Synthesis and Characterization of Hybrid Micro Crystalline Cellulose - Montmorillonite Nanoclay Filled and Sorbitol Plasticized PolyLactide Acid for Structural Application

Nehemiah Mengistu Zeleke

A Dissertation Submitted to the Department of Mechanical Engineering,

College of Mechanical, Chemical, and Material Engineering

Presented in Partial Fulfilment of the Requirement for the Degree of Doctor of Philosophy in Manufacturing Engineering

Office of Graduate Studies

Adama Science and Technology University

March/2024

Adama, Ethiopia

Synthesis and Characterization of Hybrid Micro Crystalline Cellulose - Montmorillonite Nanoclay Filled and Sorbitol Plasticized PolyLactide Acid for Structural Application

Nehemiah Mengistu Zeleke

Professor Santosh Kumar (Supervisor)

Dr. Devendra Kumar Sinha (Co-supervisor)

A Dissertation Submitted to the Department of Mechanical Engineering,

College of Mechanical, Chemical, and Material Engineering

Presented in Partial Fulfilment of the Requirement for the Degree of Doctor of Philosophy in Manufacturing Engineering

Office of Graduate Studies

Adama Science and Technology University

March/2024

Adama, Ethiopia

DECLARATION

I hereby declare that this Dissertation entitled “Synthesis and Characterization of Hybrid Micro Crystalline Cellulose - Montmorillonite Nanoclay Filled and Sorbitol Plasticized PolyLactide Acid for Structural Application” is my original work. That is, it has not been submitted for the award of any academic degree, diploma or certificate in any other university. All sources of materials used for this thesis have been duly acknowledged through appropriate citations.

Nehemiah Mengistu Zeleke _____ _____

Name of student Signature Date

RECOMMENDATION

We, the supervisor(s) of this dissertation, hereby certify that we have read and revised the dissertation entitled “Synthesis and Characterization of Hybrid Micro Crystalline Cellulose - Montmorillonite Nanoclay Filled and Sorbitol Plasticized PolyLactide Acid for Structural Application” prepared under our guidance by Nehemiah Mengistu submitted in partial fulfillment of the requirements for the degree of Doctor of Philosophy in Manufacturing Engineering. Therefore, we recommend the submission of the dissertation to the department for further review and defense.

Professor Santosh Kumar		_____
Major Supervisor	Signature	Date
Dr. Devendra Kumar Sinha	_____	_____
Co-supervisor	Signature	Date

APPROVAL PAGE OF Ph.D. DISSERTATION

We hereby certify that the recommendations and suggestions made by the board of examiners are appropriately incorporated into the final version of the dissertation entitled "Synthesis and Characterization of Hybrid Micro Crystalline Cellulose - Montmorillonite Nanoclay Filled and Sorbitol Plasticized PolyLactide Acid for Structural Application" by Nehemiah Mengistu.

_____		_____
Major Supervisor	Signature	Date
_____	_____	_____
Co-supervisor	Signature	Date

We, the undersigned, members of the Board of Examiners of the dissertation open defense by Nehemiah Mengistu have read and evaluated the dissertation entitled "Synthesis and Characterization of Hybrid Micro Crystalline Cellulose - Montmorillonite Nanoclay Filled and Sorbitol Plasticized PolyLactide Acid for Structural Application" and examined the candidate during open defense. This is, therefore, to certify that the dissertation is accepted for partial fulfillment of the requirement of the degree of Doctor of Philosophy in Manufacturing Engineering.

_____	_____	_____
Chairperson	Signature	Date
_____	_____	_____
Internal Examiner	Signature	Date
_____	_____	_____
External Examiner 1	Signature	Date
_____	_____	_____
External Examiner 2	Signature	Date

Finally, approval and acceptance of the dissertation is contingent upon submission of its final copy to the Office of Postgraduate Studies (OPGS) through the candidate's Department Graduate Council (DGC) and School Graduate Committee (SGC).

_____	_____	_____
Department Head	Signature	Date
_____	_____	_____
College Dean	Signature	Date
_____	_____	_____
Office of Postgraduate Studies, Dean	Signature	Date

ACKNOWLEDGEMENT

First of all, I would like to express my greatest thanks to God, Christ Jesus for giving me this opportunity and great effort to complete this important milestone in my life.

Then, I would like to express appreciation to my supervisor Dr. Santosh Kumar (Professor) and Co-supervisor Dr. Devendra Kumar Sinha (Associate Professor) for their continual advice, guidance, constructive comments and suggestions throughout this research work. I am incredibly appreciative of their support and courage during my Ph.D. research's highs and lows. I would also like to extend my appreciation to my doctorial committee members, Dr. Melese Workineh and Dr. Habtamu Beri for their constructive comment and suggestions.

I express my gratitude to the entire staff member of the School of Mechanical, Chemical, and Material Engineering, particularly to Mr. Sintayehu Legese, the Head of the Mechanical Engineering Department, and Dr. Getnet Asrat, School Associate Dean for Academic Affairs. I would also want to thank the staff members of the Departments of Chemistry and Biology for allowing me to use their laboratories. Moreover, I would like to also acknowledge the Madda Walabu University for his sponsorship and all individuals, mainly Dr. Gebisa Bekele, Mr. Guta Amenu, and Mr. Leta Guta who have hand in the realization of this research work.

Finally, I would like to thank my family members and friends for their support, trust and love throughout these years. Especially, to Ms. Eden Miskir, my better half.

TABLE OF CONTENTS

LIST OF TABLES

TABLE PAGE

LIST OF FIGURES

FIGURE PAGE

ACRONYMS AND ABBREVIATIONS

ANOVA	Analysis of Variance
AMw	Average Molecular Weight
ASTM	American Society Testing Methods
AT	Alkali Treatment
APS	Average Particle Size
BL	Bleaching
CH	Coffee Husk
CI	Crystallite Index
D	Density
DP	Degree of Polymerization
DSC	Differential Scanning Calirometry
DTA	Differential Thermal Analyzer
DW	De-waxing
FM	Flexural Modulus
FS	Flexural strength
FTIR	Fourier Transform InfaRed
GPa	Giga Pascal
GRA	Grey Relational Analysis
GRG	Grey Relational Grade
H_2O_2	Hydrogen Peroxide
H_2SO_4	Sulfuric Acid
HV	Hardness Value
IS	Impact Strength
IUPAC	International Union of Pure and Applied Chemistry
LA	Lactic Acid
MCC	Micro Crystalline Cellulose
MTT	Montmorillonite
Mw	Molecular Weight
MPa	Mega Pascal

NaOH	Sodium Hydroxide
PLA	PolyLactid Acid
S	Sorbitol
S/N	Signal to Noise
SEM	Scanning Electron Microscope
T	Temperature
TAPPI	Technical Association of Pulp and Paper Industry
TGA	Thermo Gravimetric Analysis
TS	Tensile Strength
UT	Untreated
WA	Water Absorption
Wt %	Weight Percentage
XRD	X-Ray Diffraction
YM	Young Modulus
^{0}C	Degree Celsius

ABSTRACT

PolyLactide Acid (PLA) is a polyester made from renewable resources such as fermented starch of corn, maize, sugarcane, etc. It's a renewable, biodegradable, biocompatible, and high strength polymer designated to substitute petroleum-based polymers. However, it has low performance in some mechanical properties, such as impact strength, and its thermal stability limits its utilization for structural applications. The main objective of this study was to modify the properties of PLA through hybrid microcrystalline cellulose (MCC)-montmorillonite (MTT) fillers and sorbitol (S) plasticizer for the structural application due to their renewability, biodegradability, nontoxicity, and less weight. Among the factors, MCC was extracted from coffee husks through sequential chemical treatments: de-waxing (DW), alkali treatment (AT), and bleaching (BL). The effect of factors such as weight percentage of MCC (0, 3, 6, and 9), MTT (0, 3, 6, and 9), S (10, 20, 30 and 40), and temperature (T) (100, 125, 150, and 175^{0}C) on flexural strength (FS), flexural modulus (FM), tensile strength (TS), young modulus (YM), impact strength (IS), hardness value (HV), water absorption (WA), and density (D) were investigated through Taguchi's based Grey relational Analysis (GRA). The obtained results of chemical composition analysis showed that the cellulose, hemicellulose, lignin, extractive and ash content were (52.9%), (12.5%), (21.9%), (9.4%), and (2.4%), respectively. The sequential chemically treated sample showed a higher crystallinity index (CI), i.e., 89.9%, in the MCC region with 54.7% yield and has great thermal stability at high temperature. The synthesized MCC/MTT/S/PLA hybrid bio-composite global optimum result obtained for FS, FM, TS, YM, IS, HV, WA and D were MCC at level 3 (6%), MTT at level 4 (9%), S at level 2 (10%), and T at level 4 (175^{0}C). ANOVA showed that MTT has the greatest significant effect on mechanical and physical properties of MCC/MTT/S/PLA bio-composite, followed by MCC, T, and S. The confirmation test indicates the improvement of weighted Grey Relational Grade (GRG) from 0.7896 to 0.846. Further, the FTIR, XRD, TGA/DTA, and SEM results indicated that the good interaction between PLA and fillers improved the thermal and morphological properties of optimal (6MCC/9MTT/10S/175^{0}C) bio-composite samples. Therefore, the multiple quality characteristics of MCC/MTT/S/PLA bio-composite material can be a possible candidate for various structural applications.

***Keywords**: Polylactide acid, Micro crystalline cellulose, Nanoclay, Plasticizer, Bio-composite*

CHAPTER 1

INTRODUCTION

1.1 Background of the Study

Polymer composites are considered as one of the most important materials used for daily life from common household to high-performance applications because of their light weight, high strength, easy fabrication, easy availability, low cost, low density, and corrosion resistance as compared to conventional metallic components (Omrani et al., 2016). The usage of polymer composites in transportation industries has gradually improved over the past few years due to environmental concern and reduction of CO_2 emissions. However, the use of polymer composites synthesized from petroleum-based chemicals, like polypropylene, polystyrene, carbon fibre, glass fibre, etc., typically results in a number of problems, including the reduction of enormous amounts of petroleum resources, waste management issues due to the non-biodegradability and non-renewability of synthetic polymers and fillers (1 billion tons annually), environmental pollution concerns (approximately 1781 million tons of CO_2 equivalent were released into the environment in 2015, and it is expected to reach up to 6500 million tons by 2050), sustainability principles, new environmental regulations, etc.. These problems has motivated the development of the next generation of fully or partially biodegradable polymer composite material, both matrix and fillers are compatible with the environment (Dejene et al., 2024; Kibria et al., 2023).

Recently, researchers are striving to produce new bio-based polymers and filler materials to address challenges related to synthetic materials. PolyLactide Acid (PLA) is a biodegradable polymer made up of lactic acid (LA) extracted from corn grain, potatoes, sugar cane, etc., and renewable agricultural products. It is extensively used in many applications areas such biomedical, packaging, automotive, composites, electronics, etc. due to its strength, high wear resistance with good performance, and ease of process ability. However, it has low performance on impact strength and poor thermal resistance, as well as high cost limits its application to automotive and structural applications (Pongtanayut et al., 2013; G. Wang et al., 2019). In order to overcome the drawbacks of PLA, it’s significant to incorporate plasticizer and different filler materials into the PLA matrix. Sorbitol is a biodegradable and low-cost plasticizer, which offers improved mechanical properties to the composite (Rico et al., 2016). Natural fiber and clay are different

types of bio-based fillers that improve the biodegradability, mechanical performance, thermal stability, and cost of polymer composites (Rajeshkumar, Seshadri, Ramakrishnan, et al., 2021).

Lately, natural fibers are considered one of the best reinforcing fillers in the development of polymer composites, and they are widely used in several application areas such as construction, automotive industries, and electrical and electronic industries due to their low cost, non-toxicity, ease of availability, renewability, biodegradability, and low specific weight but high relative strength advantageous over synthetic fillers (Oladele et al., 2020b). Natural fibers are fibers extracted from various renewable resources, namely plants, animals, or minerals. Plant fibers has better properties in terms of its stiffness and strength as compared to animal fibers. Additionally, they are advantageous in terms of easy availability, less cost, and ease of preparation (Karimah et al., 2021). Among plant fibers, coffee husk is a waste generated during the isolation of coffee bean from its cherry in the dry processing method. It is easily available (30-50% from produced coffee cherries), easy to prepare filler from it, rich in cellulose (<50%), different layers of the husk contains different cellulose content, its derivative crystalline cellulose structural performance and its reinforcing effect on bio composite development is not studied yet (Collazo-Bigliardi et al., 2019a; Poyilil et al., 2021). However, as synthetic fillers, natural fibers also have their own limitations due to their hydrophilic nature, which causes incompatibility with polymer resins (Adekunle, 2015). The hydrophilic nature is caused by the amorphous contents of natural fibers such as hemicellulose, lignin, waxes, pectin, etc., and cellulose is the semi-crystalline and crystalline content of natural fiber (Komuraiah et al., 2014).

The crystalline part of natural fibers, cellulose, is responsible for the mechanical properties of the fiber. However, the rest of the amorphous parts of the natural fiber have the tendency of water absorption, which leads to a reduction in performances (mechanical, thermal, etc.) that may not give desired results as it undergoes various loading conditions during the service life of polymer composites (Chandrasekar et al., 2017). Therefore, it is necessary to remove these amorphous parts of natural fiber in order to fabricate targeted mechanical and thermal properties of polymer composites. Different types of chemical treatments are used to remove amorphous parts of natural fibers, which increases the interfacial adhesion of polymer resin and natural fiber, which is used to boost the performances of synthesized polymer composites.

Currently, the addition of Nano clay into the PLA matrix improves the crystallization ability, mechanical and thermal properties of PLA (Othman et al., 2017). Montmorillonite (MTT) is frequently used as Nano clay because of its availability, environmental friendly, high aspect ratio, and high swelling property in polar spaces. The inclusion of Nano clay improves the performances of polymer composites, such as physical, mechanical, thermal, and shrinkage (Shah et al., 2017b).

The primary objective of this study is to modify the properties of PLA through environmental friendly MCC and MTT fillers, and sorbitol plasticizer. By extracting MCC through ecofriendly procedures, employing optimization techniques for different weight percentages of fillers and plasticizer and utilizing appropriate processing technique to develop improved performance bio composite with enhanced mechanical strength, thermal stability, and safe to the environment material for structural application. The hybridizations of MCC and MTT fillers into PLA bio composite shows a promising approach towards creating sustainable materials with improved performance characteristics. This study will contribute valuable insights into the development of bio composite materials suitable for structural applications in various areas.

1.2 Problem Statement

Currently, the widespread use of petroleum-based synthetic fibers and polymers has led to severe environmental challenges, including pollution and the depletion of finite fossil fuel resources. Since these materials are non-biodegradable, they contribute to long-term environmental contamination and complicate waste management (Gowthaman et al., 2021). According to study by the Lawrence Berkeley National Laboratory revealed that global plastic production in 2019 emitted approximately 2.24 billion metric tons of CO_2 equivalent, accounting for 5.3% of total greenhouse gas emissions. Without intervention, this figure is projected to more than double, reaching 4.75 billion metric tons by 2050 (Karali et al., 2024). Additional problems regarding the habit of using synthetic polymer and fibers restrict the natural resource derived polymer such as PLA, and fiber usage practice in the area where a high amount of natural resource waste is available. PLA is a promising candidate biodegradable polymer for automotive industry. However, it has low performance on impact strength and thermal stability. Therefore, it’s impossible to substitute this material for automotive and other structural application in its pure forms due to low mechanical performances.

Further, coffee husk is a major byproduct of coffee processing industries, constitutes 30-50% of total harvested coffee cherries, generating over 10 million tons of solid waste annually (Dadi et al., 2019). Currently, this husk is discarded, polluting land and waterways due to its 1% caffeine and 5% tannin content, which are toxic (Blinová et al., 2017b; Gómez-Salcedo et al., 2021). Since it is unsuitable for animal feed and has few practical uses, it is often burned in fields, releasing harmful smoke and posing health risks (Gaur et al., 2020). However, its abundance and low cost make it an attractive reinforcing filler for polymers.

To mitigate these environmental concerns, there is a pressing need to develop eco-friendly PLA-based bio composites enhanced with coffee husk derived fillers. Such materials could offer sustainable alternatives for automotive structural applications and other industries, reducing reliance on synthetic polymers while utilizing agricultural waste effectively.

1.3 Objectives

1.3.1 General objective:

The general objective of this research study is to synthesis and characterize the hybrid micro crystalline cellulose - montmorillonite Nano clay filled and sorbitol plasticized polylactide acid for structural application.

1.3.2 Specific objective:

- Investigate the chemical composition and extraction of MCC from outer skin isolated coffee husk
- Development of MCC/MTT/S/PLA bio-composite samples.
- Determine the mechanical and physical properties of synthesized MCC/MTT/S/PLA bio-composite samples.
- Investigate the most optimal MCC/MTT/S/PLA bio-composite sample through GRA
- Determine the mechanical, physical, thermal, structural and morphological properties of neat PLA and optimal sample.
- Recommend application for synthesized MCC/MTT/S/PLA bio-composite material.

1.4 Significance of the Study

Because of its multipurpose character, the relevance of this work includes, among other things, the eradication or minimization of environmental effect caused by synthetic polymers and fillers derived from petroleum that are employed in the manufacture of polymer composites. To further reduce the environmental impact of agro-waste, it is essential to minimize coffee husk remnants in coffee producer countries and identify new sources of cellulose. This leads to waste management and increase of a habit of reusing agro-waste materials. Particularly, explains how to extract MCC material from coffee husk. Additionally, the process for separating cellulose from agricultural waste and extracting its derivative, MCC, is identified for additional research on agricultural waste and demonstrates the capacity of biodegradable fillers to reinforce biodegradable polymer materials and also cultivates the practice of re-usage of waste materials to create valuable materials and gaining fundamental concepts related to bio-composite development and characterization for specified application. Moreover, it initiates the domestic industries that work on polymer and agro-processing to an additional composite processing sector, which leads to additional income, employment, and improved gross domestic products of the country. Finally, this study gives effective way of product extraction from agricultural residue and solid background of bio composite synthesizing method for research and academic communities.

1.5 Hypothesis of the Research

Enhancing the mechanical and physical characteristics of biopolymers involves more than just adding materials to them; it also involves the behavior of the material to be added and the interactions that occur at the interface between the new material and the biopolymer. Consequently, the properties of the constituents, the interaction at the matrix-filler material interface, and the dispersion of the filler materials within the matrix all have a significant impact on the reinforcement of bio polymers with filler materials. Additionally, the improvement of polymer bio composites can be made by chemical treatment of filler material's surface and addition of nanoparticles by increasing the interaction surface areas of the biopolymer and fillers. Furthermore, by the incorporation of diverse chemical groups, fillers and plasticizers with distinct functional groups at the surface of these materials offer the possibility of multifunctional polymer bio composite materials, such as load bearing, flame retardant, water resistant, etc. Thus, the possibility of including MCC and MTT fillers into the sorbitol plasticized PLA matrix to enhance

PLA's mechanical, physical, and thermal properties was examined in this work. The following hypothesis served as the foundation for this study:

Certain PLA may benefit by the addition of sorbitol plasticizer, MCC and MTT fillers because:

- The interaction between the plasticizer and polymer makes the fillers (MCC and MTT) more compatible with PLA.
- Because of MTT's wide surface area, adding MTT improves the MCC's compatibility with PLA.
- The filling of the spaces and gaps between PLA and MCC is made easier by the addition of plasticizer and MTT.
- An improvement in PLA's mechanical and physical performances due to increased interfacial adhesion with fillers.
- An improvement in PLA's thermal performance due to MTT's flame retardant characteristics.

1.6 Scope of the Study

To attain the aim of this study, these procedures of scope has been followed. Primarily, the isolation of outer skin from the husk was identified and the chemical composition analysis of outer skin isolated coffee husk was conducted through analytical (gravimetric) method. Then, the extraction of MCC from the outer skin isolated coffee husk was obtained after subsequent chemical treatment methods and investigated through FTIR, XRD, TGA/DTA, SEM and DP/MW. Moreover, the addition of this MCC fillers and other Montmorillonite fillers effect in bio composite polymer, PLA were investigated by preparation of bio composite samples at different weight percentages through Taguchi's orthogonal array (L16) experimental setup. Montmorillonite is a commonly utilized Nano clay because of its accessibility, environmental friendliness, high aspect ratio, and thoroughly studied chemistry (Nazir et al., 2016; Rafiee et al., 2019). The complete performance (physical, mechanical, thermal, ultraviolet, diffusional barrier, etc.) of materials are enhanced by the incorporation of Nano clay into polymers and natural fiber reinforced polymers (Shah et al., 2017b). Next, the mechanical (tensile, flexural, hardness and impact strength) and physical (water absorption and density) properties of different weight percentages of hybrid MCC - MTT fillers filled and sorbitol plasticized PLA bio composite were investigated and optimized through Taguchi's based grey relational analysis. Finally, the most

optimal sample of MCC/MTT/S/PLA bio composite material variation from the neat PLA material was determined through FTIR, XRD, TGA/DTA, SEM and OM analysis and based on the results the possible structural application areas was recommended based on the examined properties.

1.7 Outline of the Dissertation

The dissertation contains five chapters. The first chapter is the introduction chapter which explains the background of the study, objective of the study, problem of the statement, significance of the study, hypothesis of the study, scope of the study and outline of the dissertation. The second chapter is the literature review chapter which addresses the comprehensive review of literatures on the topics related to this study that gives relevant background and describes the literature gap. The third chapter is material and methods chapter which explains the material and equipment used, experimental procedure followed, testing and characterization techniques used, optimization techniques used in this study mentioned in detailed. The fourth chapter is the result and discussion which gives the result and discussion of the chemical composition of outer skin isolated coffee husk, the effects of chemical treatment on the CH fiber and the properties of the extracted MCC. Also provides the effects of loading different weight percentage of MCC and MTT filler and sorbitol plasticizer in PLA base material in order to investigate the tensile strength, tensile modulus, flexural strength, flexural modulus, hardness value, impact strength, water absorption and densities of synthesized MCC/MTT/S/PLA bio composites. Additionally, this chapter deals with the results and discussion of the optimal level combination of bio composite investigation, its variation from the base material, PLA and comparison is made with the structural components of automotive part materials. The fifth chapter is the conclusions and recommendation which gives the main investigation gained from this study and also provides the suggestion for this study area.

CHAPTER 2

LITERATURE REVIEW

This chapter presents a basic concept overview and literature assessment of a natural fiber and natural fiber-reinforced polymer composites. The review includes the procedures for isolating cellulose and extracting MCC, the efficient ways of PLA modification techniques for enhancing its performance, and the assessment of MCC and MTT reinforcing potential in the polymer composite, hybrid composite and nanocomposites. Furthermore, the synergistic effect of mixing Nano clay and MCC with plasticizers, co-polymers, natural fibers, synthetic fibers and etc. to enhance the performances of PLA matrix was reviewed. Ultimately, the review guides the development process of totally biodegradable polymer composite material as well as the gap in the literature.

2.1 Polymer Composite

Composite materials are amalgamations of two or more chemically distinct materials to form a new material with improved properties that are not achievable by any individual materials alone. They possess applications in automobiles, aerospace, buildings and electrical and electronics, general mechanical components, marine transports, rail transports, space transport, sports and recreation, cable transports, etc. (Ramchandra, 2020). They are classified at two different levels. The first level of classification is made concerning the matrix phase. The major matrix-based classifications include polymer matrix composites (PMCs), metal matrix composites (MMCs), and ceramic matrix composites (CMCs). PMCs consist of a polymer material as a matrix, which is filled with various reinforcements. Polymer matrices are the most commonly used polymer because of their low cost, low density, ease of fabricating complex parts with low tooling cost, and they also have good room temperature properties when compared to ceramic and metal matrices (Asim et al., 2017). Over the past decades, it has been found that polymers have replaced many of the conventional metals in various applications (Ngo, 2018). This class of composite is used in the greatest range of composite applications, and its properties are easily adjusted by reinforcing agents to suit the desired properties, such as high modulus/high strength requirements (Alias et al., 2021). The polymer matrix composite agent may be either petroleum-based or natural-based. Various types of petroleum-based polymers have been developed, such as polypropylene,

polyethylene, polystyrene, nylon, Teflon, polyvinyl chloride, etc. (Gowthaman et al., 2021). On the other hand, some natural-based polymers are developed for instance PLA, Polycaprolactone, Polybutylene succinate, Polybutylene succinate adipate, Polybutylene terephthalate, Polymethylene adipate, etc.

The second level of composite classification is based on the reinforcement phase. It includes particulate, fiber, structural, and nano-reinforced composites. Recently, nanoparticle-reinforced composites are considered as a new class of composite material category. The particulate and Nano-reinforced composites consist of reinforcing material in the form of particles and Nanomaterials, respectively. The particle-reinforcing material may be either synthetic or natural. Several kinds of synthetic particles have been developed, such as carbon (black), glass, aluminum, etc. On the other hand, natural particulates are particles that are derived from plants, fruits, agro-wastes, animals, etc. Natural particle reinforced polymer composite is a polymer matrix incorporated with natural particle reinforcement and widely used in various fields such as construction, automotive industries, and electrical and electronic industries due to its cost, nontoxicity, ease of availability, renewability, and low specific weight but relatively high strength.

Due to their special qualities, which result from combining the effects of their small size, high surface area to volume ratio, specific strength, and modulus, polymer composites reinforced with natural fibers have recently found widespread use in a variety of engineering applications, including aerospace, electronics, automotive, medical, structural, and catalysis (Khalid et al., 2021). These materials are smart materials in these applications because they provide excellent corrosion resistance, high durability, lightweight properties, and design flexibility (Oladele et al., 2020a).

2.2 Natural Fibers

Natural fibers are fibers extracted from various renewable resources, namely plants, animals, or minerals that are not synthetic or manmade. Fibers like seed, leaf, grass, and stalk, etc., are examples of plant fibers; hair, wool, silk are examples of animal fibers and asbestos is an example of mineral fibers. The classification of natural fibers is given clearly in Figure 1. Comparing plant fiber to animal fiber, the former has superior strength and stiffness characteristics. Additionally,

they are advantageous in easily availability, less cost, and ease of preparation (Anbupalani et al., 2020).

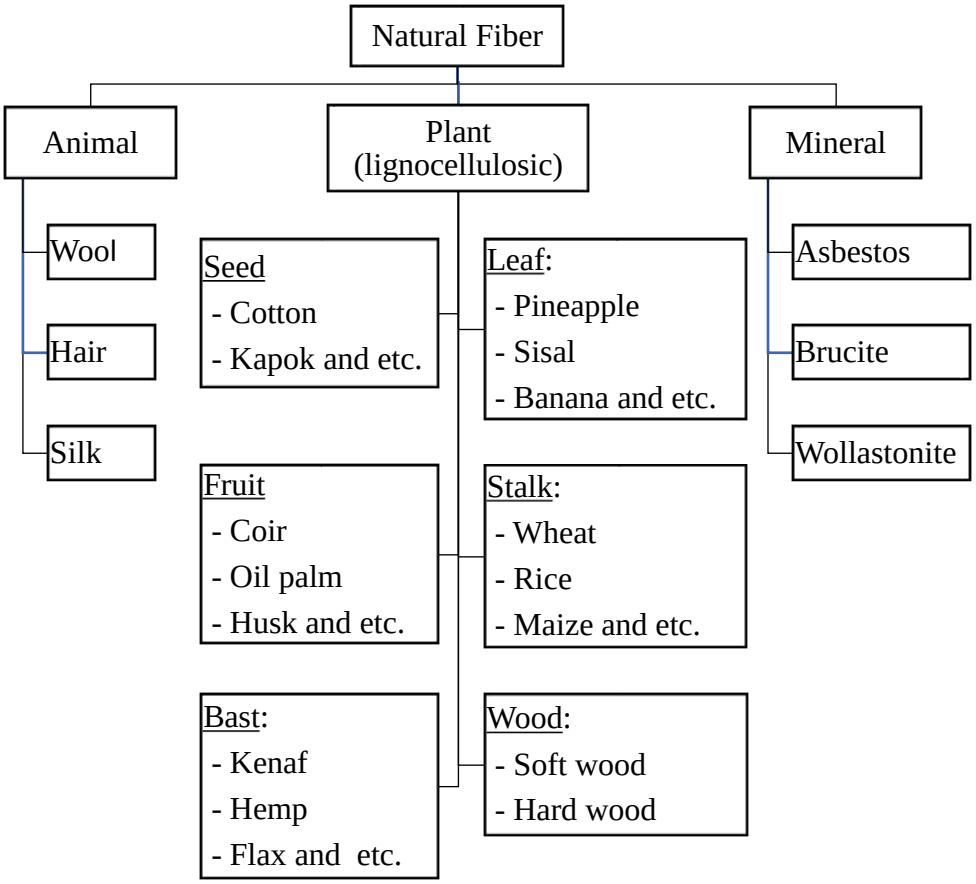

Figure 1: Natural fiber categories (Anbupalani et al., 2020; Mochane et al., 2019)

The chemical composition and structure of natural fibers differ depending on various factors, the common factors are the source of the plant and the isolation method. The composition of plant fibers typically consists of modest amounts of cellulose, lignin, hemicelluloses, and other extractives, with varying percentages found in different fibers (Mochane et al., 2019). The secondary cell wall of the fiber materials contains soft lignin and hemicellulose binder, while the stiff cellulose portion of the plant is found inside the cell wall. The natural fibers hydrophilic character, stability, and strength are mostly attributed to the semi-crystalline cellulose component. The secondary cell wall of plant fiber contains lignin, which forms linkages with hemicellulose and cellulose to provide the fibers rigidity. In addition to being hydrophobic, it serves as a reinforcing ingredient to increase the material's stiffness. Extractive (Pectin) is also utilized in the binding of cellulose to other components. In comparison to cellulose, pectin and lignin are weak amorphous materials. A polysaccharide with an amorphous structure, hemicellulose is somewhat

soluble in water and alkaline solutions. These polysaccharides include a mix of carbon rings, five and six. The hemicellulose provides the structure to the fibers and functions as a reinforcing matrix between the cellulose micro-fibrils that form the hemicellulose/cellulose network (Ali et al., 2018). The internal structure and the chemical composition of the natural fiber plays an important role in influencing the physical and mechanical properties. The lignocellulosic fiber and structure is depicted in Figure 2.

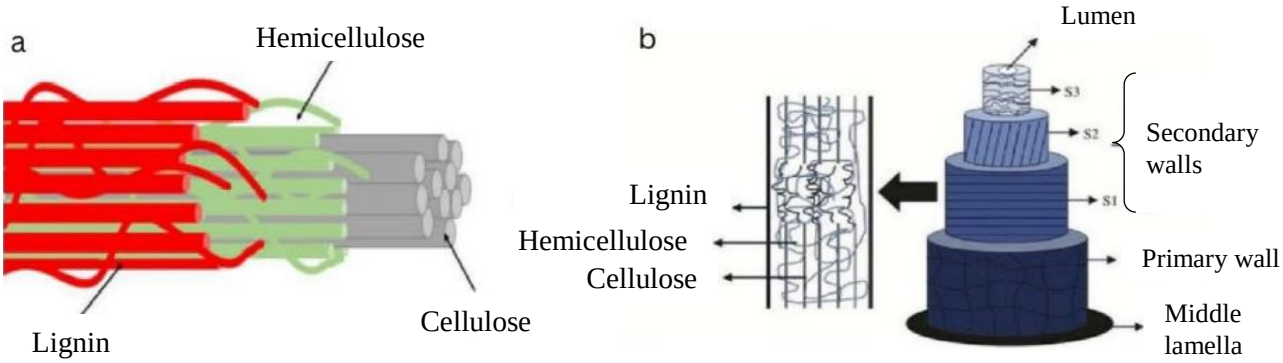

Figure 2: (a) Lignocellulosic fiber and (b) structure of Lignocellulosic fiber (Amin et al., 2022)

Natural fibres have drawn more attention lately because of their potential to replace synthetic fiber-reinforced polymers at a lower cost, with improved sustainability and other benefits. Table 1 summarizes the benefits and drawbacks of natural (plant) fibers.

Table 1: Advantage and disadvantage of natural (plant) fibers (Mochane et al., 2019; Pickering et al., 2016)

S.N	Advantage	Disadvantage
1	Renewable	High moisture absorption
2	Fibers produced at lower cost	Dimensional instability
3	Low density (light weight), and high specific strength and stiffness	Flammable
4	Non-abrasive to processing equipment	Anisotropic behavior
5	Produce non-harmful gases during processing	Limited processing temperatures
6	Less production energy require	Sensitive to microbial, fungus, UV attack
7	Good thermal and acoustic properties	Lower impact strength compared to synthetic fiber

Plant fibers are the most widely utilized type of fiber, and a significant amount of research has been done on hemp, coir, bamboo, flax, jute, and bagasse (Anbupalani et al., 2020). Table 2 provides a summary of several common natural (plant) fiber chemical compositions.

Table 2: Chemical composition of natural (plant) fibers

Fiber	Constituents in %				Reference
	Cellulose	Hemicellulose	Lignin	Others	
Pineapple	80-81	6-19	4.6-12	-	(Bondesson, 2015)
Banana	60-65	6-19	5-10	-	(Cesarino et al., 2020)
Sisal	43-78	10-13	4-12	0.8-2	(Collazo-Bigliardi, Ortega-Toro, & Boix, 2018)
Hardwood	31-64	25-40	14-34	0.1-7.7	(Malkapuram et al., 2009)
Bamboo	26-43	30	21-31	-	(Bondesson, 2015)
Rice husk	35-45	19-25	20	-	(Cesarino et al., 2020)
Rice straw	41-57	33	8-19	8-38	(Collazo-Bigliardi, Ortega-Toro, & Boix, 2018)
Wheat straw	38-45	15-31	12-20	-	(Malkapuram et al., 2009)
Sugarcane	55-57	24-25	24-26	-	(Cesarino et al., 2020)
Coffee husk	41-43	5-10	23-23.7	-	(Bondesson, 2015)

2.3 Cellulose

Cellulose is the most essential and abundant polymer in nature, which can be obtained from renewable resources. Braconnot in 1819 and Payen in 1838 were the first to study its existence as the common substance of plant cell walls (El Amri et al., 2022). Its dense microfibril structure, combined with a linear chain of β-1,4-glycosidic D-glucose units as the fundamental building blocks with strong hydrogen bonding and crystallinity, provides high mechanical strength, biodegradability, and nontoxic properties (Sung et al., 2017). According to Khenblouche et al. (Khenblouche et al., 2019), it is a promising renewable resource that decomposes naturally and has the potential to replace synthetic fibres in industrial applications. Figure 3 illustrates the structure of glucose and beta-cellulose.

There are four different crystalline structural types of cellulose: I, II, III, and IV. Since it comes from natural resources like plants, trees, algae, and bacteria, cellulose-I crystal structure is also

known as native cellulose. When native cellulose is in its crystalline form, it exhibits two distinct compositions, Iα and Iβ, which have a fairly similar chain organization. However, Iα and Iβ cellulose crystallize in triclinic and monoclinic unit cells structures, respectively (Peter, 2021). While beta cellulose (Iβ) is found in plants, alpha cellulose (Iα) is found in bacteria and algae. Furthermore, certain procedures are needed to create cellulose II, III, and IV crystal structures. The main difference between Iα and Iβ is the relative movement of the single-plane parallel stacking of cellulose chains along hydrogen-bonded planes [(110) and (200)] in the direction of the chain axis. Natural fibres' mechanical characteristics are determined by the kind of cellulose that makes up the fibres. There are four different types of cellulose: type I, II, III, and IV. Type IV cellulose has better mechanical qualities (Hafid et al., 2021).

Numerous industries, including the food industry, water treatment, biomaterial composites, textile and paper manufacture, and the pharmaceutical sector, use cellulose extensively as a raw material (Morán et al., 2008). A wide variety of plants, including cotton, jute, flax, wood, hemp, and bamboo, are high in cellulose (Kausar et al., 2022). Additionally, cellulose has been extracted from a variety of sources, including hop stems (Szymańska-Chargot et al., 2022), milkweed stems (N. Reddy et al., 2009), rice husk (Hafid et al., 2021), cissus quadrangularis root (Manimekalai et al., 2021), and many more. As a result, numerous academics throughout the world are currently working to identify substitute sources for cellulose extraction.

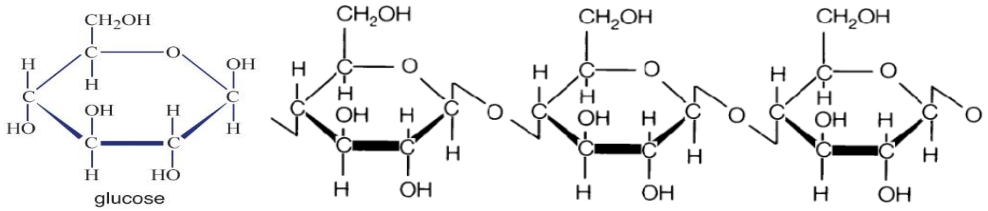

Figure 3: Structure of glucose and cellulose (Shahruzzaman et al., 2022; Swift)

2.4 Micro Crystalline Cellulose

MCC is a naturally occurring, tasteless, micro-sized material derived from partially depolymerized and pure cellulose. Microfibrils are created by combining cellulose chains, while "cellulose macrofibers" are created by further combining these microfibrils. As a result, "cellulose microfibers," which comprise both "amorphous" and "crystalline" cellulose domains, are what are known as natural fibers that retain cellulose structure (Risite et al., 2022). In order to achieve crystalline domain separation, cellulose macro-fiber characteristics are reduced through the use of

an acidic assault treatment, which eliminates the amorphous domain. The most popular technique involves treating cellulose with acid to remove the amorphous domain. Then, the crystallites' increased size allows them to travel freely. The β (1→4) glycoside link is broken by the acidic attack, which lowers the degree of cellulose polymerization and the ensuing other structure. This structure is commonly referred to as "microcrystalline cellulose" in research studies. The resulting, MCC mechanical properties are greatly controlled by crystallization degree and particle sizes (Abolore et al., 2023). There are numerous methods for extracting it, such as chemical, biological, and mechanical processing. The most common way for extracting MCC from these procedures is chemical treatment, such as acid hydrolysis (Haldar et al., 2020).

MCC possesses remarkable mechanical and thermal properties, making it a promising material for reinforcing in polymer composites (Platnieks et al., 2020). Compared to inorganic fillers (glass, carbon, and other fibres), MCC has several advantages as a reinforcing material in polymer composites, including nontoxicity, low cost, low energy required for manufacture, low density, high specific strength, and modulus. MCC fillers have hydrophilic (loving water) qualities, much unlike other inorganic fillers (glass fibres), and they don't work well with hydrophobic polymers. Therefore, it is necessary to use agents that strengthen the link between MCC and hydrophobic plastics (Teramoto, 2021). Furthermore, because MCC begins to break down or breakdown at temperatures close to 230 °C, the processing temperature of MCC-filled composites is limited to approximately 200 °C (Trache et al., 2016).

2.5 Coffee and Its Industry Residues

Plenty of evidence agree that coffee has been discovered for the first time in South-western highlands of Ethiopia. The term ‘coffee’ was named after the area of Kaffa where the place coffee first produced. In the sixth century, the excitement of goats of a man kaldi after chewed a coffee plant. So that kaldi tried this coffee cherries for himself and this moment is considered as the beginning of an incredible journey of this famed coffee beans (Duressa, 2018). For the last 1100 years coffee has been raised to the position of the sanctified, social, spiritual, and economic life of Ethiopians (Bredin, 2012). Coffee in Ethiopia is collected from garden, plantation, forest, and semi-forest locations. Garden coffee indicates around 50% of the total yield of coffee and grows around the farmhouse with extra crops. Plantation coffee represents about 10% yield in huge plantation areas in a mechanized method. On the other hand forest coffee is naturally self-growing

coffee that require minimum management system to grow under the shadow of other trees. While, the other group is semi-forest coffee which covers around 35% of total production and wherever human involvement is required to discard useless plant species that delay development (Woyesa et al., 2021).

Coffee is one of the most widely held commercial commodities next to petroleum, and therefore, the coffee industry is blamable for the generation of huge amount of residues. Ethiopia is the first in Africa and sixth in the world coffee producing country (Degaga, 2020). The coffee industry produces a large quantities of waste, in both liquid and solid forms. Basically two varieties of coffee called as Robusta and Arabica are responsible to support 100% production in the world. They vary typically in their chemical constituents, and on the other hand, produce comparable volumes of waste (Piotr Konieczka et al., 2020). Based on the processing method 30–50% of the weight of the total coffee cherry produced is waste, the variation is based on the production techniques (wet or dry) (Poyilil et al., 2021). The residues coffee husk (peel+pulp+parchment) (Figure 4a), coffee pulp (hull) (Figure 4b), coffee silver skin (Figure 4c) and spent coffee grounds (Figure 4d) are the key coffee industries residues. These residues are generated based on the processing techniques (wet or dry) of the coffee bean. In wet processing, the pulp and outer skin are removed from cherries, and parchment is removed after drying. However, in the dry processing, the dried green coffee cherries and the skins (skin or peel, pulp, and parchment) are isolated in a single process.

Coffee husk is a waste generated on a processing of isolating coffee bean from its cherry during dry processing. Coffee husk mainly contains three layers; exocarp (outer skin/peel), mesocarp (pulp) and endocarp (parchment). Each layers basically contains cellulose, hemicellulose, lignin and extractives in different percentages. The inner part (mesocarp and endocarp) of the husk contains more amount of cellulose than the outer part (exocarp) of the husk (Bekalo et al., 2010), which is responsible for the stiffness of the materials (Collazo-Bigliardi et al., 2019a). Coffee silver skin is an enveloping layer of green coffee beans separated as the first by-product during the roasting of coffee and contains about 4% weight of coffee beans (Ballesteros et al., 2014).

Figure 4: Major coffee industry residues (a - coffee husk, b – pulp (hull), c – silver skin, d - spent coffee grounds) (Blinová et al., 2017a)

2.6 Proposed Properties and Application of Coffee Industries Residue

Recently, numerous studies on different areas of coffee industry residues have been reported for various industrial applications. Some of researchers report on the chemical composition, properties, reinforcing potential and etc. of coffee industries residue are presented as follows;

According to studies of Sung et al. (Sung et al., 2017), nanocrystal cellulose reinforced polylactide acid bio nanocomposite films were developed by means of a twin-screw extruder. The nanocrystals were extracted from coffee silver skin through alkali treatment method followed by sulfuric acid hydrolysis. They were used different concentrations of nanocrystals (1%, 3%, and 5%) for preparation of PLA/CNC nanocomposites samples. Their results indicates that the tensile strength and Young's modulus improved with both 1% and 3% CNCs. Additionally, they reports that the water vapor permeability reduced progressively with increasing adding of CNCs up to 3% and worthy oxygen barrier properties were found for all nanocomposites. This shows that the agglomeration of CNCs at higher concentrations could disturb the reinforcing effect on the tensile properties of bio nanocomposite films. The developed films can be proposed for biopolymer materials with improved barrier and mechanical properties.

Reis et.al (Reis et al., 2020), conducted to examine the influence of alkaline treatment followed by a steam explosion process assisted by mechanical high shearing to get microfibrillated cellulose from coffee parchment fiber. Their results shows that around 22% of cellulose is available in the parchment and the treatment processes were carried out to increase the cellulose content. The micro and nanometric sizes cellulose are exposed during the treatment and this make sure a potential for composite reinforcement with microfibrillated cellulose.

Additionally, Collazo-Bigliardi et.al (Collazo-Bigliardi, Ortega-Toro, & Chiralt Boix, 2018), the cellulose fibre extracted from coffee and rice husks for reinforcing glycerol plasticised thermoplastic starch films. The 1 wt%, 5 wt% and 10 wt% percentage of coffee and rice husk derived cellulose were incorporated into the thermoplastic starch film and the film was obtained by melt blending and compression moulding. The result indicates that both kinds of micro-fibres improve the film stiffness while reduced the film stretchability. However, coffee husk cellulose maintained improved the film ductility at 1 and 5 wt% and thermal stability of composites was slightly greater than net thermoplastic starch films. Further, coffee husk derived cellulosic fibres and cellulose nanocrystals for enhancing the useful properties of compatibilized starch-PLA blend films were performed to determine the tensile functional performance. The result shows CNC were the most effective at reinforcing tensile properties of the material (148% and 45% improve in elastic modulus and tensile strength, respectively) (Collazo-Bigliardi et al., 2019b).

Moreover, Ilangovan et al. (Ilangovan et al., 2021), performed fabrication of bio based composites, coffee husk (CH) was used for reinforcing polypropylene (PP). The effects of different weight percentage and densities of coffee husk on the mechanical properties, flame retardancy, water stability, sound, and thermal insulation were studied. Results showed that the 1.0 g cm^{-3} composite at 80:20 ratio had the highest mechanical properties (Tensile, 24.5 MPa and Flexural strength, 21.5 MPa), sound absorption coefficient of 0.9 and thermal insulation coefficient of 51.8 mW mK^{-1}.With increase in density, the water stability and flame retardance of the composites improved. The developed CH/PP composites show excellent properties to be used in false ceiling and insulation panels. Therefore, literatures tells us tangible information about coffee industry residues potentials to yield different reinforcement, products and compounds.

2.7 Cellulose Isolation and MCC Extraction Method from Natural Sources

Cellulose isolation using several ways from different plants and animals has gained high interest as a result of their typical characteristics such as low cost, good thermal properties and high specific strength. Commonly, isolation mechanism from natural sources includes the effective way of complete removal of other constituents such as hemicellulose, lignin, pectin and other impurities (Mzimela et al., 2018). Generally two methods, namely top-down and bottom-up approach can be employed to fully separate pure cellulose from its natural sources. The top-down approach is fractionated to generate IV required quality and size of cellulose from natural sources (sisal, cotton,

bagasse, wheat straw, jute, etc.). Whereas, in a bottom-up (biological treatment method) approach cellulose is synthesized by means of microorganisms, such as fungi (white-rot) or bacteria (Acetobacter xylinum) to degrade the non-cellulosic components (Trache et al., 2016).

The common methods of top-down approach of cellulose extraction approach includes; chemical treatment and physical treatment methods. The chemical treatment method involves the use of acids, bases, or solvents to break down or dissolve the non-cellulosic components. Physical treatment method refers modifying the structure and properties of cellulose material, include mechanical, thermal, and irradiation techniques. Ball milling, ultrasonication, and high-pressure homogenization method are a few examples of mechanical technique that can break down cellulose fibres and increase their surface area, making them more accessible to chemical or enzymatic treatments. The plant cell wall can be damaged by thermal techniques, such as steam explosion, which makes the cellulose fibres more accessible. It is also possible to employ radiation, such as gamma or electron beam radiation, to enhance the crystallinity of cellulose fibres (Emenike et al., 2023). Chemical treatment is the most common method used to isolate cellulose component from lignocellulosic materials such plant biomass and agricultural residues, which contains chemical treatment such as dewaxing, alkaline treatment, dissolution or deconstruction processes and bleaching treatment (Khenblouche et al., 2019).

2.7.1 De-waxing

Organic molecules found in plant fruit peels can be extracted by in organic solvents like toluene and ethanol. In addition, organic solvent treatments break the connections between molecular chains while also removing plant fruit peel wax and oils. The literature review states that ethanol gets rid of hydrophilic substances like pigments and cell debris, while toluene greatly removes hydrophobic materials like wax and oils. For instance, powdered peel steeped for a day in a 2:1 ratio of ethanol to toluene solution. After filtering the mixture, the residue was allowed to dry at room temperature before undergoing additional processing to produce cellulose, specifically alkali treatment and acid hydrolysis. Furthermore, the fruit peel of the plant is made softer and less yellow in colour by these organic solvents (Naz et al., 2016). In a different piece of literature, the de-waxing of bamboo fibre was done using the soxhlet apparatus extraction technique and a 2:1 ratio of toluene to ethanol, which was applied for two hours at 250˚C until the colour mixture faded (Liew et al., 2015).

2.7.2 Alkali treatment

Alkaline treatment is one of the common techniques to extract hemicelluloses from fibers. The main function of alkaline treatment lies in following two aspects. First, alkaline treatment breaks down the fiber bundles into small and shorter fibers due to the distraction of hydrogen bonding between the fibers. Meanwhile, it induces a significant microstructure change in cellulose crystalline (L. Zhang et al., 2017). During the alkaline treatment procedure via reagents like potassium hydroxide (KOH) and sodium hydroxide (NaOH) solution hemicellulose is highly soluble and freely hydrolyzed than other fiber constituents. Additionally, alkali treatment helps to lessen surface tension between polymer matrix and natural fibers by modifying the surface of the natural fiber using the solution. Also bonding interface between fibres and polymer can be improved (X. Chen et al., 2014). Furthermore, as reported by the researchers; mechanical and thermal properties of sanseveria green fiber was improved by 5% NaOH treatment in a significant manner. Also characteristics of century fiber was improved in terms of mechanical, morphological properties and crystallinity by the treatment process (Devnani et al., 2019). Non cellulosic binding materials of fibers like hemicellulose is solubilized and extracted favorably via alkali treatment method using NaOH and KOH solvents. This treatment method also loosen hydrogen bonds and hydrolyze ester bonds which source the cellulose to swell and decrease in crystallinity (Martins et al., 2021). Additionally, studies shows that on kapok banana peel. The hemicellulose was eliminated by 4 wt% of NaOH solvent and stirred at 60˚C for 4 hours. Then this treated peel was filtered and cleaned with distilled water up to pH reaches 7 (Riyanti, 2023).

2.7.3 Bleaching

A subsequent bleaching treatment was conducted to eliminate residual lignin and whiten the microfibers after the removal of hemicellulose through alkaline treatment. Most studies commonly employed oxidizing bleaching agent for bleaching cellulosic natural resources are sodium chlorite ($NaClO_2$) and hydrogen peroxide solution, both methods resulted in cellulose with significant quantities removal of hemicelluloses or lignin. Bleaching with $NaClO_2$ solution is simple and environmentally aggressive (Mzimela et al., 2018). According to study reported by Nagarajan et al. (Nagarajan et al., 2018), the delignification process has been performed after de-waxed process of Saharan Aloevera cactus fibers using 0.7 wt% sodium chlorite in buffer solution at the ratios of 50:1 (g/g). This buffer solution is adjusted by 10 wt% adding acidic acid drop by drop and kept at the pH level of 4 - 4.2. The process was carried out at a temperature of 100°C for 120 min. the

mixture was then cooled and filtered by filter paper. Finally, the filtrate was washed using distilled water and 2% sodium bisulfite, then dried at 110^{o}C in an oven for 2 hrs. In the procedure of bleaching, by the existence of acidic buffer the chlorine dioxide is removed from the Sodium chlorite, bonds with the lignin, and makes lignin chloride. The lignin chloride formed misses its strength to bond with content of α-cellulose and become weak. Further, disposed paper cups (Nagarajan et al., 2020), Agave micro fibrils (K. O. Reddy et al., 2014), Ramie (Syafri et al., 2018) and cocos nucifera var aurantiaca peduncle (Nagarajan et al., 2019) are delignified by sodium chlorite solution as reported by mentioned researchers.

Bleaching with hydrogen peroxide (H_2O_2) is another chlorine-free, eco-friendly, strong oxidative bleaching agent in addition to sodium chlorite to remove the lignin content from the lignocellulosic fibers. Hydrogen peroxide is an environmental friendly bleaching agent because only water and oxygen are generated throughout the decomposition process, which is harmless to perform in an open container (Garcia-Munoz et al., 2023). Relatively to sodium chlorite, hydrogen peroxide agent is very unstable under strong alkaline condition, involves a stabilizing agent and comparatively costly. But hydrogen peroxide can be partially substituted by a chlorine-based bleaching process (Chowdhury et al., 2022). According to research work conducted to bleaching natural fibers to their maximum efficiency with H_2O_2 combined with NaOH and sodium silicate. During the process, extracted fibers were dipped in 5% H_2O_2 (vol/vol) solution for 1 hr at a temperature of 80°C and pH level of 11 was kept using the NaOH with a concentration of 0.5 M. At the end, the fibers were carefully washed with distilled water and then oven dried at 60°C for 2 days. During the process with H_2O_2, the bond formed between lignin and hemicellulose would be broken, which leads to the effective elimination of the lignin from the fiber (Nagarajan et al., 2021). To confirm the maximum elimination of the binding constituents, the bleaching can be repeated multiple times. The bleached fibers exhibit improved morphologies with greater thermal stability and crystallinity than raw natural fibers (Nagarajan et al., 2020). Additionally, two-cycle bleaching processes was implemented for jute. The first bleaching cycle was carried out using conventional hot hydrogen peroxide bleaching process and on the other hand newly developed second cycle bleaching process was performed using peracetic acid. The first cycle has essential for making white glossy base material, whereas the second one was whiteness achieved is slightly low (Chattopadhyay et al., 2022). Further, extraction and characterization of cellulose microfibers from Retama raetam stems, a subsequent bleaching process was performed to eliminate remaining lignin

and whiten the fibers. The hydrogen peroxide (H_2O_2) solvent (11%, v/v), its pH was tuned to 11 by 7 wt% NaOH. The solution was forcefully agitated constantly for 3 hours at 45 °C temperature. For highly efficient change of color, the process of bleaching was conducted two times in the similar settings, in each treatment process the microfibers were washed and filtered using distilled water (Khenblouche et al., 2019). Finally, addition to these agents another agents are used for bleaching purposes of lignocelluloic materials including sodium hypochloride (NaClO) (Rasheed et al., 2020).

2.7.4 MCC Extraction (Acid Hydrolysis)

Acid hydrolysis is a familiar chemical process for eliminating the amorphous areas of cellulosic substrate. In this process, the isolated cellulose from natural sources are subjected to acids like HCl, H_2SO_4, etc. to extract MCC. During extraction procedure, basically four factors were considered to investigate their importance, including acid concentration, fiber to solvent ratio, temperature and time. In the process the cellulose was mixed with acid solution in a closed vessel, heated to required temperature and maintained for intended time.

According to research work conducted on microcrystalline cellulose extracted by combined method of hydrochloric acid hydrolysis and fibro lytic enzyme purification of sweet sorghum. The agitation speed was held constant. At the end of hydrolysis process, the hydrolyzed cellulose was washed many times by means of distilled water using centrifugation for 30 min at 3900 rpm to eliminate acid. After cleaning of cellulose, the improved solid cellulose remains were oven dried for 6 h at 60 °C and weighed to measure the yield of MCC. The study result indicates that sweet sorghum is a possible low-cost raw material for typical cellulose I structure MCC fabrication with good thermal stability, rod-shaped morphologies, and the joined acid-enzyme extraction technique is favorable to extract great purity MCC from cellulosic material (Ren et al., 2019). Additionally, the microcrystalline cellulose (MCC) extracted from bamboo fiber was characterized its morphological, physiochemical and thermal properties. In this study, the hemicellulose free fiber was treated by 2.5 mol/L HCl acid. Hydrolysis procedure was performed for 30 min. at 85 °C and 1:30 (g/mL^{-1}) solid-to-liquor ratio was used. The process was carried out under constant stirring speed and the sample gained was kept to cool at ambient temperature followed by filtration and cleaned with distilled water to make pH neutral. The sample gained was vacuum dried at 80 °C up to constant weight was realized. Gained white product was put in storage and represented as MCC.

The produced MCC exhibited a greater crystallinity index of 82.6% and TGA analysis displayed higher thermal stability. Thus confirms its suitability for application in packaging materials and polymeric composites reinforcement with higher processing temperature (Rasheed et al., 2020). Various cellulose based natural resources that have been used for MCC production include rice husk (Bae et al., 2017), cotton wool (Rashid et al., 2017), roselle (L. K. Kian et al., 2017) and etc. Table 3 summarizes MCC extraction techniques using different hydrochloric, sulfuric acid and combination of them from various sources.

Table 3: Various sources of acid hydrolysis to produce MCC

Source	Hydrolysis Method	Reference
Roselle fibers	• 2.5 mol/L HCl acid concentration at 85 ◦C for 30 minute with solid to liquor ratio of 1:30 (g/ml−1).	(L. K. Kian et al., 2017)
Tea waste	• 1.5 mol/L HCl acid concentration at 65 °C for 90 min at ratio of 1:20	(T. Zhao et al., 2018)
Pedicle of Lagenaria siceraria fruits	• 160 mL of 40% H_2SO_4 at 85–95 °C for 40–50 min.	(Asif et al., 2022)
Bamboo	• 2.5 mole/l HCl acid at 85 °C.	(Rasheed et al., 2020)
Saccharum spontaneum (Kans grass)	• 5% H_2SO_4 acid concentration at 50 °C for 120 min in 1:15 pulp-solution ratio.	(Baruah et al., 2020)
Jute	• 375 mL of 2.0 N H_2SO_4 acid at 100 °C for 120 minute.	(Jahan et al., 2011)
Washingtonia Fiber	• 2.5 N HCl acid solution for 30 min at 80 °C.	(Azum et al., 2021)
Olive fiber	• 2.5 M of HCl acid for 30 min at 80 °C with 1:30 (g/ml) fiber to liquor ratio	(L. Kian et al., 2020)
Rice and bean hull pulps	• 2N hydrochloric acid/sulfuric acid for 45 minute at the liquor ratio of 1:10.	(Adel et al., 2011)

2.8 Polylactide Acid

Polylactide acid is a bio-degradable and eco-friendly polymer made up of lactic acid (LA), a linear aliphatic thermoplastic polyester and by-products from by-products such as starch extracted from corn grain, potatoes, sugar cane, etc., and renewable agricultural products (Shekar et al., 2018; Zwawi, 2021). Its degradation mainly caused due to cleavage of ester linkage in the monomers due to environmental factors. LA occurs in two arrangements as a result of asymmetric carbon atom in its molecule, L-LA and D-LA, as shown in Figure 5. These two arrangements have

identical chemical and physical properties in their pure forms, and are mirror images of each other. The differences between them are the plane-p, the plane-polarized light direction of rotation that is produced by a chemical is indicated by the sign of (+) and (−) (Jem et al., 2020).

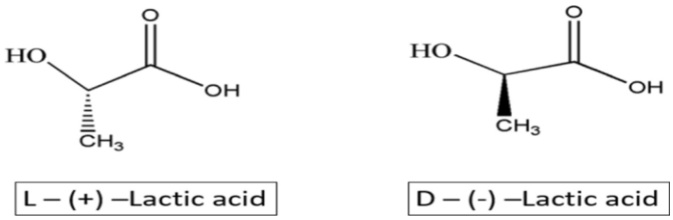

Figure 5: Enantiomeric forms of lactic acid (Casalini et al., 2019)

The PLA synthesizing methods are basically three, i.e., direct condensation of lactic acid monomers, formation of lactic acid through microbial fermentation and ring-opening polymerization. In the first, caused by the fact that the water molecule is produced in each step, there take place certain problems of eliminating water, which restricts the polymer molecular weight. The second method has more benefits such as utilization of organic waste and renewable resources apart from reduced energy consumption during the manufacturing processes, and cost of processing. In the last method which is more widely used, high PLA molecular weight is gained by the use of selected metal catalysts like tin octoate in the melt, which consequently causes the racemization of PLA (Rawoof et al., 2021).

The chains of polymers being produced by two types of lactic acid, namely L- and D- lactic acid. Depending on PLA stereo isomerism, it can be semi-crystalline or amorphous. The three types of stereo forms of poly have been produced, i.e., poly (L-lactic acid) designated as PLLA, poly (D-lactic acid), designated as PDLA and poly (D-, L-lactic acid) designated as PDLLA. Poly (D-, L-lactic acid) is also called as meso-dilactide, made when L- and D- lactic acid are combined. The most widely used type of PLA with mass fabrication is PLLA, and the second one PDLA has also certain use. The L-lactide would yield semicrystalline polymer (PLLA), while poly (DL-lactide) (PDLLA) produce an amorphous polymer (Taib et al., 2023).

Many properties of PLA such as mechanical, thermal and etc. would be adjusted based on the ratio and distribution of L- and D-LA in the polymer chains. The PLA derived from L-LA blocks is semicrystalline polymer and its structural uniformity is more. The crystalline areas up to 37% would provide more mechanical strength at high temperatures. An Important characteristic of polymer materials is glass transition temperature (T_g), it identifies the temperature over which

amorphous areas of the PLA would be changed to rubbery/softened from their brittle nature. Semi-crystalline and amorphous PLAs T_g are between 50 and 70 °C (Storz et al., 2013). The poly (L-lactic acid) (PLLA) is transparent, rigid and between 45 and 70 MPa tensile strength polymer. Whereas, the melting point of 170 –180 °C with a T_g of 53 °C and physical blending with poly-D-lactide (PDLA), PLLA's melting and heat deflection temperature can be raised by 40 - 50 °C and 60 - 190 °C, respectively. Additionally, PDLLA has no melting point but has T_g about 55 °C. These properties confirms PDLLA has lesser tensile strength (Pan et al., 2016). Commercial PLA normally uses L-LA grade polymer for production, which contains over 98–99 % L-LA and less than 1–2% of D-LA (G.-Q. Chen et al., 2012).

2.9 PLA Modification Techniques

PLA is considered as a leading candidate thermoplastic polymer that yields different components for structural, packaging, and biocompatibility applications. Currently, different bio-based polymer materials are used for binding natural fiber, among these polymers PLA has the dominant one and its intensively being studied (Debnath et al., 2021). However, it has low performance on mechanical and thermal properties as well as high cost, due to these pose great scientific challenges and limit their large scale applications to outdoor environments (Pongtanayut et al., 2013; G. Wang et al., 2019). Recently, several studies such as plasticization (Greco et al., 2021), copolymerization, blending (Martinez Villadiego et al., 2022), reinforcing with natural fiber (Rajeshkumar, Seshadri, Devnani, et al., 2021), reinforcing with synthetic fiber (K. R. Kumar et al., 2022), Filling with Nano/Micro-sized materials (R. Guo et al., 2019), Reinforcing with hybrid materials (Y. Kim et al., 2020) and combination of these techniques (Behera et al., 2020) are the common techniques used to modify the properties of PLA bio plastic. In addition to these techniques co-polymerization using PVC, ABS, etc. (Puthumana et al., 2020), modifiers such as polyglycerol esters, Talc, etc. and, physical treatments (annealing, aging, drawing, etc.) (Farah et al., 2016) are used to modify the PLA bio plastic.

2.9.1 Plasticizer

Plasticizers are a commonly used material to modify polymers, and considered as the most common plastic material additive. They are a type of non-volatile and low molecular weight organic compounds that improve the process ability and the flexibility of the polymer by decreasing the glass transition temperature. The plasticizing theory is assumed that the low

molecular weight of a plasticizer permits decreasing connecting forces such as Vander Waals forces, hydrogen bonding and etc. between the polymer chains by penetrating the intermolecular places and reducing the intermolecular frictions (Bocqué et al., 2016). The inclusion of these materials on polymers influence the viscosity, density, elastic modulus, hardness, impact resistance, water absorption, crystallization, melting temperatures, permeability and degradation rate (Alhanish et al., 2021). Plasticizers can be differentiated into petro-based or bio-based. Bio-based plasticizers are assumed as ideal green plasticizers and non-toxic, have good miscibility, efficient, low cost, high resistance to leach from polymer. The most common bio-based plasticizers are polyols (glycerol, ethylene glycol, diethylene glycol, tetraethylene glycol and polyethylene glycol, propylene glycol, xylitol, mannitol and sorbitol), monosaccharaides (glucose, fructose, mannose, sucrose), fatty acids, vegetable oils, Ethanolamine, urea, lecithin, waxes, surfactants, and amino acids (Vieira et al., 2011). Sorbitol is a type of carbohydrate called polyol, which are extracted from glucose that occur naturally in many fruits and vegetables with T_g (0), T_m (100^0C) and degradation temperature of around 200^0C (Mathew et al., 2002). The inclusion of a plasticizer to biodegradable composites reduces the composite fragility behavior noticeably (Shahmaleki et al., 2021). The addition of nucleating agent and plasticizers on the PLA as reported by Moser et.al (Moser et al., 2016), the sorbitol is the most effective nucleating agent for the nucleation of PLA 4032D. Further addition of polyethylene glycol as a plasticizer increases crystallization rate. The joint effect of sorbitol and polyethylene glycol in PLA 4032D, can enhance the impact properties by more than 500 % from 21.8 kJ/m² to a value of 131.3 kJ/m² and the heat resistance by about 20 % from 54.0 °C to 65.9 °C. The addition of sorbitol as nucleating agent on the PLA can be greatly improved the crystallization behavior of PLA. The application of 0.7% Sorbitol into PLA matrix, the corresponding crystallization temperature increase to 110℃ which is 16 °C greater than that of neat PLA. Meantime, the estimated crystallinity improved from 25.3 to 51% (H. Liu et al., 2023). The anti-plasticized influence of sorbitol on starch bio composite was up to 27% and Sorbitol plasticized films have provided the starch bio composites with low flexibility and high mechanical properties, while to glycerol plasticized bio composite exhibited increased mechanical properties and reduced flexibility (Adamu et al., 2017). Polyols plasticized starch filled with microcrystalline cellulose showed improved water resistance and mechanical properties whereas sorbitol enhanced the water resistance, stiffness and thermal stability of thermoplastic starch (Rico et al., 2016). The role of sorbitol in PLA has been summarized in Table 4.

Table 4: Sorbitol plasticizer role in plasticized PLA.

Role	Effects in PLA	References
Mechanism	Sorbitol acts by increasing the free volume within the PLA matrix, reducing intermolecular forces and enhancing flexibility.	(Eslami et al., 2023)
Mechanical property	Blends with sorbitol exhibit higher tensile strength and elongation compared to those with glycerol, indicating better ductility.	(Sirbu et al., 2024; Tian et al., 2017)
Thermal property	The addition of sorbitol decreases the glass transition temperature and melting points, improving melt processing capabilities.	(Eslami et al., 2023)
Morphology	Sorbitol plasticized blends show finer morphologies, enhancing the overall structural integrity of the material.	(Hongbo Li et al., 2011)
Bio-degradability	Sorbitol contributes to the biodegradability of PLA blends, making them environmentally friendly options for various applications	(Sirbu et al., 2024)

2.9.2 Polymer Blending

Polymer blends can be defined as the mixture of at least two macromolecular compounds, polymers, or copolymers. There have been numerous researches work conducted to address brittleness problem of PLA by blending. These works mainly focused on the mixing of PLA with elastomers like natural and synthetic rubbers and thermoplastic polyurethane elastomers. Though, these researchers mainly testified that significant improvements were attained in the ductility and toughness values due to blends (Tang et al., 2022). The addition of 50% poly (ε-caprolactone) on the PLA increases a small amount of elongation at break with respect to PLA but strong decrease with respect to thermoplastic starch (PCL) (Carmona et al., 2015). Further, the high impact strong and high elongation at break poly (butylene adipate-co-terephthalate) (PBAT) gains attention to blend with PLA in order to improve its properties. Nofar et al. (Nofar et al., 2017) studied high molecular weight amorphous PLA blend with 25% PBAT made using a twin-screw extruder. They verified that the blend ductility is 265% related to PLA.

2.9.3 Reinforcing Polymers with Natural Fiber

Natural fibers are biodegradable, renewable and environment friendly materials that are available abundantly in nature. Moreover, their properties are comparable with synthetic fiber in specific areas. Several studies are conducted to increase mechanical properties of PLA by strengthening using Natural fibers and called as “bio composite” material, i.e. reinforcing PLA using natural resources like wood (Sachin et al., 2020), coir (Sun et al., 2017), ramie (Debeli et al., 2018), bacterial cellulose nanocrystals (Wardhono et al., 2019), calotropis procera (Yoganandam et al., 2021), sisal (Liang et al., 2021), hemp (Hedthong et al., 2023) and kenaf (Mohamad et al., 2020). It was exposed that these natural fiber reinforced PLA bio composites might have not only improved mechanical properties, additionally enhanced thermal and physical properties of PLA bio plastic. In literature, there are limited number of studies are available on microcrystalline cellulose (MCC) as reinforcement in PLA matrix bio composites. Among them was conducted by (Mathew et al., 2005), (Haafiz et al., 2013) and (Xian et al., 2018), their investigation indicates that the addition of MCC within a certain range improves the mechanical properties of the bio composites, that is, the modulus, the tensile strength and the flexural strength were improved. However, the elongation at break was decreased, which might be due to poor interfacial adhesion between the phases. Further, the inclusion of MCC shows increase in thermal stability of the composites. The effects of MCC addition in PLA has been summarized in Table 5.

Table 5: Effects of MCC inclusion in PLA.

Properties	Effects of MCC	References
Mechanical	Addition of 1% MCC improves tensile strength and Young's modulus due to better crystallinity and chain mobility. Higher MCC content (3% and above) can lead to reduced mechanical properties due to restricted polymer chain movement.	(Krapež Tomec et al., 2024)
	Up to 4% of MCC filler, the tensile strength is improved from 67.3 to 73.01 MPa and young modulus is increased from 206 to 262.9 MPa due to enhanced interfacial adhesion, resulting better load transfer then starts to decline. Up to 6% of MCC, the flexural strength and modulus shows enhanced strength then sharply starts to decline.	(Xian et al., 2018)

Thermal	MCC acts as a nucleating agent, enhancing crystallinity at low concentrations (1% MCC). At higher concentrations, thermal stability may decrease, with degradation temperatures dropping from 354°C (pure PLA) to around 328°C with 10% MCC.	(Mahmoud et al., 2022)
Crystallinity	The presence of MCC increases the crystallinity from about 30.42% (pure PLA) to around 38.47% with optimal MCC content (e.g., 10% from walnut cellulose). Excessive MCC can disrupt crystal formation, leading to decreased crystallinity	(Krapež Tomec et al., 2024; Mahmoud et al., 2022)
Bio-degradability	Incorporation of MCC enhances biodegradability; composites showed weight loss in soil burial tests over 12 months. The best biodegradation properties were observed with specific MCC contents, indicating a balance between mechanical integrity and environmental performance.	(Krapež Tomec et al., 2024; Mahmoud et al., 2022)

Bio composite (also alternatively called as NFRPC) is a material made by using a natural (usually biological) material as reinforcement and the matrix is produced by a polymer from natural or synthetic sources (Manu et al., 2022) (Onyekwere et al., 2021). This composite material has numerous advantages in terms of its eco-friendliness, recyclability, biodegradability, low density, carbon dioxide neutrality (non-toxic); good insulating and acoustic properties; good thermal properties; and non-abrasive (Belkheir et al., 2022; Mohammed et al., 2021; Naik et al., 2021). As a result, it has many industrial applications in the fields of automotive, building, packaging, furniture, and etc. (Bhambure et al., 2021).

Several challenges are induced when natural fibers are incorporated into the polymers, these challenges has to be addressed to improve the performance of bio composites. One of the main challenge of using natural fiber as a filler for polymer is that hydrophilic/polar nature of natural fibers, while polymers used are hydrophobic/nonpolar properties. This produces problem in compounding, which causes in poor performance of the composite (Nechifor et al., 2022). Additionally, this hydrophilic nature of fibers seriously affects absorption of water properties of the composite as fiber content increases water absorption of composite also increased due hydroxyl

groups present in the fibers (Sahu et al., 2022). Additional challenge of reinforcing plastics with natural fibers for composites is their limited thermal stability. They are limited to around 200^{o}C processing temperature, this limited selection of the binding material to a low melting temperature plastics like PE, PP and PS, which are weak in mechanical properties when compared to engineering thermoplastics like acrylonitrile butadiene styrene (ABS), polycarbonate (PC) and polyethylene terephthalate (PET) (Väisänen et al., 2017). Further, various studies have indicates that processability is another challenge of bio composites when the fiber amount go beyond a certain limit (Pickering et al., 2016). This is caused by the accumulation of fibers, which ultimately weakens the characteristics of composites material and leads to for additional problems, such as increased absorption of water. The accumulation of fiber is produced due to the inter-fiber hydrogen bonding caused from the incapability of the polymer matrix to efficiently wet the fibers (Väisänen et al., 2017).

Bio composite applications are currently limited to non-structural and semi-structural applications that not require significant role in supporting the structure of the intended components at all. It support its own weight in addition to bearing light external loads like impacts or soft knocks. The applications of bio composites has been very limited to structural use because of the lack of superior mechanical strength (Chandrasekar et al., 2021; Islam et al., 2022). Both the matrix and reinforcing materials constitute the mechanical performance of the bio composite. The fabrication of bio composites with uniform mechanical performance could be difficult as the structure, due to natural fibers properties fluctuate significantly based on source of the fiber, growth conditions of the fiber and fiber treatments such as mechanical, chemical and biological treatments (Dixit et al., 2017). The key reason for deficiency of mechanical properties of bio composite is due to poor matrix-fiber interaction, which is generated as a result of different chemical properties of the fiber and matrix constituents. The chemical inconsistency or interaction of these materials results in insufficient stress transfer from the matrix to fibers. The phenomenon of stress transfer is additionally complicated by constituent properties of natural fibers, including impurities, orientation, volume fraction, moisture absorption and other characteristics (Väisänen et al., 2017). As a result, the strong interfacial compatibility allows the composite material to carry stress even if several fibers are damaged because the load can be shifted to the complete portion of the fibers. So it is critical to have a good interfacial compatibility between the matrix and fibers to enhance

the mechanical properties of bio composites. The schematic model of interfacial compatibility between polymer and fillers is shown in Figure 7.

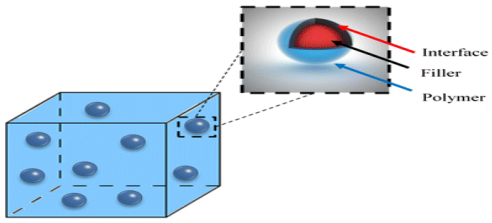

Figure 6: Schematic model of filler interface in a polymer composite (Kashfipour et al., 2018)

In general, the main causes that affecting mechanical properties of bio composites are; fiber type, fiber aspect ratio, fiber content, fiber treatment method, matrix type, interfacial strength, dispersion of fiber, orientation of fiber, additive used, fabrication process and others. These are essential factors that are considered to attain specific engineering properties and applications.

2.9.4 Reinforcing Polymers with Nano-sized materials

Nanomaterials are materials having at least one dimension which is nanometer range (1-100 nm). Nanomaterials have been the most studied material in the last decade because of their wide applications in academic and industrial areas such as automotive, aerospace, electronics, pharmaceutical and biotechnology. Reinforcing plastics with nano-sized materials is named “Polymer Nano composites”. Polymer nano composites have greater physical and mechanical properties than host polymers in part because of the high interfacial region between nano-fillers and polymers. Nano-scale fillers have several sizes and shapes; and they form ultra large interfacial areas when united to polymer resin. Polymer nano composites can be usually categorized into three main types, depending on the dimensions of the dispersed nano-scale fillers (Fu et al., 2019). In the first type, the two dimensional nano-scale fillers for instance layered graphene and silicate in the form of sheets of one to a few nanometer thick and of hundreds to thousands nanometers long are exist in polymeric matrices and it’s called Sheet-like nanoscale fillers. Layered silicates are the common type of this category and follow to the structural family identified as the 2:1 phyllosilicates. Saponite, Hectorite and montmorillonite are the frequently used layered silicates and their structure is presented in Figure 8. The second type of polymer nano composite is the two sizes are in nano-size dimensions and the third is higher. They make longer size single structure, these nano-sized fillers best examples are carbon nanotubes and nanofibers. The third type category is the polymer nano composites having a filler of all its dimensions in nano-sizes, the

typical examples of this category is spherical fillers (quantum dots) and spherical silica (Fu et al., 2019).

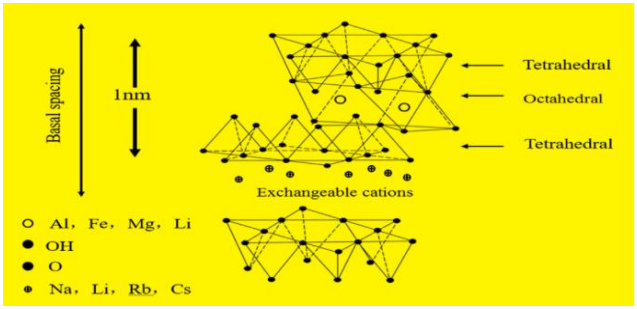

Figure 7: Structure of commonly used 2:1 phyllosilicates (Fu et al., 2019).

Furthermore, the inclusion of nanoparticles in polymer matrix acts as a great tool for advancing the polymer composite properties such as rigidity, strength, barrier, electrical conductivity, and thermal stability. The interfacial adhesion of nanoparticle filled polymers are very high compared to conventional fillers due to large surface energy which permits to have increased chemical interactions with polymer and great surface area to volume ratio. The only reason to get excellent nano composite material is not only restricted to these reasons additionally good dispersion and distribution of nanoparticles in the polymer affects the properties. The main challenge associated to realize intended properties of nano composites. Several researches testifies that polymer nano composite properties were determined by the nanoparticles dispersion degree in the polymer matrix (Idumah et al., 2021).

2.9.5 Reinforcing Polymers with Hybrid Material

Previously, the term hybrid material were limited to specific materials composition like bone, shells, and teeth that are found in nature, these materials usually composed of bio macromolecules and nano scale inorganic ingredients. However, currently hybrid materials definitions given by the International Union of Pure and Applied Chemistry (IUPAC): "A hybrid material consists of an intimate mixture of organic components, inorganic components, or both kinds of component. Usually in IUPAC components are defined on the size of less than 1 μm. A more common exact definition of Hybrid material would be; A hybrid material is composed of as a minimum two components; usually an organic and an inorganic components that are molecularly (nanoscale) dispersed/distributed in the material (Kickelbick, 2014). Based on this description hybrid materials are an exceptional case of composites showing a combination of the dissimilar components on the molecular length scale, a feature that makes them dissimilar from traditional composites where the

components are at the macroscopic size. Therefore, hybridization in the context of inorganic and organic mixture is a synergistic amalgamation of inorganic and organic compounds in one material to attain better properties. Most of the times such material amalgamations were developed, for the reason there was an insufficiency of the required material properties in the traditional setting of materials which could only be filled by merging two absolutely dissimilar single components. These method would made optimal trade-offs between properties (physical, mechanical, thermal), and additional functions such as biocompatibility, permeability, hydrophilic or hydrophobic properties, etc. Stimulated by material performances, an increasing group of studies have involved on organic-inorganic hybrids as the request for exceptionally functionalized and environmentally friendly materials. Scholars generally define organic-inorganic hybrids as the combination of organic and inorganic materials of micro or nano-scale levels (Park et al., 2020). Due to the combined effect of dissimilar constituents, organic-inorganic hybrid materials are estimated to produce different characteristics other than the original characteristics of organic and inorganic components (Nguyen et al., 2015).

In material hybridization, inorganic components can carry out a lot of responsibilities: improve mechanical, chemical, electronic, and thermal properties, while organic components offer unique roles such as guest molecule loading, stimuli responsiveness, and keep stable chemical environment and compensate for the defects of the inorganic phase (Xiaoyang Liu et al., 2021). Hybrid materials can be classified into two classes based on the interface between organic and inorganic components, that is, according to the type of chemical interaction between the parts. Class I category includes materials in which weak interactions such as ionic, van der Waals bonds, hydrogen bonds, and weak electrostatic bonds between organic and inorganic components are seen, and Class II category hybrid materials would be those materials the organic and inorganic parts are interacted together through strong chemical bonds such as covalent, ionic-covalent or coordination bonds (Park et al., 2020). The organic-inorganic hybrid materials development is gain a great attention in numerous applications for their potential to associate the required characteristics of more than one class of materials.

Hybridization, in the context of natural fiber reinforced polymers, commonly mentions to the amalgamation of two natural fibers or in some cases, with one synthetic fibers. The key argument beside fiber hybridization is that closely all of the advantages of natural fibers such as recyclability,

easy handling, biodegradability, processing and etc. are negated by being mixed with synthetic/polymer fibers. Although assumed that, hybridization can be used to lessen cost and weight, and offer some advantage to environmental effects. Current studies have showed hopeful results with hybridization of natural fibers for strengthening. The evaluation effect of hybridization on mechanical performances of banana/sisal hybrid fiber reinforced polyester (Okafor et al., 2021), kenaf and pineapple leaf fiber reinforced high-density polyethylene (HDPE) composites (Pickering et al., 2016), sisal and banana fiber reinforced hybrid epoxy composites (Siva et al., 2021) and abaca/sisal fiber reinforced epoxy resin based hybrid composites (Rajaram et al., 2023) show better performances.

2.9.6 Hybridization of Techniques for Polymer Modification

Modification of polymer material properties usually not only conducted through one method. Additionally, combinations of improvement techniques are used by several researchers, literatures shows that to improve further the limitation of this materials researches comes to blending of PLA with other matrix material then reinforcing with natural fibers (Bhasney et al., 2019; Bhasney et al., 2020), surface improvement of reinforcing material with other agents (Bin et al., 2018; H Li et al., 2016; B. Zhao et al., 2020) and hybridization of reinforcing material with other natural fiber materials (Ramesh, Durga Prasad, et al., 2020; Ramesh et al., 2021; Siakeng et al., 2019). Their investigation indicated that blending of PLA with other matrix material noticeable modifications in various properties of the polyblend composites like mechanical, morphological, and crystallinity were observed. In the technique of surface modification of reinforcing material, the crystallization, mechanical (tensile, modulus, elongation at break) and thermal (heat distortion temperature) properties were increased significantly after modified reinforcing (MCC) material was added. Further, hybridization adding of MTT clay or other material improves the physical (water resistance and biodegradability), mechanical and thermal properties of the bio composite. Finally, the PLA modification techniques are summarized in Table 6.

Table 6: Summary of reported PLA modification techniques

Modifier	Materials	Findings	Reference
Natural fibers	Sisal, jute and elephant grass	- Increases the tensile, flexural and impact strength of PLA noticeably.	(Gunti et al., 2018)

		- The water absorption rate increased in all the composites as the fiber content increased.	
	Wheat straw	- There is no tensile and flexural strength improvement was observed with the addition of wheat straw only due to poor interfacial adhesion. However, when compatibilizer (maleic anhydride-grafted polymers) added on the composite highly improved tensile and flexural strength were shown.	(Nyambo et al., 2011)
	Corn straw	- The tensile strength and elongation at break properties were increased up to 13% and 10%, respectively.	(Ding FangFang, 2018)
	Palm and Kenaf fiber	- The tensile strength was improved at all fiber type loading of 20 - 60%. - At 40% palm fiber addition maximum tensile strength (47.8%) improvement was recorded. Also at 40% alkali treated kenaf fiber loading showed the greatest improvement 54% while only 12.6% was recorded for the untreated kenaf fiber.	(Neoh et al., 2012)
	Bamboo, wood and coconut fibers	- The tensile strength is improved significantly in each fiber composite sample, whether fibers were modified or not. - the tensile strength of PLA first increased and then decreased with increasing the content of fibers from 1 to 8 wt %, and reached the highest when the fiber content was 2 wt %. - The thermal properties was not improved in each fibers addition.	(Q. Zhang et al., 2012)
Plasticizer	Poly (ethylene glycol) (PEG) (0 –20 wt %)	- Tensile strength, strain at break and impact strength increased up to 10 wt% incorporation of PEG and decreases upon higher PEG content.	(Sungsanit et al., 2012)

		- The incorporation of PEG increased the chain mobility and at the same time facilitates crystallization of PLA. - Decreases the glass transition temperature and lowers the stiffness.	
	Epoxidized palm oil and epoxidized soybean oil.	- Each Plasticizer improved the impact strength almost doubled at 15 wt%. - Increases the chain mobility and reduces the temperature of PLA.	(Tee et al., 2014)
	Polyethylene glycol mono-acrylate (PEGA). Content (0-40 wt%).	- The elongation at break was increased - The glass transition temperature, tensile strength and modulus were reduced. - The optimum PEGA content was found to be 20% as achieved higher elongation at break with acceptable strength.	(Choi et al., 2013)
Blending	Poly (ϵ-caprolactone) (PCL)	- Impact strength was increased with acceptable stiffness and modulus was decreased. - Sufficient interfacial adhesion between PLA and PCL was observed.	(Ostafinska et al., 2015)
	Acrylonitrile butadiene styrene, biomax, Polybutyrate adipate co-terephthalate, polyether block amide, ethylene-vinyl acetate and ethylene acrylic elastomer.	- Each blends showed improvement in impact strength and elongation at break. But the highest impact strength was obtained for PLA blended with ethylene acrylic elastomer at 20 phr. - In order to achieve tougher blend, tensile strength and modulus were sacrificed, but still at acceptable values.	(Likittanaprasong et al., 2015)

Synthetic fiber	Carbon black (CB) Content varied (4 -12 wt%).	- Increases the mechanical properties and hydrophobicity of PLA, but an excessive addition of CB reduced the mechanical properties of PLA/CB composites. - Improves the crystallinity and glass transition temperature of PLA. - CB and PLA had no chemical bonding reaction, thus, the oxygen permeability was greatly increased with increase of the CB content.	(J. Guo et al., 2021)
Fillers	Zinc oxide (ZnO) Loading (0-6 wt%)	- Tensile strength and toughness were enhanced at 2 wt% ZnO loading due to high aspect ratio of ZnO powder attribute, allowing good interfacial interaction. - Increases the thermal stability.	(Jayaramudu et al., 2014)
Hybrid technique	Blend: Natural Rubber (NR) Filler: Calcium carbonate (CaCO3) and vetiver grass	- Incorporation of NR into PLA increased the impact strength, especially with the addition of NN-g-GMA as a compatibilizer. - Compared to vetiver fiber, the composite with CaCO3 showed higher impact strength. - The tensile strength and modulus of the composite were lower than neat PLA. However, the elongation at break was higher when NR was added due to the rubbery nature of NR. - The thermal stability of PLA increased when blended with NR, then the addition of CaCO3 reduced the thermal stability of blend because it catalyzed the depolymerization of ester bands of PLA.	(Juntuek et al., 2012)
	Blend: Natural rubber	- Incorporation of NR into PLA reduces the PLA crystallization temperature as it gave the nucleating effect. Similar observation showed for	(Bitinis et al., 2014)

	Filler: organoclay (Cloisite® Na+, 15A, and 30B)	nanocomposites with 3 wt% Cloisite® Na+. However, the addition of Cloisite® 15A and Cloisite® 30B increased the crystallization temperature. - Thermal degradation temperature of PLA/NR blend were improved with the loading of organoclay.	

2.10 Nano Clay

Clay is a material class having layered clay minerals or silicates with traces of organic matter and metal oxides. The classes of clays are classified in terms of their crystal structure and chemical compositions. Based on the ratios of its building block (silica tetrahedron and aluminium (or other) octahedron) natural clay are catagorized into three groups kaolinite (1:1), montmorillonite and vermiculite (2:1) and chlorite (2:2) related with constitutive interchanging layers of "SiO_2" and "AlO_6" units. Montmorillonite (MMT) is frequently used nanoclay because of its availability, environmentally friendly, high aspect ratio, high swelling property in polar spaces and well analysed chemistry (Nazir et al., 2016; Rafiee et al., 2019). The chemical formula of montmorillonite is $(Na, Ca)_{0.33}(Al, Mg)_2(Si_4, O_{10})(OH)_2 \cdot nH_2O$. This indicates that montmorillonite is a hydrated sodium calcium aluminum magnesium silicate hydroxide and it is water content is varied based on the environmental conditions.

The literatures shows that the inclusion of MTT into PLA matrix improves the tensile strength of PLA/MTT bio composites with MTT content up to a certain threshold. For example, at 3 wt% MTT, the tensile strength reached approximately 58 MPa, while elongation at break improved from 4.46% to 10.19% and the maximum decomposition temperature increased from 336.84 °C for pure PLA to 339.08 °C when mixed with 3 wt% MTT. However, increasing MTT content beyond this point also resulted in decreased thermal stability (Huang et al., 2021). In another study, the addition of MTT improves the Young's modulus of PLA bio composites by 54% compared to pure PLA (N. Ibrahim et al., 2019). Furthermore, incorporation of nanoclay into polymers and natural fiber reinforced polymers improves the whole performances (physical, mechanical, thermal, ultra violet, diffusional barrier etc.) of nano composites (Shah et al., 2017b). The mechanical property of polymer matrix composite is greatly enhances due to the interfacial level

interaction among the constituent and better dispersion of nanoclay in the polymer matrix. These insures better load transfer between them and highly uniforms stress distribution for better properties (Rajeshkumar, Seshadri, Ramakrishnan, et al., 2021). For insuring better thermal stability; in combustion, nanoclays move to the surface of the matrix material and to form a compact silicate layer, which fight against the fire as defending layer that slow down the polymer composite for more degradation (Shah et al., 2017a). Previously, conducted research work have been shown to produce good quality bio composites, containing nanoclay is considered as a basic constituent.

In other matrix material inclusion of nanoclay shows improved mechanical performances. For instance the addition into polyester matrix improves the mechanical performace and decreases the shrinkage of the composite material (Rajamani et al., 2022). On the same matrix material incorporation of graded nanoclay improves the tensile strength, modulus with flexural strength (Shuvo et al., 2015). Additionally, the loading of nanoclay, Nanomer I30 E, into epoxy resin enhanced the tensile strength with reduce in strain at failure (Ferreira et al., 2013). The addition of Cloisite 20A, nanoclay enhanced the mechanical properties of vinyl ester composites specifically fracture toughness with insignificant reduction in flexural strength (Bui et al., 2010). Furthermore, it has been verified that the flammability behaviour of polymer composite with charging of 2 % of nanoclay was improved (Alex et al., 2017).

Based on the processing and interaction of the nanoclay and polymers, the principle of nanoclay/polymer composites can be experimentally synthesized through different (four) strategies, such as solution intercalation, in situ intercalative polymerization, melt intercalation and in-situ direct synthesis. Among these strategies solution intercalation was the easiest technique, which consist of an intercalation of polymer from the solution, and includes a continuous process, i.e. the nanoclay are dispersed in the solvent, in which the polymer is soluble and accordingly adsorbed by the nanoclay platelets. Then the nanoclay platelets and the polymer resin are reunited to a structure after the evaporation of the solvent (A. Banerjee et al., 2020; Prevot et al., 2020). The effects of MTT incorporation on the mechanical and thermal properties of PLA material was summarized in Table 7.

Table 7: The effects of MTT filler in the PLA matrix material.

Property	Conclusion	Value	References
Tensile Strength	MTT/PLA nanocomposites showed an increase in tensile strength with MTT content.	45 MPa (PLA) to 60 MPa (5 wt% MTT)	(Arjmandi et al., 2014)
Flexural Strength	Addition of MTT improved flexural modulus and strength.	60 MPa (PLA) to 75 MPa (5 wt% MTT)	(R. Liu et al., 2013)
Impact Strength	MTT addition increased impact strength significantly.	~90% increase 5 wt% MTT with 1 phr CNW	(Arjmandi, Hassan, Eichhorn, et al., 2015)
Maximum Degradation Temperature	The addition of MTT increases the degradation temperature.	336 °C (PLA) to 339 °C with 0.5% MTT addition	(Shar et al., 2021)

2.11 Synthesizing Methods of Bio Composite Materials

Selection of an appropriate synthesizing method for the preparation of bio composites is a significant assignment with the intention of improving the physical, mechanical and thermal performance of the end product. The common and effective synthesizing method of polymer bio composite materials are melt mixing, compression molding, solution casting, injection molding, extrusion, resin transfer molding, etc.

2.11.1 Melt Mixing

Melt mixer is a common polymer mixing tool for the mixing particularly for the production of particle and short fibers reinforced polymer composites. Primarily polymer was heated to its melting temperature and then the reinforcing ingredients were added to the mixing equipment to disperse the reinforcing material into polymer matrix. This method is broadly used in small scale laboratory studies, reinforcing polymers with short fiber and nanoparticles to synthesizing polymer composites because of its good mixing results. But, the main weaknesses of melt-mixing can be used only for mixing and additional processing tools are required to produce the polymer composites. It is well reported in the literature that PLA- Cellulose nanofibrils-epoxidized soybean oil tertiary nanocomposite fabrication method using melt-mixing processing method followed by compression molding. A morphological study with SEM exhibited a good dispersion of Cellulose nanofibrils as confirmed by well-distributed fiber “pull outs” with no visible aggregates (Meng et

al., 2018). Additionally, the lesser mixing (rotor) speed (< 50 rpm) and lesser mixing time (<10 min) cause poor dispersion of the reinforcing constituents through the polymer matrix which leads to a great amount of reinforcing material accumulation in one place of polymer composites and directly affects the mechanical properties of polymer composites. Lesser mixing temperature also causes intense loss of the base and reinforcing material in melt mixing (J. Banerjee et al., 2019).

2.11.2 Solution Casting

Solution casting or sometimes called solvent casting is a polymer nanocomposite synthesizing method in which the polymer is dissolved in solution, the filler material is added and dispersed in dissolved polymer, and then the water or solvent is removed by drying or evaporation to make a composite material. This technique usually used to fabricate polymer films for pharmaceutical, biomedical and food applications. The molds used in this method are made of non-sticky materials such as Teflon that are easily peeled off the films from the mold after drying.

2.11.3 Compression Molding

Compression molding also called hot pressing is a commonly used technique for the processing of polymer composites. The composite material fabrication using compression molding starts by loading a precise amount of mixed fiber-matrix, called the charge, into the bottom half of a heated mold. Then bringing the mold halves together to compress the charge, forcing it to flow and conform to the shape of the cavity. Next heating the charge by means of the hot mold to polymerize and cure the material into a solidified part and finally, opening the mold halves and removing the part from the cavity. This process is effectively used for manufacturing large, thin, strong, stiff, and light weight fiber-reinforced composite materials. In compression molding process, selection of suitable parameters is important in order to yield the optimum composites products. Among the compression molding parameters, molding temperature, pressure, and heating time are the most important parameters that influence the mechanical properties (Jaafar et al., 2019). Composite materials fabricated by using compression molding have comparatively good mechanical properties as compared to other fabrication methods. Table 8 summarizes the PLA based some common bio composite processing methods.

Table 8: Processing method of some popular PLA based bio composite materials

Processing	Fiber	Content %	Reference
Injection molding	Wood flour	30	(Getme et al., 2020)

Extrusion/compression molding	Coconut	0.5	(Getme et al., 2020)
Solvent casting	rice straw	30%	(Saidi et al., 2018)
Blending, mixing followed by compression molding	Starch/cellulose/ carnauba wax	63/24/2.9	(Ranakoti et al., 2022)
Brabender mixer and hot press machine	kenaf	60	(Asaithambi et al., 2014)
Brabender internal mixer and hot press mold	kenaf bast fiber	30	(N. A. Ibrahim et al., 2010)
Melt mixing	Posidonia oceanica	20	(Scaffaro et al., 2018)
Compression molding	Cellulose	20	(Kowalczyk et al., 2011)
Hot pressing	Pineapple leaf	30	(Siakeng et al., 2019)

2.12 Design of Experiments

Experimental design is a well-established statistical methodology that assists to study the relationship between controllable (input) factors and response (output) factors. It's a powerful tool used to; determine the cause and effect knowledge of factors, observe each factors at the same time, conduct experiment at the extent of our factors possible experimental ranges, and makes us to recognize the cooperative effects of factors (Evans, 2022). Designing the experimental design considers basically different procedures mainly follows these steps; defining the research question, defining the factors and its levels, forming the hypothesis, selecting the design type, conducting the experiment and recording the observations (Panke, 2018).

Factors are the variables that affects the response during the experiment and its levels are the values of that factor in the experimental study. Factor and its levels are important inputs into the experimental studies. Their selection has no particular exact method to choose factors and its levels. The selection criteria mainly considers the objectives of the study, scope of the study, earlier procedure knowledge, available resource and constraints/limitations. Before selection these questions should be answered in order to focus relevant factors and levels that can help to achieve the defined objectives; problems should be addressed, response to be measured and improved, and available constraints are defined (Czitrom, 2003; Jankovic et al., 2021). For composite material synthesis and development factors to be considered for experimentation are constituent material and additive properties, as well as processing parameters that are highly affects the performances (mechanical, thermal and physical properties) of the material. However, in factor level selection

the range and behavior of the material to be effectively work without compromising its performance. Understanding the thermal behaviors of constituent materials such as glass transition temperature, T_g and melting temperature, T_m of the matrix material, in addition to the thermal stability of the reinforcement materials. These factors offer a suggestion of the temperature range the composite can resist without substantial degradation or loss of mechanical properties. Additionally, the temperature range should align with the application of material, fabrication process used to prepare the samples and guidelines provided by the material supplier. Polymer composite processing is usually done above glass transition temperature of matrix material. The exact processing temperature may differ based on factors such as processing method, the existence of other additives and etc. (Ghadi et al., 2017).

The design of experiment quality tool approaches are used in many engineering and material development process solving problems. These tool can be used for investigating significant factors in the process, effects of each factor in the outcome, modelling the process, the variance in the process and screening the process parameters. Among DOE tools Taguchi technique has been successfully implemented by numerous researchers in various studies related to composite material synthesizing and development (Antony, 2023). Taguchi technique meaningfully reduces the number of experiments that are required to model the response function. A key advantage of this technique is to investigate the possible interaction between the various parameters with reduced experimental run (Gao et al., 2022).

2.13 Optimization Technique

Optimization is important method used to determine the set of design parameters that will give the optimal (minimum or maximum) solution for a problem. Optimization problems are basically solved by conventional and non-conventional optimization techniques (Kurda et al., 2019). Conventional method is statistical design of experiment which includes Taguchi technique and response surface methodology. These methods were used for optimization of single performance characteristics. Non-conventional optimization techniques were used for optimization of multi-response characteristics. Currently, for many engineering and other design problems numerous multi- response optimization techniques are implemented by various researchers, such as Grey relational analysis (Kopparthi et al., 2021; Onyekwere et al., 2021), principal component method (Zadorozhnyy et al., 2022) and genetic algorithm (A. Kumar et al., 2022) and etc. Taguchi based

GRA is applied for decision-making in multi-response problems and it stands for uncertain, incomplete or improper. It defines situations with no information as black and those with perfect information as white. One of the advantages of GRA is that from several factors with inadequate data, quantitative and qualitative relationship can be obtained. It analyzes the interrelationships between the multiple responses. The performance characteristics were combined into a single value (Grey relational grade) that was treated as a single characteristic in gray relational optimization. It measures the degree of relationship between sequences through it. Grey relational analysis has been applied by several researchers to optimize the control parameters having multi-responses through grey relational grade (Chanda et al., 2015). It's mainly significant to several design problems, particularly complicated problems. For example, in a composite material design, there is need to determine the percentage content of each constituent, to achieve the best properties of the composite. In numerous studies, Taguchi based GRA method is used due to its ability to find the best and worst alternative from the given set of data.

2.14 Application of Bio Composite

Applications of bio composite materials are increased from time to time in various areas. The suitable properties of bio composite has shown high attention in infrastructural and structural uses where less cost, eco-friendly and moderate strength characteristics are sought. Currently, applications of bio composite has been made for various areas such as automotive, building and construction, furniture, socket prosthesis, packaging, storage device, electronics and etc. (Bharath et al., 2016). In automotive industries numerous bio composite materials are used for various components such as seat back rests, bumpers, luggage shelves, door inner trim panels, inner section of the front door linings, rear trunk covers, rear panel shelves, side trims, door scuff plates, tool box area, floor finishing plate, and package trays and others, for these components bio composites has been showing outstanding performance (Akampumuza et al., 2017; Alam et al., 2021).

Bumper is a guard made of aluminium, steel, rubber, or plastic that is attached to the front and rear of a car. The bumper system absorbs the shock to prevent or reduce damage to the car when a low speed collision occurs (Begum et al., 2020). In the existing bumper (conventional bumper, steel) the weight is more (Prabhakaran et al., 2012). In the present trends, weight reduction has been the main focus of automobile manufacturers and the requirement of the bumper material are absorb more energy while collision, has good rust resistance, has high strength, is light in weight, easy to

manufacture in large quantity and low cost. Recently numerous materials like composites experiment in almost all parts of automobiles and it has also been attempted into the bumper. Due to weight reduction, collision energy absorption, corrosion resistance, and impact strength, composite materials are preferred over conventional steel bumpers. Findings of composite material research work conducted to replace existing bumper materials for the application of automotive bumper over the last decade are presented as follows;

Q. Liu et al., 2014, conducted study on the crushing performances of carbon fibre reinforced plastic structures that are commonly led by delamination of inter-ply, growth of fracture, and micro-cracking broadening, which can be tailored over structural and material characteristics, such as orientation of fibre, stacking layers number, and each layers property. Carbon fibre reinforced plastic directed to outstanding merits in absorption of specific energy on such particular crushing response and lightweight characteristics. Additionally, carbon fibre reinforced plastic has higher strength and lower density compared to glass fibre reinforced plastic, and as a result carbon fibre reinforced plastic bumper has improved characteristics in crashworthiness and lightweight (Q. Liu et al., 2014).

Jalauddin et al., 2012, examined crashworthiness of three dissimilar bumper beams which made of carbon fiber reinforced polymer, aluminium AA5182 and glass fiber reinforced polymer through applying finite element method. They indicated that the carbon fiber reinforced polymer bumper has noticeable merits than others in absorption of energy and lightweight (Jalauddin et al., 2012). In addition study conducted by D.-H. Kim et al., 2012, bumper made of glass/carbon mat thermoplastic to design optimal bumper beam. They investigated that the optimized glass/carbon mat thermoplastic bumper beam design had 33% reduced amount of weight and enhanced performance of impact strength compared to the conventional GMT bumper (D.-H. Kim et al., 2015).

Belingardi et al., 2015, suggested design analysis and characteristics of GFRP for the application of front bumper systems. They verified that the design of the combined crash box and bumper beam has enhanced crashworthiness physical characteristics, and it can also lessen the assembly price successfully. Additionally they optimize section profile and curvature of the bumper beam for crashworthiness by applying finite element method, and they showed that the optimized bumper beam presented the better capacity of energy absorption (Belingardi et al., 2015).

According to Selwyn, 2021, study Aramid fiber layers with various interior angles are joined to produce a composite plate to increase the mechanical properties of the aramid composite. His result shows that the aramid composite has a high flexural strength of 86.8 MPa and high tensile strength of 147 MPa, these result verified that the bumper made of aramid material is exceptionally suitable for automobiles (Selwyn, 2021). Additionally, Achema et al., 2017, studied glass fibre reinforced composite material mechanical properties for lightweight car bumper system applications using E-glass bi-directional laminate and epoxy resin. The test result shows that the tensile strength of 3852.8 kJ, impact strength of 100 kJ/m2 and satisfactory flexural strength above a load of 0.5 KN. Further, a 60% weight reduction was examined when compared to steel car bumper system (Achema et al., 2017).

Onyedum et al., 2015, conducted their research on okra fibre and banana fibre comparative analysis of mechanical properties for application of automotive car bumper. Vinyl ester resin is used as a matrix material to bind okra and banana. Hand layup production technique were implemented to produce the composite in the mould. The weights percentage of fibre used for this study were 10 wt%, 30 wt% and 50 wt% and the length of fibre considered for this work is 10 mm, 30 mm and 50 mm. They result showed that the optimum tensile strength value was found for percentage: length composition is (30 %:10 mm) for okra and (30 %:50 mm) for banana fibre. The NaOH treatment process was used to remove the moisture content of the fibre and also to improve the tensile strength (Onyedum et al., 2015).

Adesina et al., 2019, conducted their work on the effects and analysis of natural fibre polymer composite plates produced from sisal fiber used for passenger car bumper. The production technique of the composite plate of sisal fiber mat reinforced with epoxy and polyester resin were made through hand lay-up method. The mechanical (tensile, flexural and impact) properties were tested over these sisal reinforced composite plates in order to propose its possibility to replace the conventional steel bumper. They result indicates that a 35.69% reduction of weight was realized with sisal fibre reinforced polymer composite compared to conventional steel bumper without compromising the mechanical performance, impacts of bumper beam and also it has a cost advantage (Adesina et al., 2019).

Hasanzadeh et al., 2017, carried out the effect of carbon Nano-tube reinforced polymeric Nano composite material selection for the automotive bumper beam. In their experimental setup six

samples of polymeric material were fabricated via injection moulding in order to investigate mechanical properties (tensile and impact) and cost. Three polyamide-6 Nano composites foam samples blended with weight percentage of multi walled carbon nanotube 0.5, 1.0 and 1.5, and weight percentage of three polycarbonate samples Nano composite blended with Nano alumina 0.5, 1.0 and 1.5. Based on their investigation 0.5 weight percentage polycarbonate with multi-walled carbon nanotube composite has greater tensile and impact strength with reduced cost. So, it was proposed as a proper nano material for the application of bumper beam (Hasanzadeh et al., 2017). Table 9 exhibits the general bio composite material used for selected automotive components.

Table 9: Bio composite material for selected automotive components (Hill et al., 2012).

Model	Fiber	Matrix	Application
Ford Fiesta	Kenaf	Polyurethane	Interior door panel
Mercedes Benz C class	Flax	Polyethylene	Engine and transmission cover, underbody panels
Mercedes Benz A class	Abaca/banana, flax	Polyethylene	Underbody panels, seatbacks, cover for spare tire
GMC Terrain	Cotton, kenaf	Polyester	Acoustic insulator, ceiling liner Trim, rear shelf
Ford Focus BEV	Coconut	Polypropylene	Luggage-compartment speakers
Mazda 5 hydrogen	Corn	Polylactic acid	Console, seat fabric
Mercedes-Benz S-Class	Hemp, flax, sisal, coconut	N/A	Interior components
Toyota Lexus ES300	Kenaf	Polylactic acid	Package shelves

2.15 Literature Gap

From the referred literature review, it could be realized that there are important research investigations in coffee industries residues potentials to reinforce polymers and be used to extract various components. Subsequently, PLA based polymer composites were promised for various applications such as packaging, film, medical, and more. The properties of PLA were also modified using different modification techniques including by compromising its biodegradability for numerous applications. However, the availability of literatures for tuning the properties of PLA such as mechanical and thermal properties for structural and automotive part application is limited. In addition the extraction of MCC from coffee husk and the amalgamation of MCC and MTT filled sorbitol plasticized PLA bio composite was not reported yet. In this study, the MCC and MTT

filled and sorbitol plasticized PLA bio composite is synthesized for structural application and the effects of each parameters on the mechanical and thermal properties is endeavored.

CHAPTER 3

MATERIALS AND METHODS

3.1 Materials

White PLA Powder reagent grade was utilized as the matrix material, and sorbitol powder Technical grade was used as plasticizer, both of them were purchased from Aritech Chemazone Pvt Ltd, Haryana, India. Coffee husk fiber were collected from bale zone Dello Menna, the southern part of Ethiopia in the form of short fiber, in 2022 and the other reinforcing material, known as Montmorillonite Nanoclay, Reagent Grade was purchased from Nanochemazone Private Limited, Alberta, Canada and their information are tabulated in Table 10. Reagents used to isolate cellulose and extract MCC from the outer skin (exocarp) separated coffee husk were toluene, ethanol, sodium hydroxide, hydrogen peroxide, and sulfuric acid. All reagents were purchased from Techno tech, Addis Ababa, Ethiopia, and were used without further purification.

Table 10: Important information of commercialized material

Material	**Grade**	**Density** (g/cm^3)	**T_g (^oC)**	**T_m (^oC)**	**APS**	**Appearance**	**Purity (%)**
PLA	Reagent	1.25	75	175	1-5 um	Powder	99.9
MTT	Reagent	1.77	-	-	<80nm	Powder	99.9
Sorbitol	Technical	2.16	-	-	1-5 um	Powder	≥ 99

3.2 Research Methodology

The methodological design employed for this study was integrating both exploratory and experimental methodologies. This makes a systematic determination of outer skin isolated coffee husk chemical composition and extraction of MCC from it for strengthening PLA with MTT, combining qualitative approach with quantitative approach. Exploratory methodology were carried out to initially understand the chemical composition, possibility of MCC extraction from outer skin isolated coffee husk, assess the possible extraction techniques of MCC from agricultural wastes, assess interaction between fillers and matrix material and PLA modification techniques. Whereas, experimental methodology were conducted to quantify each chemical composition of outer skin isolated coffee husk, the effects of each chemical treatments on fiber, and effects of different weight percentage concentrations of fillers and plasticizer on the bio composite material properties. The mixed approach of the methodology, quantitative data was collected through

measurement, analytical analysis, and physical and mechanical testing of synthesized MCC/MTT/S/PLA bio composite, while qualitative insights are gathered through literature review and qualitative assessments of previous studies related to PLA bio composites.

3.3 Sample Size and Sampling Techniques

The sample size of coffee husk collected for this study was 1 sample approximately 5 kg from Bale zone, Dello Menna woreda, through composite bulk sampling technique from local dry coffee processing industries. This technique is easy, cost effective and effective for relatively uniform population. The sample size utilized for the chemical composition analysis of outer skin isolated coffee husk was 1 sample which weight 200 g and the technique employed was stratified convenience with sub sampling technique. This size was taken based on the literature, being controllable in laboratory situations and also sufficient material was collected for further measuring and characterizations and the technique represents, typical chemical untreated and treated groups. The sample size employed for bio composite sample preparation is 4 sample at varied weight percentage of fillers and plasticizer using snowball purposive sampling technique. Then, the sample size utilized for testing mechanical and physical properties of synthesized bio composite was 16 samples for each testing and randomization sampling technique was utilized by Taguchi's experimental setup for ensuring unbiased results. Further, for the validation of optimal sample 1 sample size was taken for each test and validate purposive sampling technique was employed. Finally, for study structural variation analysis of optimal sample for neat sample 2 sample size was taken using validate purposive sampling technique.

3.4 Data Collection Procedures

Data collection procedures employed for this study were include several key procedures such as fiber preparation, sequential chemical treatments, extraction procedures, bio composite sample preparations, structural, thermal and morphological analysis of untreated and chemical treated samples of fibers, physical measurement of extracted MCC, physical and mechanical testing of synthesized bio composite samples, neat PLA and the most optimal samples structural analysis, thermal analysis, morphological analysis, and physical and mechanical testing.

3.4.1 Preparation of Fiber: From the collected coffee husk fiber part, the pulp and parchment were separated from the outer skin (exocarp) via strip (manually) because of pectin and lignin

made up the majority of exocarp (Rodiah et al., 2019). The coffee husk (pulp and parchment) isolated from the outer skin were washed away with distilled water and dried up in an oven at 70^{o}C for 2 days, then cooled in a desiccator for 30 minutes to prevent moisture absorption of the fiber . Finally, it was crushed with a grinding machine and put through a sieve using a sieve dimension of 2 mm. Figure 8 confirms the collected coffee husk, outer skin isolated coffee husk and sieved outer skin isolated coffee husk.

Figure 8: a) waste coffee husk, b) outer skin (peel) isolated coffee husk (pulp and parchment), c) ground outer skin isolated coffee husk

3.4.2 Chemical Composition Analysis: The chemical composition investigation of the lignocellulosic components present in the outer skin isolated coffee husk fibers was carried out in three steps, which follow the conventional methods of the Technical Association of Pulp and Paper Industry (TAPPI) and standards which involves an analytical approach (gravimetric method) to find extractive, hemicellulose, lignin, ash and cellulose contents. For a piece of sample, three replicates were conducted to determine the average value. This step was then followed by micro crystalline cellulose extraction process for obtaining higher yield value.

Step 1: - The extractive content was investigated through the TAPPI standard technique (T-264 om-82) (Reis et al., 2020). In a Soxhlet extraction (Fig. 9 (a)), about 20g of dry outer skin isolated coffee husk was added to a beaker filled with 750 mL of the solution combination (1:1, ethanol: toluene). The extract was collected and placed in an oven at 110 ^{0}C with the aim of drying up for precede weighing. This extractive-free dried coffee husk was considered as a base for the subsequent processes. The yield of extractive was determined by the expression (1) mentioned below.

$$\% \text{ of Extractives} = \frac{W_i - W_f}{W_i} \times 100 \quad (1)$$

Where; W_i - is the weight (gm) of oven-dried sample before extraction and W_f - is the weight (gm) of the oven-dried sample after soxhlet.

Step 2: - The content of the lignin sample was calculated by putting in the residue in a sulfuric acid solvent of 72% as per TAPPI approach (T-222 om-83) methodology (Alotaibi et al., 2019) (see Fig. 9 (b)). About 3 gram weighed extractive free sample was immersed in a beaker, to the 51 mL of sulfuric acid (72%) solvent was placed, rigorously stirred in electromagnetic stirrer at room temperature for 8 hours. Then this hydrolyzed sample was washed away using distilled water up to the PH become neutral and dehydrated in an oven for 3 hours at 105^0C. The lignin content was determined by expression (2) mentioned below.

$$\% \text{ of Lignin} = \frac{W_i - W_L}{W_i} \text{ x } 100 \quad (2)$$

Where w_i is the weight of oven-dried sample before extraction and w_L is the weight of oven-dried sample after extraction.

Step 3: - The content of hemicellulose was studied according to the technique broadly mentioned in the literature (Geng et al., 2019). Extraction process was carried out using 4gm extractive free and dehydrated sample were placed in a 200 mL boiling flask at a ratio of 20/1 (liquid/solids) by the use of 10% NaOH solvent for 24 h at room temperature with stirring (Fig. 9 (c)). The extracted samples were washed away by distilled water until the pH was neutral and dried up in an oven for 3h at 110 ◦C. The yield of the extracted hemicellulose was determined by the expression (3) mentioned below.

$$\% \text{ of Hemicellulose} = \frac{W_i - W_b}{W_i} \text{ x } 100 \quad (3)$$

Where w_i is the weight of the oven-dried sample before extraction and w_b is the weight of the oven-dried sample after extraction.

Step 4:- Ashing or the content of ash was determined according to Dawit (Dawit et al., 2020), furnace dried empty crucible weight was measured and crucible having 3 gram of sample was placed in furnace for 5 hours at 600 °C and cooled by silica gel at room temperature and weighed (Fig. 9 (d)). The cooling and heating process was continued up to the difference of the two consecutive weights becomes insignificant. Finally, the content of ash is determined by the equation (4).

$$Ash \text{ content } (\%) = \frac{Final\ weight\ of\ the\ sample}{Initial\ weight\ of\ the\ sample} x\ 100 \quad (4)$$

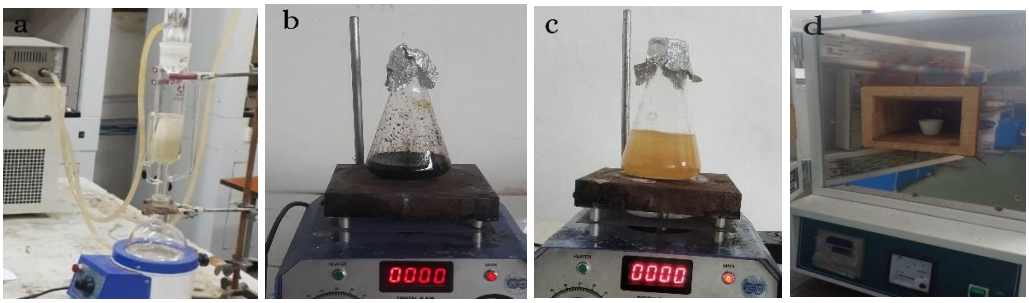

Figure 9: (a) Soxhleting, (b) Acid hydrolysis, (c) Alkalization, (d) Ashing

Then, the cellulose percentage was calculated according to equation (5) and the chemical composition analysis schematic diagram has been illustrated in Figure 10.

$$\% \text{ Cellulose} = 100 - (\% \text{ extractive} + \% \text{ hemicellulose} + \% \text{ lignin} + \% \text{ ash}) \quad (5)$$

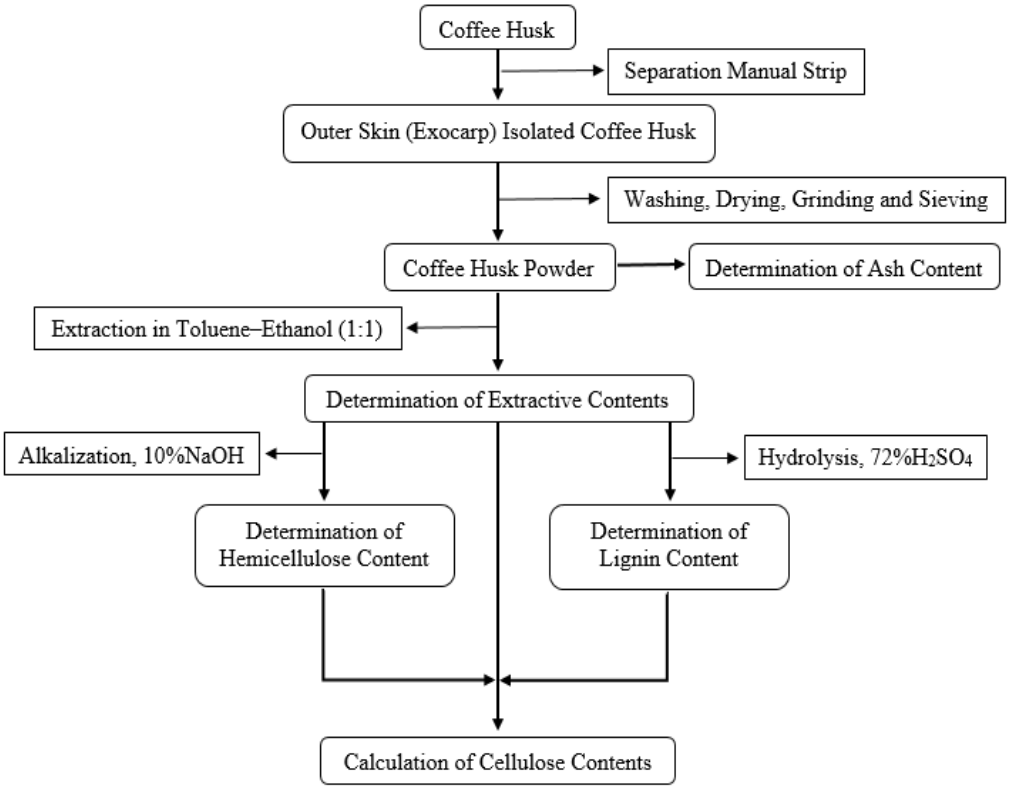

Figure 10: Schematic diagram of chemical composition analysis

3.4.3 Micro Crystalline Cellulose Extraction and Yield: The extraction and yield of micro crystalline cellulose was carried out using fully chlorine free extraction procedure, which was proposed according to the method reported by khenblouche (Khenblouche et al., 2019) with the addition of one bleaching cycle (hydrolysis). This method eliminates the traditional method uses a chlorine containing chemical such as sodium hypochlorite which is easily available and low cost. But following extraction, purifying the waste liquid can be challenging and lead to significant

environmental contamination. Thus, the method overcomes the environmental impacts (Shi et al., 2021). The process is chemical treatment with execution in de-waxing (removal of extractives), alkalization, and bleaching treatment procedures.

De-waxing: was carried out to remove tannins, sugars, fatty acids, wax, and extractives from powder material (outer skin separated coffee husk) using toluene-ethanol (2:1, v/v) in a Soxhlet setup at 65^0C for 8 hours as per TAPPI standard (T264 om-97) (see Fig. 12 (a)). After de-waxing, the sample was dried in an oven at 50^0C for 2 days and then cooled in a desiccator to take away traces of residual reagents and moisture absorption.

Alkali treatment: was performed for an extractive free (de-waxed) sample to remove hemicellulose and insignificant amount of lignin. It was done at 70 °C for 4 hours with electromagnetic stirring using a 7 wt% NaOH with an extractive free sample to solvent ratio of 1:10 (Fig. 12 (b)). This action was conducted twice, after a piece of action, the sample was filtered and washed away with distilled water till the pH became neutral. Finally, the sample was dried at 80 ^{0}C for 24 hours in an oven.

Bleaching: for removal of lignin and remaining amount of hemicelluloses and extracting MCC was carried out with the de-waxed and alkali-treated sample placed in hydrogen peroxide (H_2O_2) solvent (11%, v/v), the pH was tuned to 11 by 8 wt% NaOH. The solution was forcefully agitated constantly for 4 hours at 50 °C temperature and a 1:25 sample to a solvent ratio (Fig. 12 (c)). Further Purified cellulose was bleached for the second time or hydrolyzed with H_2SO_4 (7 wt%) solvent for 3 h at room temperature under stirring with 1:20 fiber to liquid ratio (g/mL) (Fig. 12 (d)) as reported by Baruah (Baruah et al., 2020), this process break downs the β(1→4) glycoside bond of cellulose. Thus, decreases the DP of the resulting MCC. The micro crystalline cellulose sample obtained from this process was filtered and washed away with distilled water till pH reach neutral (Fig. 12 (e)). The treatment of each process is carried out twice in the same settings and weighed for taking the sample yield. The outer skin isolated CH, MCC extraction process has been illustrated in Figure 11.

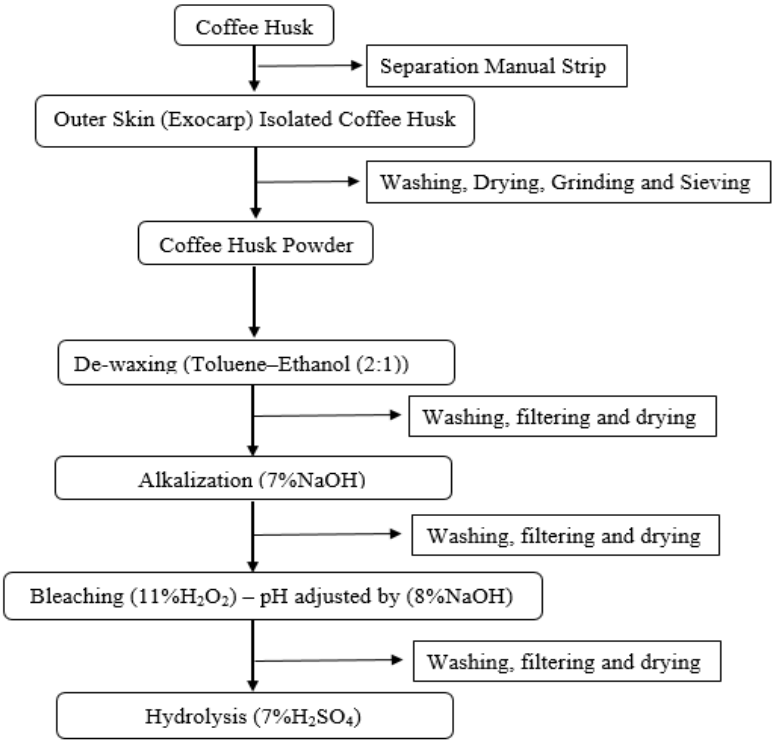

Figure 11: Schematic diagram of MCC extraction from outer skin isolated coffee husk

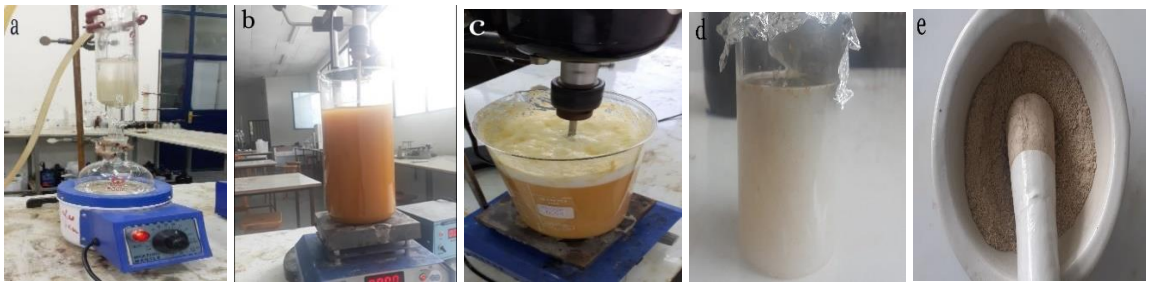

Figure 12: (a) De-waxing, (b) Alkalization, (c) Bleaching, (d) Hydrolysis, (e) MCC

Yield Determination of MCC: The percentage yield of the samples was calculated using equation (6).

$$\text{Yield (\%)} = \frac{\text{weights of the sample before treatment}}{\text{weight of the sample after treatment}} \text{ x } 100 \qquad (6)$$

3.4.4 Preparation of MCC/MTT/S/PLA Bio Composites Samples: All samples of MCC/MMT/S/PLA bio composite were fabricated using melt-mixing method followed by hot pressing technique as shown in Figure 14(a-e). Initially, the designated weight percentage of PLA and sorbitol were mixed and heated at required temperature on heating plate. Then pre calculated amount of MCC and MMT were added on the heated blend of PLA and sorbitol, and stirred

properly to make uniform distributions of reinforcing agent. After that the molten MCC/MTT/S/PLA material was poured into a mild steel mold of 100x50x4mm and continuously pressed at 2 MPa for 24 hrs to allow it to solidify and form desired mold shape. In order to simplify the removal of the sample from the mold and protecting sticking of material on the mold, aluminum foil was used inside the mold. Moreover, the solidified MCC/MTT/S/PLA material cut into the specimens using hacksaw according to ASTM standards and sanded using sand paper. Finally, the post curing of specimens were carried out at 40 °C temperature in an oven for 3 hours to remove existence of moisture that may affect the final results.

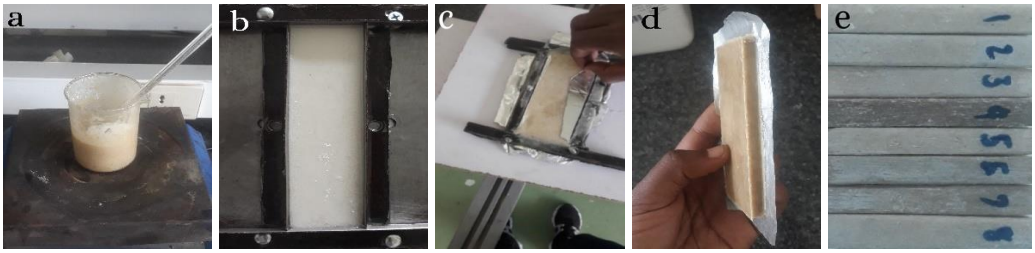

Figure 13: (a) Melt-mixing, (b) Mold pouring, (c) Mold removal, (d) Curing and (e) Samples

3.4.5 Experimental Characterization, Measuring and Testing Methods

Fourier Transform IR-Spectroscopy Analysis: Infrared spectroscopy investigation was carried out to obtain the existence of chemical variations which occurred in the intended (UT, DW, AT and BL) samples. Additionally, conducted to find the existence of chemical variations occurred between neat PLA and optimal sample due to the additions of plasticizer and fillers in neat PLA. For each investigation one sample with 0.25 gm were used in both cases. The peaks were obtained with Jasco FT/IR-6600typeA analyzer (Easton, Maryland, USA), at scanning speed of 2 mm/sec in the range of 400-4000 cm^{-1} (standard) and 4 cm^{-1} resolution.

X-Ray diffraction (XRD): The XRD pattern of untreated, chemically treated, neat PLA and optimal samples were recorded using MAXima_X XRD-7000 X-Ray Diffractometer (Japan) with Cu Kα radiation. For each investigations one sample with 0.25gm was used. The x-ray was operated at 30 mA and 40 kV with a scan rate of 3^0 min^{-1} and in the range of 5^0 – 60^0. The crystallinity index (CI) was investigated by the XRD amorphous subtraction method developed by Ruland for the first time and states that, the ratio of the sum of areas under the peaks of the crystalline component (I_{cry}) to the overall area under all peaks (I_{tot}) as shown equation (7) and the crystallite size was calculated by using Scherrer equation, equation (8) (Thygesen et al., 2005).

$$\text{Crystalline index (\%)} = \frac{I_{cry}}{I_{tot}} \text{ x } 100 \quad (7)$$

$$\text{Crystallite size (D)} = \frac{k\lambda}{\beta\cos(\theta)} \quad (8)$$

Where; λ is the radiation wavelength (1.54 Å), 2θ is the diffraction angle, β is the peak width at half maximum intensity in radian, k = 0.94, is a dimensionless shape factor.

Morphological characterization: The surface morphology of untreated CH fiber, chemical treated samples (DW and AT) and CH derived MCC, and fracture surfaces of neat PLA and optimized bio composite samples were examined using JOEL scanning electron microscope, JCM-6000 plus model (JOEL Ltd., Tokyo, Japan) operating under 10 KV accelerating voltage and ZEISS EVO 50 scanning electron microscope. The surface morphology of the neat PLA and synthesized bio composite was examined through Huvitz HRM – 300 series optical microscope (Huvitz Co., Ltd, Anyang-si, South Korea). For each examinations, one 0.25 gm sample was prepared.

Thermal Stability Analysis (TGA/DTA): The thermal endurances of the untreated, chemical treated, neat PLA and optimized samples were carried out using BJHENVEN simultaneous TGA – DTA/DSC instrument, HCT-3 model, Beijing, China. For analysis, the samples were heated between 0 to 600 °C under a nitrogen atmosphere at 10 °C/min. For each analysis, one 0.25 gm sample was used.

Determination of average molecular weight and degree of polymerization: The average degree of polymerization, DP of extracted MCC was determined by viscometry method at 25^0C in 6 wt% NaOH/4wt% Urea solvent using Ostwald viscometer (Xiong et al., 2012; Zhou et al., 2021). The flow time was recorded and relative viscosity, η_r was determined based on recorded flow time (ratios of time flow of extracted MCC solution and NaOH/ Urea solvent). Then intrinsic viscosity, η was determined according to the equation (9) in cm^3g^{-1}. The result shows an average of three measurements (Fig. 13 (a)).

$$\log\left[\frac{\eta_r - 1}{C}\right] = \log[\eta] + 0.13[\eta]C \quad (9)$$

Where, C is solution concentration of the sample in gmL^{-1}

Average degree of polymerization then determined from the equation (10).

$$DP^{0.905} = 0.75\ [\eta] \quad (10)$$

True Density of MCC :- The true density was determined by the liquid displacement method by completely immersing the sample in a pycnometer (density bottle) (100 ml) capacity using xylene as the immersion fluid (Haruna et al., 2020). The empty weight of a pycnometer was obtained, filled with xylene, and its weight determined. A sample of the powder weighing 2.5 g was added into the bottle and the excess liquid spilled wiped off. The new weight was determined and the volume of the liquid that was displaced was measured (Fig. 13 (b)) and the density was computed according to equation (11).

$$\rho_T = \frac{\text{Sample weight x Xylene density (0.864)}}{\text{Weight of xylene displaced by sample}} \quad (11)$$

Bulk Density of MCC: - The bulk density was examined by 1.4 grams of cellulose powder were placed into a 10 mL clean and dry measuring cylinder. The volume occupied without tapping was determined (Fig. 13 (c)). This was done in triplicate to ensure data reliability, and the average volume was calculated and recorded. The bulk densities were determined using Equation (12) (Adeleye et al., 2022).

$$\text{Bulk density} = \text{Sample weight} / \text{Bulk volume} \quad (12)$$

Porosity of MCC: The powder porosity was determined from Equation (13) (Adeleye et al., 2022).

$$E = 1 - (D_b / D_t) \times 100 \quad (13)$$

Where; D_b is the bulk density, D_t is the true density, and E is the porosity

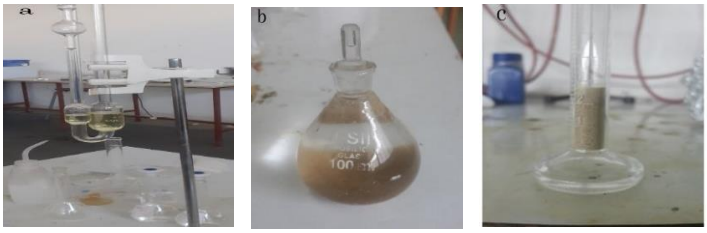

Figure 14: (a) Flow recording using viscometer, (b) True density determination in pycnometer, (c) Bulk density measuring using dry measuring cylinder.

Flexural Testing: the flexural strength of the samples was determined as per American Society for Testing and Materials (ASTM) D790 through three point bend testing method by universal testing machine i.e. Bongshin Model DSCK machine. The 40 mm span length and cross head speed

for test is keep at 5 mm/min. The bio composite samples has dimensions of 55×10×4 mm and three times test is conducted for each samples to obtain the mean value of the flexural strength (Jena et al., 2019; Kelleci et al., 2022). The flexural strength and modulus were determined with equation (14) and (15), respectively;

$$\text{Flexural strength, FS} = \frac{3FL}{2wt^2} \quad \ldots\ldots\ldots\ldots\ldots\ldots\ldots\ldots\ldots\ldots\ldots\ldots \quad (14)$$

$$\text{Flexural modulus, FM} = \frac{L^3F}{4wt^3\delta} \quad \ldots\ldots\ldots\ldots\ldots\ldots\ldots\ldots\ldots\ldots\ldots\ldots \quad (15)$$

Where; F - is the applied load, L - is the length of specimen, w - is width of specimen, t - is the thickness of the specimen and δ - is the deflection.

Tensile Testing: tensile test was performed based on ASTM D638 in order to measure tensile strength of the samples. The samples were cut into 60x6x3mm and then to get smooth surface grounded using sand paper. The investigation was performed by universal testing machine (Model DSCK) with a cross head speed 5mm/min and the test is recorded repeatedly three times for all samples to get the average value of the tensile strength (Ihueze et al.).

Hardness Testing: Hardness is the ability to penetrate the top layer of the specimen. In this study, the hardness test was carried out according to ASTM E384 using a digital display Vickers hardness tester Model HVS – 50 at room temperature and a load of 20 kg.f (0.2 N) using diamond pyramid indentation. The hardness value, HV was determined from the residual projected area of indentation as shown in equation (16).

$$HV = 1.854\,(F/d_2) \quad \ldots\ldots\ldots\ldots\ldots\ldots\ldots\ldots\ldots\ldots\ldots\ldots\ldots\ldots \quad (16)$$

Where; F - is the contact load (kgf) and d - is the length of the imprint crosswise (µm). The test results were recorded for each sample repeatedly for three times and the final results are calculated based on the average value of the three data (Budin et al., 2019).

Impact Testing: the impact tests of each samples were conducted as per ASTM D256 by Charpy impact testing machine method, Model SI42 (Jinan Tianchen Testing Machine Co Ltd., China). The samples dimension 75 mm x 15 mm x 3 mm were placed and subjected to 5.5 J pendulum impact blow and the amount of impact energy absorbed by the samples were display on the calibrated scale fixed to the machine as a measure of impact strength in Joules (Ramasubbu et al., 2022).

Water absorption: the materials water absorption is important study in case of developed materials has been used for determining water uptake in contact with water, this can adversely affect mechanical and aging properties. The investigation was conducted according to ASTM D570-98, sample size of 20x20x3mm to find out the water absorption of specimens (Chandramohan et al., 2017). The bio composite sample were dried in oven for 3hrs at 50 °C before tested, then dipped in water bath contain distilled water for 3 days at room temperature. At fixed time intervals, the samples were moved out from distilled water and cleaned by filter paper to avoid surface water and weighed using digital balance. The weighing was performed within a minute to remove the inaccuracy caused by dehydration. The samples continually were dipped in water bath to allow the extension of absorption up to maximum bound was achieved. Three samples were tested for all experimental setup and their mean outcomes were presented. The water absorption of the specimens was determined as increase in weight % with the equation (17) (Ramasubbu et al., 2022).

$$\text{Increase in weight \%} = (\text{wet weight-dry weight})/\text{dry weight} \times 100 \quad \ldots\ldots\ldots\ldots\ldots (17)$$

Density: the density of developed bio composite specimens were carried out according to ASTMD792-98, sample size of 20x20x3mm. The samples were weighed in a digital balance and their mass recorded. The volumes were determined from their recorded sizes. Then, the density was determined through the equation (18) (Kandasamy et al., 2020).

$$\text{Density} = \text{Mass (g)}/\text{Volume (mm}^3\text{)} \quad \ldots\ldots\ldots\ldots\ldots\ldots\ldots\ldots\ldots\ldots (18)$$

3.4.6 Experimental Design and Plan of Investigation

In the present research investigation, bio-composite material based on Polylactide acid with coffee husk derived MCC and reagent grade MTT filler, and sorbitol plasticizer at different processing parameter of temperature was prepared using a melt mixing setup. The intended amount of MCC and MTT particles were mixed properly to make homogeneous distributions. For preparation of bio composite material, four effective parameters (MCC, MTT, S and T) with four levels for each parameters were used to investigate responses. Temperature is considered as one of the main parameter that affect the process in addition to fillers and plasticizer materials, it's variation changes the mechanical, physical, morphological, and other properties of polymer composites and accordingly, its effects should be considered along with the main other important factors in analyzing such systems (Sharifzadeh et al., 2021). The temperature range considered in this study bases from the first level, melting temperature of sorbitol and glass transition temperature of PLA,

and the last level taken below degradation temperature of fillers (MCC and MTT), sorbitol and PLA. The control factors and their levels are exhibited on Table 11. The response factors tensile strength and modulus, flexural strength and modulus, hardness value, impact strength, water absorption and density values were measured according to their perspective ASTM standards.

Table 11: Control factors and their values at four levels

S.N	Coded Factor	Uncoded Factors Name	Unit	Levels			
				1	2	3	4
1	A	MCC	Wt %	0	3	6	9
2	B	MTT Nanoclay	Wt %	0	3	6	9
3	C	S	Wt %	0	10	20	30
4	D	T	^{0}C	100	125	150	175

Taguchi method has special experimental design method called orthogonal array used to combine each level of factor with all other levels of factors with a lesser observation number. This structure allows for comprehensive analysis while keeping costs and time manageable. The arrays are typically represented in tabular form, where rows correspond to experimental runs and columns represent different factors and their levels. The result drawn from this small experiments are acceptable over the whole experimental domain varied by the control factor and their levels. The Taguchi orthogonal array (L16) experimental design made by "Minitab" software are shown in Table 12.

Table 12: L16-OA Design matrix for bio composite development

Sample No.	Coded Factor				Uncoded Factor			
	A	B	C	D	MCC (Wt %)	MTT (Wt %)	S (Wt %)	T (^{0}C)
1	**1**	**1**	**1**	**1**	0	0	0	100
2	**1**	**2**	**2**	**2**	0	3	10	125
3	**1**	**3**	**3**	**3**	0	6	20	150
4	**1**	**4**	**4**	**4**	0	9	30	175
5	**2**	**1**	**2**	**3**	3	0	10	150
6	**2**	**2**	**1**	**4**	3	3	0	175
7	**2**	**3**	**4**	**1**	3	6	30	100
8	**2**	**4**	**3**	**2**	3	9	20	125
9	**3**	**1**	**3**	**4**	6	0	20	175
10	**3**	**2**	**4**	**3**	6	3	30	150
11	**3**	**3**	**1**	**2**	6	6	0	125
12	**3**	**4**	**2**	**1**	6	9	10	100
13	**4**	**1**	**4**	**2**	9	0	30	125
14	**4**	**2**	**3**	**1**	9	3	20	100
15	**4**	**3**	**2**	**4**	9	6	10	175

16	**4**	**4**	**1**	**3**	9	9	0	150

3.5 Instruments, Devices and Machines Used for Data Collection and Experimentation

The instruments used for data collections were comprises both qualitative and quantitative instruments. Qualitative instruments such as observational notes, scanning electron microscope, optical microscope, photos and videos were used for recording. While quantitative instruments such as digital weight balance, FTIR, XRD, TGA/DTA, Ostwald viscometer were used to assess the removal of constituents through absorbance, diffraction, weight loss, flow measurements and etc. The comprehensive information of instruments, devices and machines used for data collections and experimentations for this study were provided as follows;

Digital laboratory analytical weighing balance machine: FET - N model machine were used to measure the removal of constituents from the fiber after each chemical treatment, and water absorption and density of synthesized bio composite samples.

Fourier Transform InfraRed Spectroscopy: Jasco FT/IR-6600typeA analyzer (Easton, Maryland, USA) were used to collect structural data of untreated, chemical treated, neat PLA and the most optimal bio composite samples.

X-Ray Diffraction: MAXima_X XRD-7000 X-Ray Diffractometer (Japan) with Cu Kα radiation were utilized for data collection of untreated, chemical treated, neat PLA and the most optimal bio composite samples.

Thermo-Gravimetric Analysis/Differential Thermal Analyzer: BJHENVEN simultaneous TGA – DTA/DSC instrument, HCT-3 model, Beijing, China were used for collecting data of untreated, chemical treated, neat PLA and the most optimal bio composite samples thermal stability and reaction takes place in the material.

Scanning Electron Microscope: JOEL scanning electron microscope, JCM-6000 plus model (JOEL Ltd., Tokyo, Japan) were employed for morphological analysis of untreated, chemical treated, neat PLA and the most optimal bio composite samples fractured surface.

Universal Testing Machine: Bongshin Model DSCK machine used for flexural and tensile strength testing of synthesized bio composite samples and the most optimal sample.

Digital Display Vickers Hardness Tester: Model HVS – 50 hardness testing machine were employed for investigating the indentation resistance of the developed bio composite samples and the most optimal sample

Impact Testing Machine: charpy impact testing machine, Model SI42 (Jinan Tianchen Testing Machine Co Ltd., China) were used to evaluate the energy absorption of synthesized bio composite and the most optimal sample material in its plastic range.

3.6 Data Analysis Method

Generally, the data analysis method used employed for this study was both qualitative and quantitative techniques. Qualitative data collected were analyzed systematically to identify the behavior of the material changes. Whereas, quantitative analysis was conducted through analytical and statistical methods using excel spreadsheet program, Origin and Minitab softwares.

The data analysis method used for measuring weight loss of cellulose, hemicellulose, lignin, extractive and ash content of outer skin isolated coffee husk was conducted using analytical method called gravimetric technique and the crystalline index of each chemical treatments were investigated through amorphous substraction method with the help of Origin software. The experimental result analysis and optimization of synthesized bio composite samples were conducted through Taguchi's orthogonal array technique. This technique used to achieve robust result by minimizing variation, succeeding consistent performance across different conditions and compatible with statistical analysis such as ANOVA. The result of observations are changed into a signal to noise ratio. Then further analysis of multi-objective optimization were carried out through grey relational analysis. The overall processes of S/N ratio, statistical analysis and grey relational analysis are given as follows;

Signal-to-Noise Ratio Calculation: - is used to evaluate the variation of the response from the preferred value. Based on the type of desired response, S/N ratio analysis are categorized into three, i.e. the higher the better, the lower the better, and the nominal the better. For developed bio composite flexural strength, tensile strength, hardness value and density have been thought as larger-the-better and for water absorption is smaller-the-better. This process used to investigate the optimal levels for each factor level across different experimental runs. The S/N ratio for the corresponding responses was calculated using the following cases.

Case 1: Larger-the–better performance characteristics are utilized for a problem when maximization of interest is required.

$$S/N \text{ ratio} = -10 \log_{10} \left(\frac{1}{n}\right) \sum_{i=1}^{n} \frac{1}{y_{ij}^2} \quad (19)$$

Where; y_{ij} - observed response value, n - Number of replications, i=1, 2, ...n; j=1, 2, …k

Case 2: Smaller–the–better performance characteristics are used for a problem where minimization of interest is required.

$$S/N \text{ ratio} = -10 \log_{10} \left(\frac{1}{n}\right) \sum_{i=1}^{n} y_{ij}^2 \quad (20)$$

Analysis of Variance: - was conducted to identify significant factors influencing the mechanical and physical properties of the developed bio composites. This analysis provides F-values and p-values for each factor, indicating their influence on the performance metrics at 95% confidence level.

Regression analysis: - the factors (MCC, MTT, S, and T) were considered in the development of mathematical models for the responses value (TS, YM, FS, FM, HV, WA, and D) accuracy. The correlation between factors (MCC, MTT, S, and T) and responses value (TS, YM, FS, FM, HV, WA, and D) accuracy of developed bio composite were obtained by multiple linear regression, which is a technique analyzes numerous explanatory factors to forecast the result of a performance characteristics (Kus et al., 2018). A linear model is developed to control the response (TS, YM, FS, FM, HV, WA, and D) data fitness to represent a characteristics as a form of equation (21), as follows:

$$Y = b_0 + b_1MCC + b_2MTT + b_3S + b_4T + \varepsilon \quad (21)$$

Where Y is the response; b_0 is y-intercept; b_1, b_2, b_3, and b_4 are estimates of the factors and ε is the models error term (residuals). The statistical software package MINITAB was applied to develop the models.

Grey Relational Analysis: - for multi response optimization Taguchi based grey relational analysis was employed for converting the multi objectives into the single criterion and by following few steps optimal combination is identified. This process of converting multi objective into single objective has three major steps that are normalization, calculation of grey relational coefficient (GRC) and grey relational grade (GRG).

Normalization: - the experimental result normalization was set to the range of 0 to 1 by signal-to-noise ratio obtained from Taguchi analysis. The S/N ratio for the maximum is the better and smaller is the better characteristics was calculated using equation (19) and (20), respectively. To convert S/N ratio into the normalization, equations (22) and (23) were used for larger is the better and smaller is the better, respectively. Normalization is a transformation performed on a single data input to distribute the data evenly and scale it into an acceptable range for further analysis.

$$\text{For larger the better;} X_{ij} = \frac{Y_{ij} - \min Y_{ij}}{\max Y_{ij} - \min Y_{ij}} \quad \ldots\ldots\ldots\ldots\ldots\ldots\ldots\ldots \quad (22)$$

$$\text{For smaller the better; } X_{ij} = \frac{\max Y_{ij} - Y_{ij}}{\max Y_{ij} - \min Y_{ij}} \quad \ldots\ldots\ldots\ldots\ldots\ldots\ldots\ldots\ldots \quad (23)$$

Where X_{ij} - is normalized S/N ratio, Y_{ij} - is signal-to-noise ratio obtained from Taguchi analysis, and Min Y_{ij} and Max Y_{ij} are the minimum and the maximum values of signal-to-noise ratio, respectively.

Grey Relational Coefficient: - to identify the grey relational coefficient were calculated from the normalized signal-to-noise ratio. Primarily the determination of deviation sequence of the location order is determined by equation (24) in order to determine the GRC. High value of grey relational grade indicates stronger relational degree between ideal sequence and present sequence. The ideal sequence is the best response and the equation for calculating GRC is as follows:

$$\Delta_{oi}(k) = x_o(k) - x_i(k) \quad \ldots\ldots\ldots\ldots\ldots\ldots\ldots\ldots\ldots \quad (24)$$

Where; $\Delta_{oi}(k)$ is deviation sequence; $x_o(k)$ is location sequence and $x_i(k)$ is comparability sequence.

$$GC_{ij} = \frac{\Delta_{min} + \varphi\Delta_{max}}{\Delta_{ij} + \varphi\Delta_{max}} \quad \ldots\ldots\ldots\ldots\ldots\ldots\ldots\ldots\ldots\ldots\ldots\ldots \quad (25)$$

Where GC_{ij} is the grey relational coefficient, Δ_{min} and Δ_{max} are the minimum and maximum difference in absolute value, respectively, which is a deviation from the target value. φ is the distinguishing coefficient, which is defined in the range $0 \leq \varphi \leq 1$. The distinguishing coefficient can be used to distinguish the important of each response based on the particular application. φ was assumed to be 0.5 for all responses in this study because all the fabrication parameters influence the responses almost equally.

Grey Relational Grade (GRG): - the grey relational grade values is calculated with the help of equation (26) to determine the best parametric combinations.

$$G_i = \frac{1}{K} \sum_{j=1}^{m} GC_{ij} \quad \text{.....} \quad (26)$$

Where G_i is the grey relational grade, k is the number of performance characteristics and m is the number of response variables. The overall procedures from experimental design to plan of investigations are summarized in Figure 15.

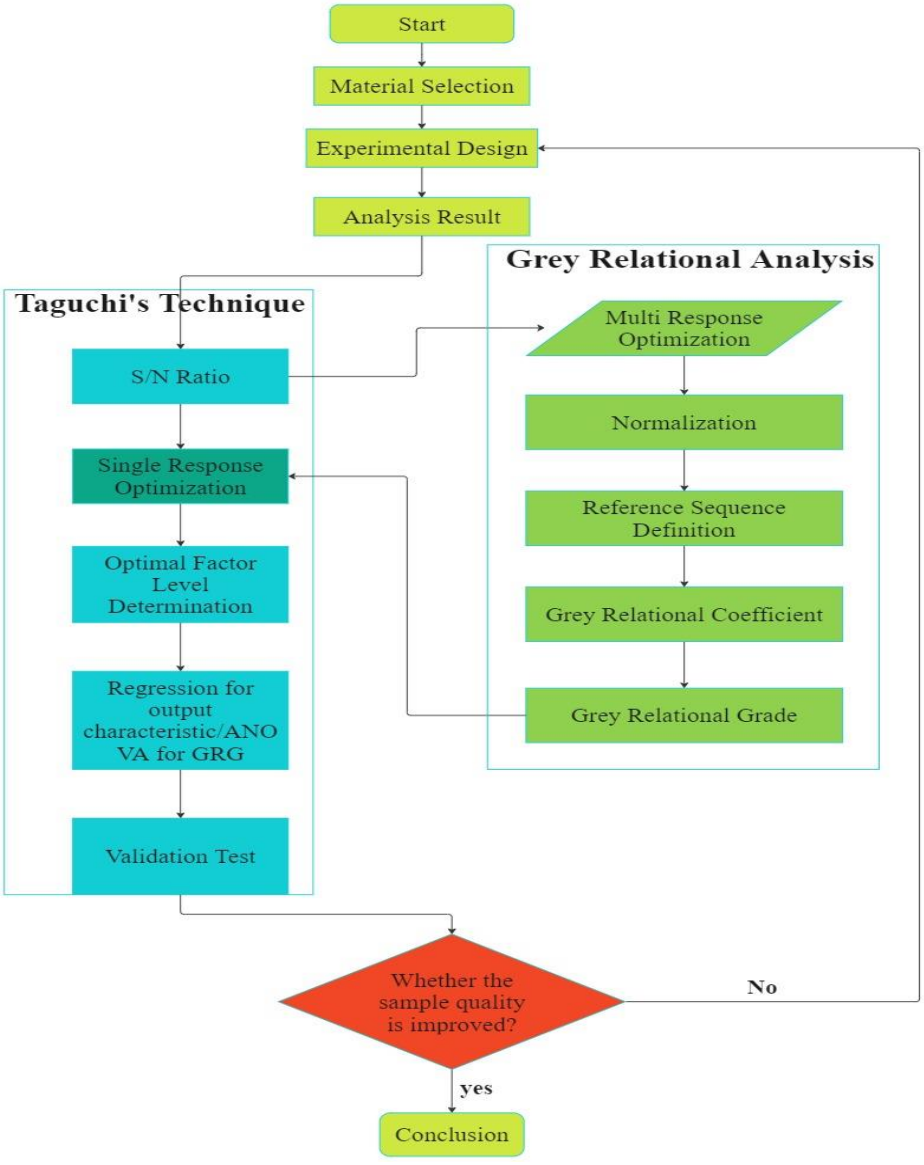

Figure 15: Flow chart of experimental design and plan of investigation

Finally, possible applications for synthesized bio composite material was assessed and compared with obtained results. The assessment and comparison were made with an existing material used

for structural application in automotive components and other possible materials proposed by researchers for automotive part applications.

This chapter outlined a comprehensive and systematic approach to investigate the chemical composition of CH, extraction of MCC, measuring, and characterization of extracted MCC, preparation of PLA-based bio composite, testing and characterization of prepared samples and etc. The chemical composition analysis provided a foundational understanding of the raw materials, while the MCC extraction process ensured the isolation of crystalline cellulose from agricultural wastes and further measuring. The bio composite sample preparation was carefully designed to maintain consistency and reproducibility, enabling reliable testing and characterization. Advanced analytical techniques were employed to evaluate the structural, physical and mechanical properties of the bio composites, ensuring a detailed understanding of their behavior. Optimization processes were implemented to refine the parameters for enhanced performance, and application recommendations were derived based on the findings. Together, these methodologies established a robust framework for developing viable bio composite materials with potential applications in various industries. This chapter serves as a critical foundation for the subsequent analysis and interpretation of results in this study.

CHAPTER 4

RESULTS AND DISCUSSION

4.1 Chemical Composition Analysis

The chemical composition of outer skin isolated coffee husk was determined using the gravimetric method and was determined to be 52.9 % of cellulose, 21.9 % lignin, 12.5 % hemicellulose, 9.4 % extractives, and 2.4 % ash content. This yield value is higher than the cellulose yield of wheat straw (32.5 %) (Hernandez et al., 2016), coffee husk (24.5%) (Bekalo et al., 2010) and parchment (22%) (Reis et al., 2020), and lower than the yield values of cellulose extracted from coffee husk through chlorine based extraction techniques (61.8%) (Collazo-Bigliardi, Ortega-Toro, & Boix, 2018) reported in the literature. Further, the yield value is comparable to yield values of cellulose extracted from bagasse (55.2 %) (K. O. Reddy et al., 2016) and kenaf fiber (53%) (Suriani et al., 2021). The obtained cellulose from outer skin isolated CH is compared with other renewable source has been summarized in Table 13 and Figure 16 which shows different samples of outer skin isolated coffee husk in order to determine their chemical composition and changes.

Table 13: Cellulose obtained from different renewable sources

S. No	Renewable Source	Cellulose Content (%)	Reference
1	Wheat straw	32.5	(Hernandez et al., 2016)
2	Coffee Husk	24.5	(Reis et al., 2020)
3	Parchment	22	(Reis et al., 2020)
4	Bagasse	46	(K. O. Reddy et al., 2016)
5	Kenaf	53	(Anbupalani et al., 2020; Suriani et al., 2021)
6	Giant Reed	35.52	(Tarchoun et al., 2019)
7	Jute	60	(Sharma et al., 2019)
8	Sisal	73.5	(Anbupalani et al., 2020)

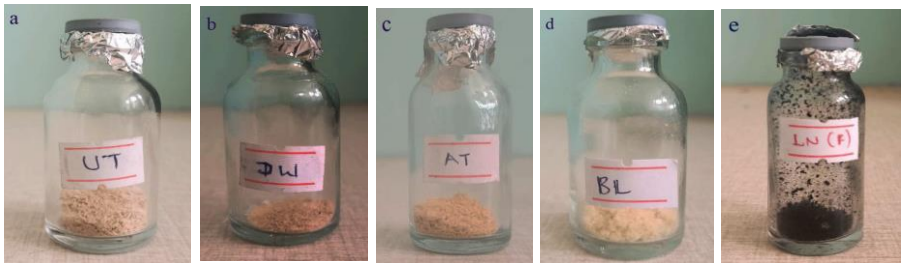

Figure 16: a) Untreated sample, b) Extractive free sample, c) Alkali-treated sample, d) Bleached sample, e) Acid-treated sample (to determine the lignin content)

4.2 Fourier Transform Infrared Spectroscopy

Infrared spectroscopy is a simple technique used to obtain information continually on chemical changes that takes place throughout chemical treatments. Figure 17(a) shows the IR spectra of untreated (UT) sample, dewaxed (DW) sample, alkali-treated (AT) sample, and bleached (BL) sample. The IR spectra analysis shows UT and DW sample spectra exhibited matching absorption bands. The spectra at 1030 cm^{-1} shows the O–H and C–O stretching vibration of polysaccharide occurred in cellulose, and the peak at 1630 cm^{-1} may cause by water absorption of the samples (Romruen et al., 2022). The spectrum at 1739 cm^{-1} is a typical behavior of the carbonyl C=O stretching of the uronic ester and acetyl groups of polysaccharides. It is moreover associated to the p-coumaric acids of hemicellulose or/and lignin (Nie et al., 2019), the removal of this spectra after continuous chemical treatments shows the elimination of excessive content of hemicellulose and lignin from the samples. Additional sign of hemicellulose and lignin elimination through the treatment is the substantial reduction in the absorption of the small spectra at 1220 cm^{-1} which is associated to the C–O stretching of the aryl group in hemicellulose and lignin. A small spectra exhibited at 1430 cm^{-1} can be associated to the CH_2 symmetric bending of cellulose (Hachaichi et al., 2021). The absorption in the range of 3600–3100 cm^{-1} are associated to the O–H stretching vibration and hydrogen bonds of the hydroxyl groups. The absorption at 2920 cm^{-1} are typical characteristics of the C–H stretching frequency in cellulose (Hachaichi et al., 2021). Furthermore, typical FTIR spectra of AT sample shown in Fig.17 (a) exhibits the peaks observed at 1516 cm^{-1} which are associated to aromatic ring stretching frequencies of lignin (Nie et al., 2019). The alkali treatment removes this peak apparently from the cellulose so that these spectra was eliminated from the AT sample spectrum. The absorption at 3440 cm^{-1} is correlated to the –OH stretching vibration of cellulose (Azum et al., 2021). The cellulose did not show the absorption band located at 1739 cm^{-1}, which is a typical behavior of the stretching vibration of C=O and C–O. Due to The alkali treatment disappeared these groups from the spectra.

Finally the FTIR spectra of BL sample shown in Figure 17 (a) shows, the delignification process of sample and further extraction of MCC. In this spectra the elimination of almost the remaining lignin was proven by the removal of peak at 1516 cm^{-1} and the peak band around 3440 and 2920 cm^{-1} are related with the characteristic values of purified cellulose and the broadened peak and sharp peaks in the BL sample implying enhanced cellulose content and increasingly exposed

cellulose content in the sample (Azum et al., 2021). In addition, the spectra around 1430 cm^{-1} is connected to the crystallinity of cellulose and related to CH_2 symmetric stretching. Additionally, the spectra at 898 matching to the C–O–C pyranose ring skeletal stretch, β-glycosidic bond stretch, and C–H asymmetric deformation (Beroual et al., 2021). This peak appearance on the BL sample spectra confirms the breaking of cellulose chains and extraction of MCC. Table 14 exhibits all IR spectra of detected peaks and their representations.

Table 14: The IR spectra of detected peaks and their representations

Wave no. cm^{-1}	Spectra	Represents	Reference
1030	All	C–O–C pyranose ring skeletal vibration	(Khenblouche et al., 2019)
1141	BL	C–O–C stretching at the b-(1→4)-glycosidic linkages	(He et al., 2022; Rasheed et al., 2020)
1220	UT	C–O stretching of the aryl group in hemicellulose and lignin.	(He et al., 2022)
1430	AT, BL	C-H bond of cellulose	(Hachaichi et al., 2021)
1516	UT, DW	C-C aromatic ring stretching vibrations of lignin	(Rasheed et al., 2020)
1630	AT, BL	OH bending of the absorbed water	(Romruen et al., 2022)
1739	UT, DW	C=O stretching in hemicellulose	(Nie et al., 2019)
2920	AT, BL	C–H stretching	(Hachaichi et al., 2021)
3440	AT, BL	-OH groups stretching of cellulose	(Azum et al., 2021)

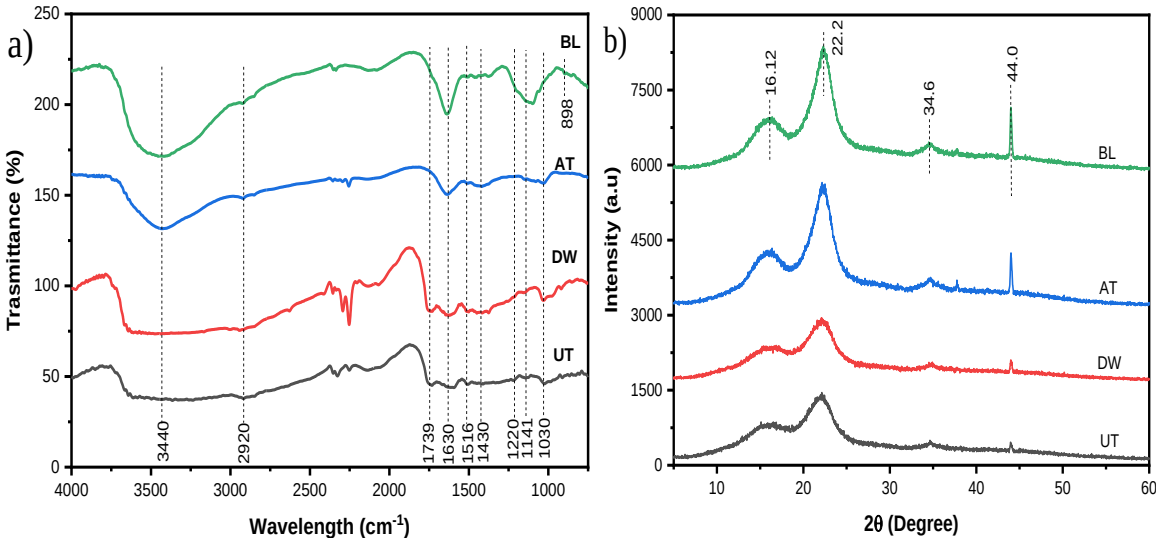

Figure 17: (a) Infrared spectra and (b) X-Ray diffraction pattern of UT, DW, AT, and BL samples

4.3 X-Ray Diffraction Measurements

XRD is an important method to characterize the structure of crystalline material. Figure 17(b) represents the XRD patterns of chemical untreated and treated outer skin isolated coffee husk samples. The samples showed outstanding peaks around 16.7^0, 22.4^0, 34.6^0, and 44.1^0, which match all peaks with Joint Committee on Powder Diffraction Standards (JCPDs) data (JCPDs Card Number: 00-003-0192) that corresponds to the crystallographic plane of (110), (200), (004), and (100) (Rasheed et al., 2020; Yan et al., 2008). This JCPDs Card Number: 00-003-0192 refers to coated cellulose-II type structure and these planes reveal that each cellulose sample has a cellulose type structure (Fouad et al., 2020) and the bleached (BL) sample shows coated cellulose-II type structure. The cellulose to be coated cellulose is due to treating the husk with NaOH. When lignocellulose materials are treated with NaOH fibers starts to swell and become highly accessible to subsequent chemical treatment steps, mainly under mechanical stress. Consequently, some of the cellulose fibers can break down into smaller fragments during the other chemical treatments. When these degraded cellulose fragments come into contact with the NaOH solution, they can undergo a process called regeneration. This process involves the formation of a thin layer of cellulose on the surface of the degraded fragments, which is known as coated cellulose. Therefore, coated cellulose is a type of cellulose that has a layer of regenerated cellulose on its surface, which can improve its mechanical and physical properties (Xi Liu et al., 2020). The peak observed at 16.12^0 was related to the cellulose crystals domain and it has increased intensity for alkali-treated (AT) and bleached (BL) samples. It was suggested that the two-cycle NaOH – alkali treatment and H_2O_2 and H_2SO_4 – based bleaching processes promote highly ordered coated cellulose-II crystallites in outer skin isolated coffee husk through improving intra and intermolecular hydrogen bonding. Meanwhile, the peak 22.2^0 34.6 and 44.0 were observed gradually sharpen and have high intensity for both AT and BL samples when compared to UT and DW samples. This was likely due to the alkali treatment and bleaching processes that removed residual compounds and produced coated cellulose-II crystalline structure with 54.7% yield. Accordingly, the highest crystalline index of cellulose possessed 89.9 % with the BL sample, followed by the AT with 81.2%, DW with 76.2 %, and lastly UT with 69.7 % as shown in Table 15. Thus, the outer skin isolated coffee husk bleached sample could offer it as a promising agent in bio composite reinforcement application.

Table 15: Crystalline index of UT, DW, AT, and BL samples

Sample	The total area of crystalline peaks	Areas of all peaks	Crystalline index (CI %)
UT	5207.2	7462.2	69.7
DW	6611.9	8667.5	76.2
AT	6386.1	7863.2	81.2
BL	8394.4	9328.3	89.9

4.4 Morphological Analysis

Fig. 18 exhibits SEM micrograph of untreated CH fiber and CH fiber subjected to de-waxing, alkaline, and bleaching treatment. Fig. 18 (a) and Fig. 18 (b) shows the feature of any typical lignocellulosic fiber characteristics which clearly shows surface impurities. The de-waxed sample Fig. 18 (b) further exhibits the microfibers in pack form more densely with a rough surface and the alkali-treated sample Fig. 18 (c) exhibits less dense microfibers with a smooth surface and fibers try to isolate each other. This indicates partial hemicellulose, lignin, and surface impurity removal at this stage, while the smooth structure of cellulose was still preserved (K. O. Reddy et al., 2016). The two-cycle bleaching process Fig.18 (d), causes the fiber to split into isolated cellulose microcrystalline. According to reported pieces of literature, the acidic attack disintegrates the cellulose structure into individual small micro crystalline size, and penetration of acidic ions into the inner part of fiber could depolymerize the cellulose by degrading the amorphous regions (Azum et al., 2021). The chemically treated cellulose microcrystalline average diameters are about 1-2 μm but the exact length is difficult to determine. The reduction in diameter refers to the disappearance of hemicellulose, lignin and other impurities (Hashim et al., 2017). This extracted CH cellulose microcrystalline is less in diameter than those extracted from various sources such as sisal (Fan et al., 2022), coconut (Maheswari et al., 2012), and wheat straw (Nehra et al., 2022) with different extraction methods which uses chlorine-based extraction methods. This makes the extracted MCC a potential candidate for polymer reinforcing application.

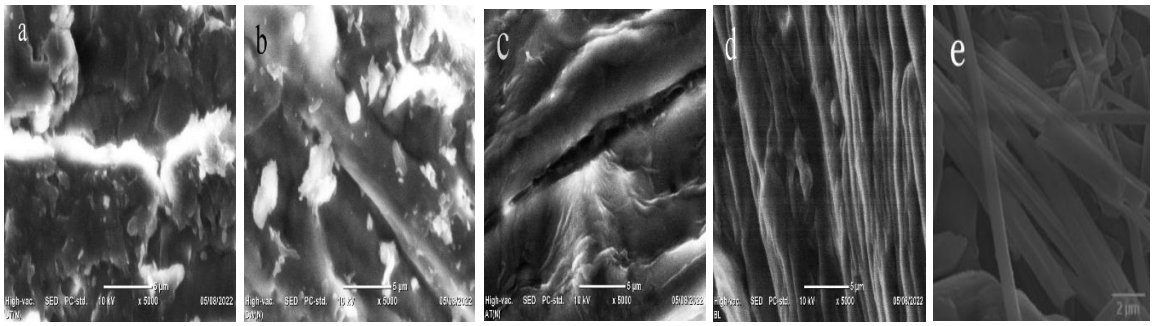

Figure 18: (a) untreated, (b) de-waxed, (c) alkali-treated, (d) first cycle bleaching, and (e) second cycle (hydrolysis) sample of SEM micrograph of outer skin isolated coffee husk fiber.

4.5 Thermal Stability Analysis

Figure 19 (a) and (b) exhibit the TGA and DTA curve respectively, environmentally friendly chemical treated and untreated outer skin separated coffee husk samples. Initially, all samples mainly UT and DW samples demonstrated a decreased weight curve in the range of 30 -135 ^{0}C, which is a typical characteristic of adsorption of water and disappearance of constituents of low molar mass (X. Wang et al., 2021). However AT and BL samples showed increase in the same way with a flattened curve and the weight loss was also relatively low. This was probably caused by water adsorption of the high amount of cellulose content in both samples. Consequently, AT and BL samples exhibit higher decomposition temperatures than UT and DW samples, for the reason of the existence of micro crystalline cellulose structure that increases the thermal endurance of samples from high temperatures (Fouad et al., 2020). The second range 135-250 ^{0}C is associated with the degradation of hemicellulose which contains numerous saccharide types that form amorphous structures and thermally less stable lignocellulosic components (Reis et al., 2020). The third range 250 – 375 ^{0}C corresponds to a portion of hemicellulose, and cellulose. Cellulose is a crystalline and ordered structure that forms strong material with thermal stability (Barzegar et al., 2020). Finally, the degradation takes place at the range of 375 – 520 ^{0}C related to lignin, which is more thermally stable and difficult to degrade (Nakason et al., 2019). The DTA curve tries to show a slight an endothermic reaction at the initial stage of the curve due to the sample's dehydration around 100 ^{0}C, then undergoes a sharp exothermic reaction between temperature around 270 ^{0}C – 375 ^{0}C. The sharp exothermic reaction at these temperature range indicates the degradation of cellulose and remaining hemicellulose. Variation in the structure of cellulose due to heat primarily take place through depolymerization (begins at 310 ^{0}C due to breaking the chain at 1,4 glycosidic

bond), dehydration (occurs at initial range of degradation temperature, 280 ^{0}C), and the formation of Glucosan (Safaei et al., 2019). Additionally, the exothermic peak around the temperature of 410 ^{0}C and above indicates the release of lignin from the samples. Finally, the curve BL sample shows that the temperature resistance is high relative to other samples. This indicates that the two stage bleaching process highly improves the thermal resistance of the sample. The weight loss in each range of the samples was summarized in Table 16. The weight loss of sample BL in the range: initial, second, and final was lower than other samples, and in the third range AT sample, the loss was low. These characteristics makes the extracted MCC a potential candidate, where stable filler is required for polymer strengthening in the range of <270 ^{0}C.

Table 16: Weight loss of the samples at each range

% of weight loss in each Ranges	UT	DW	AT	BL
Initial range	7.7	6.1	3.5	3.3
Second range	3.4	4.0	3.4	0.9
Third range	48.0	60.8	45.2	46.9
Final range	20.1	26.2	22.3	17.9

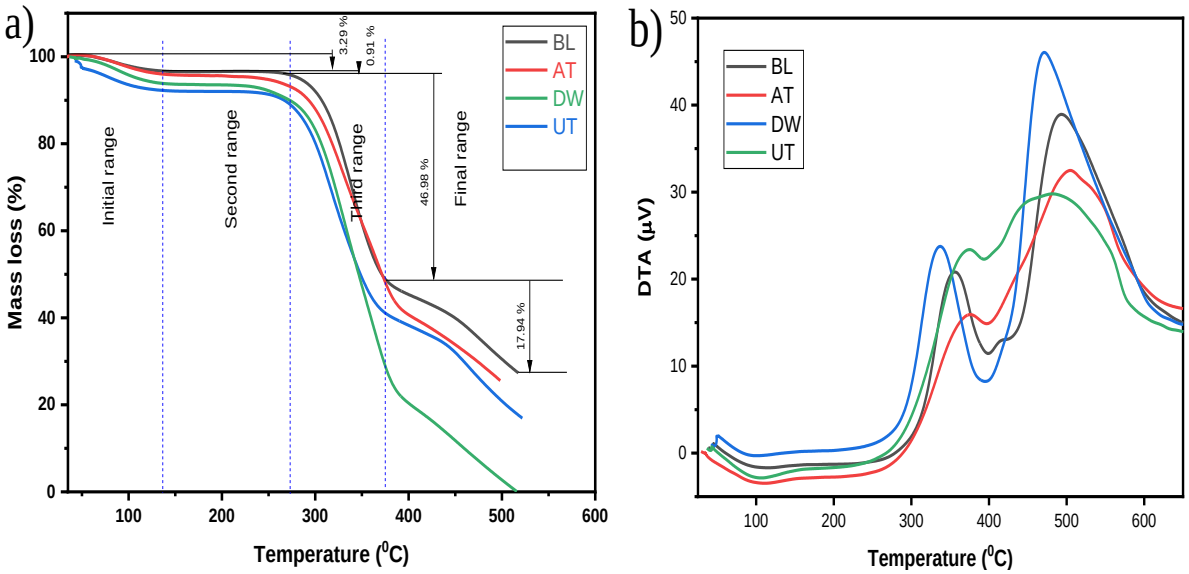

Figure 19: (a) TGA and (b) DTA curves of UT, DW, AT, and BL samples.

4.6 Average molecular weight and degree of polymerization

The η and extracted MCC average DP was determined to study the effect of H_2SO_4 treatment on the cellulose structure. During the first bleaching cycle using H_2O_2, the η and DP is 901 and 1340, respectively. For the second bleaching cycle or hydrolysis, using H_2SO_4 for preparation of MCC,

the η and DP significantly reduced to 365 and 281, respectively. This could be described by the degradation of amorphous region for the extracted MCC. The result shows that the DPs of extracted MCC is in the range (150 -300) of currently available commercial MCC and the DPs of extracted MCC higher than DPs of commercial MCC, 117.2 and MCC extracted from bacterial cellulose, 250 (de Oliveira et al., 2011). The molecular weight (Mw) of extracted MCC from outer skin isolated CH was determined by multiplication of DP of extracted MCC with Mw of unit cellulose, 162 (Lee et al., 2009), then the Mw of extracted MCC is around 21,300 g/mol. With considering to the plenty of coffee husk waste material, large scale fabrication of MCC with adequate DP and Mw could be realized for various applications such as medical, packaging, and composites.

4.7 Density (True and Bulk) and Porosity

True density determines the density of a material with the exclusion of any open and closed voids. It can show the closeness of the material to the crystalline state or the proportions of a binary mixture (Achor et al., 2014). High true density indicates high crystallinity, which states that the degree of crystallinity of cellulose increases directly with true density when determined in a non-polar solvent (Nwajiobi et al., 2019). The true density value of coffee husk derived MCC (1.4 g/ml) was slightly greater than that reported for Mango kernel (1.36 g/ml) (Nwadiogb et al., 2015) and slightly lower than that of sugar palm bunches (1.47 g/ml) by (Adedokun et al., 2014). Thus, it might exhibit better compressibility and possess higher crystallinity. Whereas, bulk density of MCC related with pressing behavior of particles which varies as the particle combines (Adedokun et al., 2014). Higher bulk density indicates that the necessity of larger amount of compression (Pachuau et al., 2014). The obtained bulk density of coffee husk derived MCC is 0.518 g/ml, which is higher than that of reported for Muli bamboo (Melocanna baccifera) (0.35 g/ml) (Pachuau et al., 2014) and African breadfruit seed hulls (0.382 g/ml) (Nwajiobi et al., 2019).Therefore, coffee husk derived MCC may have improved flow property, additionally it would require moderate amount of pressing load in material processing. Porosity is the voids within and between particles. The place between particles is known as void and the volume occupied by this void is called void volume. The high value of total porosity of MCC (63%) corresponds with the high tapped density. Degree of material densification correlates to its porosity which is a function of the void volume (Olorunsola et al., 2016).

4.8 Flexural Strength and Modulus of Bio Composite

The flexural strength and modulus of bio composite samples at different weight percentage of MCC, MTT and S in PLA at various temperature level were shown in Table 17 with its S/N ratio and Figure 20. Under flexural loading, the Table 17 and Figure 20 exhibits that the addition of MCC, MTT and S improved the flexural strength and modulus of neat PLA. The flexural strength values of the MCC and MTT reinforced and S plasticized PLA (MCC/MTT/S/PLA) bio composites could be higher than the neat PLA except 9MCC/0MTT/30S/125T values at experiment 13, which has lower FS value due to higher amount of MCC and sorbitol concentration can increase agglomeration and lessen the intermolecular forces and deteriorate the material (Kormin et al., 2019). The experimental setup 3MCC/9MTT/20S/125T combination shows the highest flexural strength with the value of 93.75 Mpa as shown in experiment 8, which improves 78.5 % greater than that of the neat PLA experiment 1. It is easily assumed that at these contents the fillers are dispersed uniformly within the PLA material and fillers size (Nano and micro) have a high surface area that are greatly enhances interfacial interactions of bio composite material at molecular level and ends with other properties (Turku et al., 2014). It is clearly shown in Table 17, the flexural modulus of each MCC/MTT/S bio composite samples is greater than that of the neat PLA, this is mainly caused due to flexural 3-point bending tests, upper half part of the cross-section of the sample is in compression, whereas lower half part of the cross-section is revealed to tensile loads. Therefore, at the parting boundary would be hindered in the sample on the side of compressive, resulting to improved load transfer mechanism from the matrix material to the fillers (Dogu et al., 2016).

Table 17: Flexural strength and modulus of bio composite with S/N ratios

S.N	Factors				Responses			
	MCC	MTT	S	T	FS (Mpa)	S/N Ratio	FM (Gpa)	S/N Ratio
1	0	0	0	100	52.50	34.40	4.1	72.19
2	0	3	10	125	60.00	35.56	5.3	74.53
3	0	6	20	150	75.00	37.50	6.7	76.59
4	0	9	30	175	82.50	38.32	7.5	77.54
5	3	0	10	150	60.00	35.56	5.5	74.89
6	3	3	0	175	71.25	37.05	7.1	77.01
7	3	6	30	100	75.00	37.50	7.5	77.58
8	3	9	20	125	93.75	39.43	9.7	79.79
9	6	0	20	175	63.75	36.08	6.7	76.58
10	6	3	30	150	63.75	36.08	7.1	77.00

11	6	6	0	125	67.50	36.58	7.7	77.79
12	6	9	10	100	71.25	37.05	8.4	78.57
13	9	0	30	125	45.00	33.06	5.0	73.97
14	9	3	20	100	56.25	35.00	8.1	78.22
15	9	6	10	175	56.25	35.00	7.8	77.85
16	9	9	0	150	60.00	35.56	8.6	78.78

The best S/N ratios shown in Table 17 for FS is 39.43 at experiment number 8 and also offer the higher FS value 93.75. The weakest S/N ratio is 33.06 observed at experiment 13. The best S/N ratios of FM is observed at the same experimental setup, experiment 8 with the value of 79.79 and the weakest S/N ratio is observed at experiment 1 with the value of 72.19. These results suggests that the consistency of the results, both best FS and FM happens at the same sample (experiment 8) because the sample at 3% MCC and 9% MTT fillers, and 20% S reinforced the matrix material better than other fillers and plasticizer weight percentages. This caused due to improved interfacial adhesion and enhanced load transfer between fillers and matrix material. Additionally, the fillers (MCC and MTT) increases the delays in crack growth and restrict the mobility of polymer chains, leads to increase in FS and FM of synthesized bio composite sample.

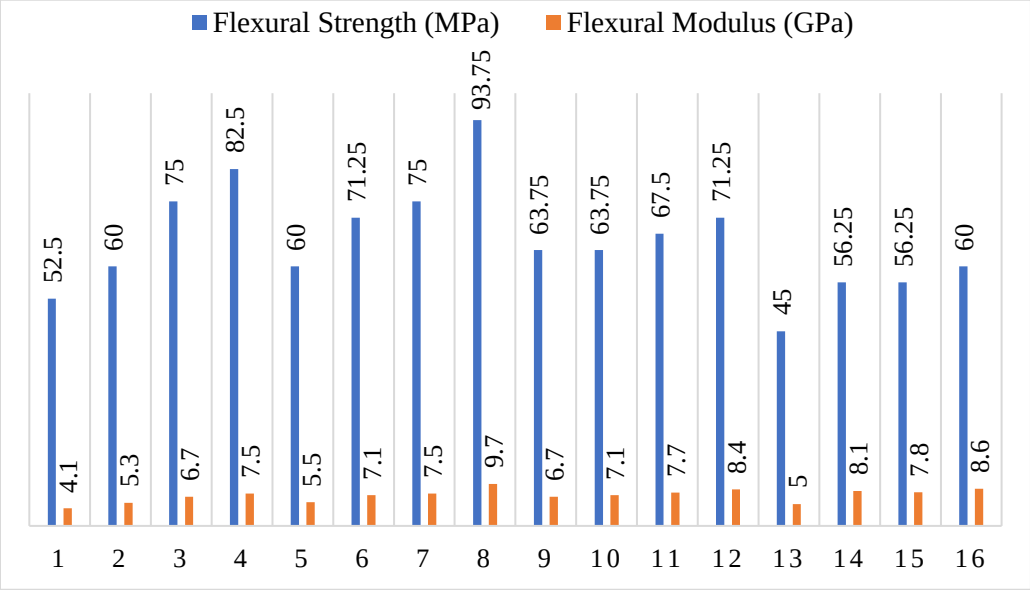

Figure 20: Flexural strength and modulus for each experimental design

Probability Plot

Figure 21 presents that the probability plot of flexural strength and modulus of all samples. As exhibited in Fig. 21 (a) and (b) all data are under normal distribution at the confidence level of 95%. The two lines beside the center line on the left and right shows the upper and lower limit of

confidence interval. There is no any sample value is out of the confidence interval. Additionally, the p-values 0.657 and 0.544, which is higher than the significance level of 0.05 presents that the data follow a normal distribution.

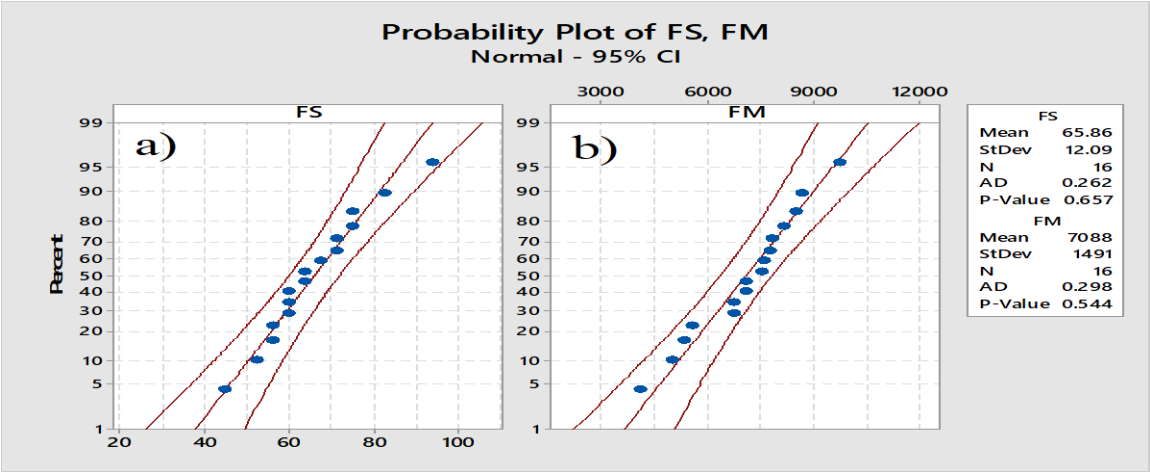

Figure 21: Probability plot for flexural strength (a) and flexural modulus (b) of samples

S/N Ratio Analysis of FS and FM

Table 18 and 19 presents that response table for the S/N ratio of flexural strength and flexural modulus, respectively. The delta value shows the significance of the control variables and helps to identify optimal setting that generates higher flexural strength and modulus. The higher values of delta shows the more significant variable, and based on values of delta, the whole significant variables are ranked properly. The value of delta ranking in Table 18 indicates, the MTT content as the most significant parameter in influencing the flexural strength of the bio composite, followed by MCC content and then S and T respectively. The value of delta ranking in Table 19 indicates, the MTT is the highest significant factor in influencing the flexural modulus of the bio composite, followed by MCC content and then S and T respectively. These caused due to MTT's layered structure with high surface area and aspect ratio (length to thickness), when dispersed in a PLA, these layers can significantly increases the interfacial area between the MTT and the PLA, leads to improved FS and FM properties.

Table 18: Response Table for S/N Ratios of FS (Larger is the better)

Level	MCC	MTT	S	T
1	36.45	34.78	35.90	35.99
2	37.39	35.93	35.80	36.16
3	36.46	36.65	37.01	36.18
4	34.66	37.60	36.25	36.62
Delta	2.73	2.82	1.21	0.63

Rank	2	1	3	4

Table 19: Response Table for S/N Ratios of FM (Larger is the better)

Level	MCC	MTT	S	T
1	75.22	74.41	76.45	76.64
2	77.32	76.70	76.47	76.53
3	77.49	77.46	77.80	76.82
4	77.21	78.67	76.53	77.25
Delta	2.27	4.26	1.35	0.72
Rank	2	1	3	4

The S/N Ratio graphs are plotted for flexural strength and flexural modulus responses in Figure 22 (a) and (b). The graph is drawn using the optimal control factors and the optimal value is the one with the highest value of mean S/N ratio. It has been found that the maximum flexural strength was obtained for developed bio composite at 3%MCC, 9%MTT, 20%S and 175^0C T as shown in Figure 22 (a), at this level FS is 96.5 MPa. For flexural modulus 6%MCC, 9%MTT, 20%S and 175^0C T showed the maximum S/N ratio as shown in Figure 22 (b), at this level FM is 9.8 GPa. As observed the effects of the MTT in the developed bio composites, the contribution of MCC in the FS and FM of developed bio composite also observed due to its lower aspect ratio and surface area than MTT.

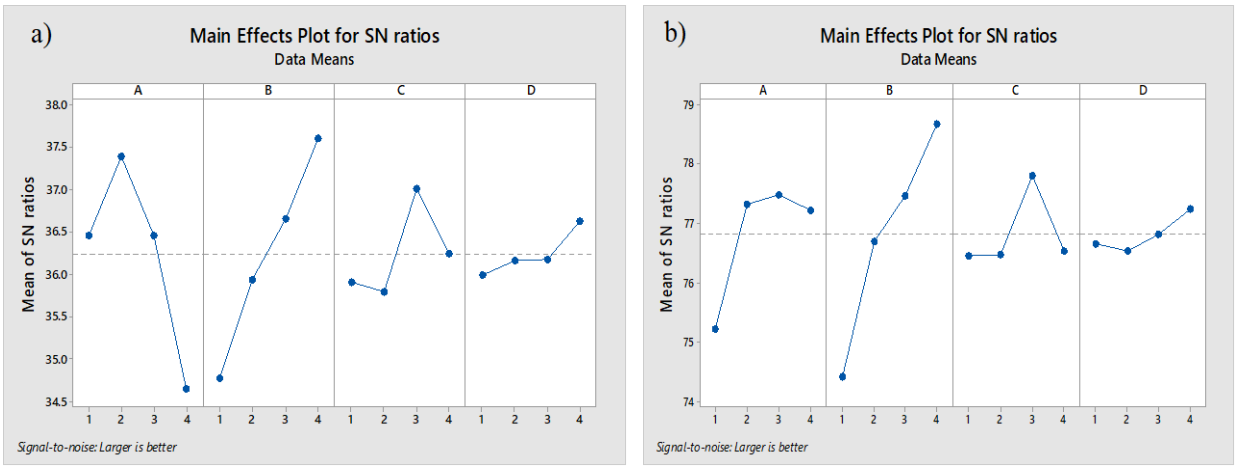

Figure 22: Main effect plot for S/N ratios of FS (a) and FM (b)

Regression Analysis

The relationship between factors that affects the flexural responses and outcomes are expressed by using regression equation as follows;

$$FS = 51.80 - 4.78\ MCC + 7.03\ MTT + 2.16\ S + 1.22\ T \quad \ldots\ldots\ldots\ldots\ldots\ldots\ldots\ldots\ (27)$$

FM = 2.997 + 0.450 MCC + 1.039 MTT + 0.074 S + 0.074 T …….…….. (28)

Table 20 presents the significances of factors incorporated in regression equation of flexural strength. The Table 20 clearly shows that regression P-value 0.005 suggests that the factors incorporated in the experimental setup are statistically highly significant for the linear model and factors P-value lesser than 0.05 shows the most significance parameter that influences the regression equation. Additionally, the larger F-value shows the more significant factor that influence the regression response. Table 20 exhibits that MTT and MCC P-value 0.002 and 0.016, respectively indicates that they are the most significant factor that affect the regression model of bio composite flexural strength, and factor S and T has less significances, respectively. These result agrees with the S/N ratios analysis of FS.

Table 20: ANOVA for regression model of FS

Source	DF	Seq SS	Adj SS	Adj MS	F-Value	P-Value
Regression	4	1568.67	1568.67	392.17	6.91	0.005
MCC	1	457.21	457.21	457.21	8.06	0.016
MTT	1	988.77	988.77	988.77	17.42	0.002
S	1	92.99	92.99	92.99	1.64	0.227
T	1	29.71	29.71	29.71	0.52	0.484
Error	11	624.20	624.20	56.75		
Total	15	2192.87				

Table 21 presents the significances of factors incorporated in regression equation of flexural modulus. Table 21 indicate that regression P-value 0.001 suggests that the factors incorporated in the model are statistically highly significant and factor MTT and MCC P-value 0.000 and 0.033, respectively indicates that they are the most significant factor that affect the regression model of bio composite flexural modulus, and factor S and T has less significances, respectively. These result agrees with the S/N ratios analysis of FM.

Table 21: ANOVA for regression model of FM

Source	DF	Seq SS	Adj SS	Adj MS	F-Value	P-Value
Regression	4	25.855	25.855	6.463	9.47	0.001
MCC	1	4.042	4.042	4.042	5.92	0.033
MTT	1	21.594	21.594	21.594	31.63	0.000
S	1	0.110	0.110	0.110	0.16	0.695
T	1	0.108	0.108	0.108	0.16	0.698
Error	11	7.509	7.509	0.682		
Total	15	33.365				

4.9 Tensile Strength and Young Modulus of Bio Composite

In order to analyze tensile strength and young modulus properties as responses, Table 22 and Figure 23 present different specimen configurations of PLA-based bio composites with varying loading conditions of plasticizer, MCC and MTT contents, and temperature. All data converted to S/N ratio are also displayed in Table 22. It can be shown from Table 22 and Figure 23 that PLA's tensile strength is increased by loading S, MCC, and MTT. The experimental setup 6MCC/9MTT/10S/100T combination shows the highest tensile strength, followed by the 9MCC/6MTT/10S/175T experimental combination, and experimental combination 6MCC/0MTT/20S/175T shows the lowest tensile strength following the neat PLA. The highest tensile strength experimental setup 6MCC/9MTT/10S/100T bio composites has 83.3 MPa, which improves 50 % greater than that of the neat PLA. It is easily assumed that at these contents the fillers are dispersed uniformly within the PLA material and Nano and micro sized fillers, have a great surface area, can meaningfully improves interfacial interactions of the materials, results increase in tensile strength and modulus (Arjmandi et al., 2016; Turku et al., 2014). The lowest bio composite combination improves 5% greater than that of the neat PLA. This probably due to the absence of MTT and increment of S reduces the tensile strength relative to the rest of experimental setup (Arief et al., 2021). As presented in Table 22 and Figure 23 the addition of fillers improves the modulus of elasticity of the neat PLA and plasticizer reduces the modulus of elasticity of neat PLA (Tian et al., 2017). Therefore, it is important to consider the tradeoff to achieve the ideal or optimal level of parameters. At the minor inclusion of fillers without plasticizer at higher temperature shows the highest young modulus at experiment 6 (3MCC/3MTT/0S/175T) with value of 4.28 GPa. At this experimental combination the young modulus is increased with 23% more than neat PLA. This improvement basically caused due to the presence of MCC and MTT contents which restricts the molecular chain movement in the PLA and forms physical and chemical interlock with the PLA matrix.

Table 22: Experimental setup and result of TS and YM with S/N ratio

S.N	Factors				Responses			
	MCC	MTT	S	T	TS (MPa)	S/N Ratio	YM (GPa)	S/N Ratio
1	0	0	0	100	55.5	34.8945	3.28	10.3175
2	0	3	10	125	68.8	36.7630	3.60	11.1261
3	0	6	20	150	72.2	37.1734	3.93	11.8879
4	0	9	30	175	77.7	37.8171	3.70	11.364
5	3	0	10	150	66.6	36.4782	3.38	10.5783

6	3	3	0	175	77.7	37.8171	4.26	12.5882
7	3	6	30	100	67.7	36.6217	3.44	10.7312
8	3	9	20	125	75.5	37.5653	3.53	10.9555
9	6	0	20	175	58.3	35.3178	3.12	9.8831
10	6	3	30	150	72.2	37.1734	3.75	11.4806
11	6	6	0	125	78.8	37.9403	4.13	12.319
12	6	9	10	100	83.3	38.4164	3.95	11.9319
13	9	0	30	125	66.6	36.4773	2.55	8.1308
14	9	3	20	100	70.5	36.9706	2.63	8.3991
15	9	6	10	175	81.6	38.2409	2.89	9.218
16	9	9	0	150	78.8	37.9403	3.21	10.1301

The best S/N ratios shown in Table 22 for TS is 38.41 at experiment number 12 and also offer the higher TS value 83.3 MPa. The weakest S/N ratio is 34.89 observed at experiment 1. The best S/N ratios of YM is observed at the experimental 6 with the value of 12.58 and the weakest S/N ratio is observed at experiment 13 with the value of 8.13.

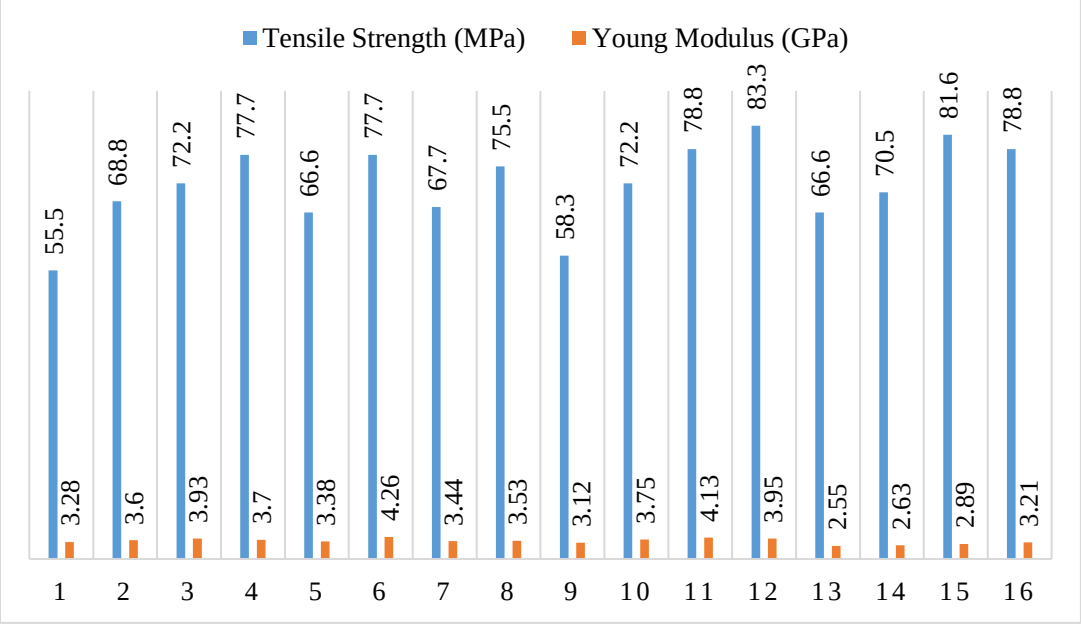

Figure 23: Tensile strengths and young modulus of each experimental design

Probability Plot

Probability plot shows each value of experimental setup against the percentage of values in the specimen that are less than or equal to it, along a fitted distribution line. Figure 24 exhibits that all sample values are under normal distribution at the confidence level of 95%. The two lines beside the center line on the left and right shows the upper and lower limit of confidence interval. There

is no any sample value is out of the confidence interval. This tendency offers improved outcome for future estimation of process characteristics.

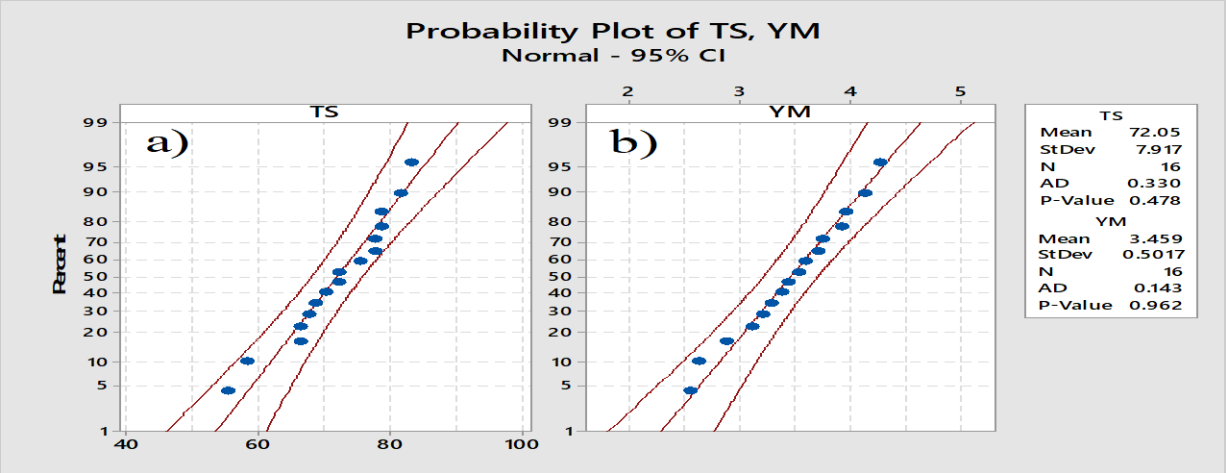

Figure 24: Probability plot of TS and YM

Signal to Noise Ratio Analysis of Tensile strength and young modulus

Table 23 shows the S/N ratios of TS for greater is the better characteristic in order to maximize the tensile strength of bio composite material. For larger is the better, tensile strength features, the optimal experimental setting is 9%MCC, 9%MTT, 10%S, and 1750C. MTT has the greatest effect on tensile strength, followed by MCC, and then S and T, respectively. The validation test experiment indicates that the TS of the synthesized material is 85.2 MPa at this optimal level combination. The main effects plot for S/N ratios of TS is presented in Fig. 25 (a).

Table 23: Response Table for S/Noise Ratios of TS (Larger is the better)

Level	MCC	MTT	S	T
1	36.66	35.79	37.15	36.73
2	37.12	37.18	37.47	37.19
3	37.21	37.49	36.76	37.19
4	37.41	37.93	37.02	37.30
Delta	0.75	2.14	0.72	0.57
Rank	2	1	3	4

Table 24 presents the S/N ratios of young modulus of bio composites. The optimal experimental setup for larger is the better characteristics of young modulus is at 6%MCC, 9%MTT, 0%S and 150^0C and primarily affects by MCC followed by MTT, then S and T affects, respectively and at this level, the YM of synthesized material is 4.22 GPa. The main effects plot for S/N ratios of young modulus is presented in Fig. 25 (b).

Table 24: Response Table for S/N Ratios of young modulus (Larger is the better)

Level	MCC	MTT	S	T
1	11.174	9.727	11.339	10.345
2	11.213	10.898	10.714	10.633
3	11.404	11.039	10.281	11.019
4	8.969	11.095	10.427	10.763
Delta	2.434	1.368	1.057	0.674
Rank	1	2	3	4

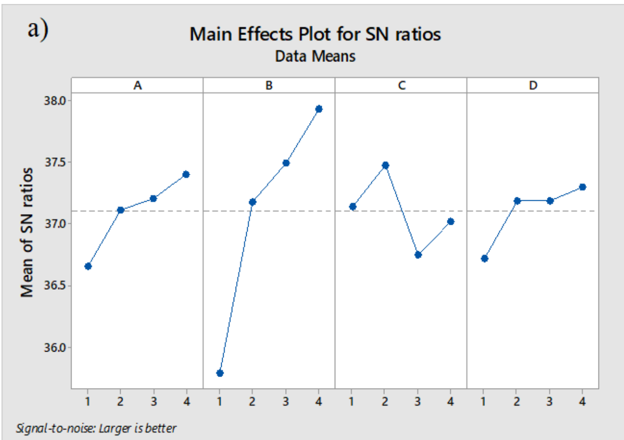

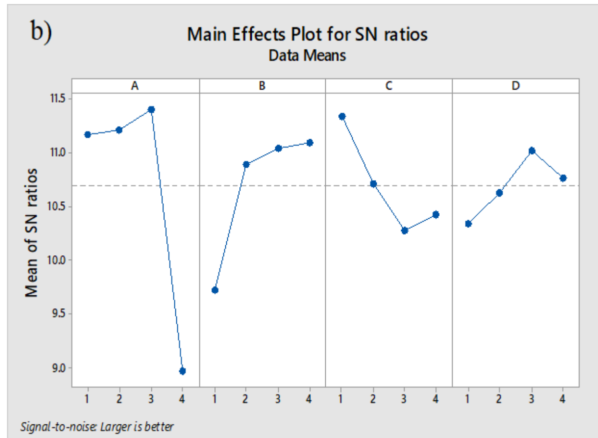

Figure 25: Main effects plot for S/N ratios of (a) tensile strength and (b) young modulus

Regression Analysis

The regression analysis is a statistical technique that explains the correlation between factors and one or more responses. The relation between tensile strength and young modulus has with the input parameters i.e. MCC content, MTT content, S content and temperature are given by regression equation as follows;

TS = 53.16 + 1.87 MCC + 5.40 MTT - 1.10 S + 1.37 T ………………………….. (29)

YM = 3.802 – 0.2338 MCC + 0.1583 MTT – 0.1232 S + 0.0618 T ……………… (30)

ANOVA for regression model of TS and YM of bio composite

The significances of factors incorporated in regression equation of tensile strength is given in ANOVA Table 25. The regression P-value (0.002) lesser than 0.05 suggests that a statistically significant relationship occurs between factors and responses in the experimental design and factors P-value lesser than 0.05 shows the most significance parameter that influences the regression equation. Additionally, the larger F-value shows the more significant factor that influence the response. Table 25 presents that MTT P-value 0.000 and F-value 28.68 indicates that

MTT is the most significant factor for regression model of tensile strength, and factor MCC, T and S has less and less significances respectively.

Table 25: ANOVA for regression equation of TS

Source	DF	Adj SS	Adj MS	F-Value	P-Value
Regression	4	716.14	179.04	8.79	0.002
MCC	1	70.27	70.27	3.45	0.090
MTT	1	583.96	583.96	28.68	0.000
S	1	24.10	24.10	1.18	0.300
T	1	37.81	37.81	1.86	0.200
Error	11	223.97	20.36		
Total	15	940.11			

Table 26 presents the significances of factors incorporated in regression equation of young modulus. The Table 26 clearly shows that regression P-value 0.066 suggests that the factors incorporated in the experimental setup are satisfactory for the linear model and factors P-value lesser than 0.05 shows the most significance parameter that influences the regression equation. Additionally, the larger F-value shows the more significant factor that influence the regression response. Table 26 exhibits that MCC P-value 0.025 and F-value 6.67 indicates that MCC is the most significant factor that affect the regression model of bio composite young modulus, and factor MTT, S and T has less and less significances, respectively.

Table 26: ANOVA for regression model of YM

Source	DF	Seq SS	Adj SS	Adj MS	F-Value	P-Value
Regression	4	1.97372	1.97372	0.49343	3.01	0.066
MCC	1	1.09278	1.09278	1.09278	6.67	0.025
MTT	1	0.50086	0.50086	0.50086	3.06	0.108
S	1	0.30381	0.30381	0.30381	1.85	0.200
T	1	0.07626	0.07626	0.07626	0.47	0.509
Error	11	1.80158	1.80158	0.16378		
Total	15	3.77529				

4.10 Hardness and Impact Strength

The hardness and impact strength of developed bio composites has been improved compared with that of the neat PLA as shown in Table 27. The results show that the hardness for neat PLA is 87.1 HV whereas the hardness of developed bio composites are higher. The maximum bio composite is recorded at experiment 12 with the hardness value of 134.6, which is 54.5% higher than that of neat PLA value. Similar trends are recorded on the best and weakest S/N ratios as shown in Table 27. The finding is consistent with tensile strength of developed bio composite. The increase in

hardness values of the synthesized bio composite is most probably due the higher crystallinity of both MTT and MCC leads to greater hardness because crystalline regions are more rigid and resistant to indentation compared to amorphous regions. Additionally, MCC and MTT can form hydrogen bonds with the PLA matrix. These bond restrict the mobility of PLA chains, leading to increased hardness. Further, the impact strength of PLA is improved with the addition of fillers and plasticizer and the higher result is observed at experiment 16 with the value of 53.8 J/m, at this experimental setup higher concentration of MCC and MTT improve the material's ability to absorb energy during impact, decreasing the risk of failure under sudden loading conditions. These increase in impact strength maintaining its brittleness caused mainly due to the incorporation of plasticized, micro and Nano fillers. The addition of nanoparticles and fibers combination can offer energy absorption mechanisms and crack bridging, resulting in enhanced impact resistance. Additionally, improvement of interfacial bonding between matrix and reinforcing agent can improve the impact strength without meaningfully affecting brittleness.

Table 27: Experimental setup and result of hardness value and impact strength with S/N ratio

S.N	Factors				Responses			
	MCC	MTT	S	T	HV	S/N	IS	S/N
1	0	0	0	100	87.1	38.800	26.7	28.5302
2	0	3	10	125	91.4	39.219	30.9	29.7992
3	0	6	20	150	108.9	40.741	35.2	30.9309
4	0	9	30	175	119.0	41.511	36.9	31.3405
5	3	0	10	150	102.4	40.206	30.6	29.7144
6	3	3	0	175	113.6	41.108	37.1	31.3875
7	3	6	30	100	106.1	40.514	37.9	31.5728
8	3	9	20	125	110.7	40.883	44.1	32.8888
9	6	0	20	175	98.6	39.878	40.1	32.0629
10	6	3	30	150	108.4	40.701	43.0	32.6694
11	6	6	0	125	124.3	41.889	45.3	33.1220
12	6	9	10	100	134.6	42.581	51.2	34.1854
13	9	0	30	125	94.6	39.518	39.6	31.9539
14	9	3	20	100	104.3	40.366	45.3	33.1220
15	9	6	10	175	127.6	42.117	52.2	34.3534
16	9	9	0	150	123.8	41.854	53.8	34.6156

Probability Plot

Figure 26 displays the probability plots for the hardness values and impact strength of all samples. As shown in Fig. 26(a) and (b), all data points fall within a normal distribution at the 95% confidence level. The upper and lower bounds of the confidence interval are represented by the

two lines flanking the central line. Notably, none of the sample values exceed these confidence limits. Furthermore, the p-values of 0.956 for HV and 0.885 for IS both exceeding the significance threshold of 0.05 confirm that the data follow a normal distribution.

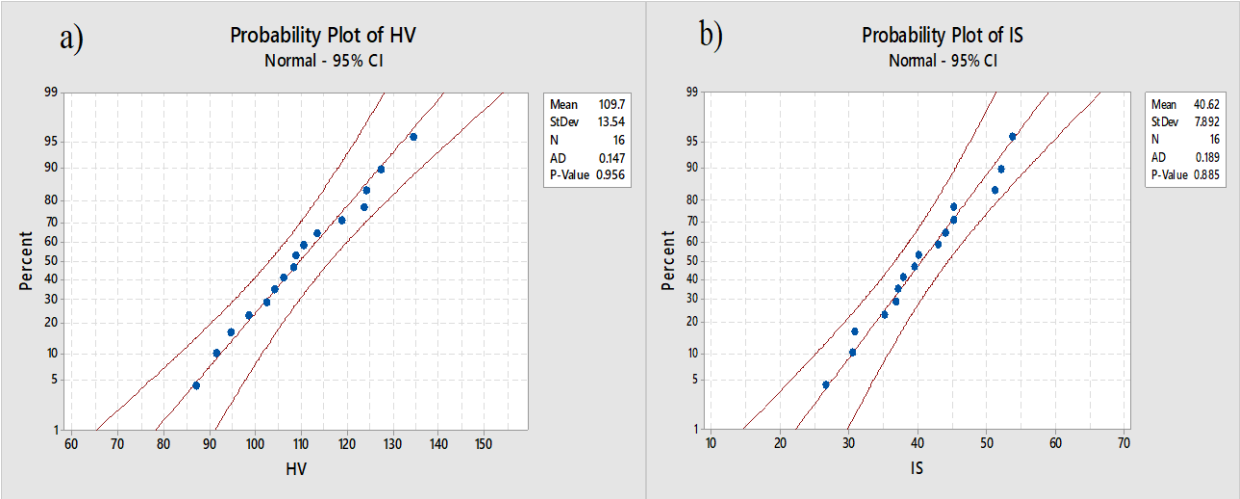

Figure 26: Probability plot for (a) hardness value and (b) impact strength

S/N Ratio Analysis of Hardness Values and Impact Strength

Table 28 and 29 shows the S/N ratios of hardness value and impact strength for higher is the better characteristic in order to maximize the values of developed material. The hardness value optimal experimental setup for larger is the better characteristics is 6%MCC/9%MTT/10%S/175T at this experimental levels its value is 138.2 and MTT primarily affects the hardness value followed by MCC, then T and S affects respectively. The main effects plot for S/N ratios of hardness value is presented in Figure 27 (a). The optimal impact strength is obtained at experimental setup of 9%MCC/9%MTT/20%S/175T at this experimental level its value is 54.2 J/m. This indicates that the energy absorption of the samples increases with the higher content of fillers and up to 20% of plasticizer and MCC highly affects the IS followed by MTT, T, and S, respectively as shown in Table 29 and Figure 27 (b).

Table 28: Response Table for Signal to Noise Ratios of Hardness value (Larger is the better)

Level	MCC	MTT	S	T
1	40.07	39.60	40.91	40.57
2	40.68	40.35	41.03	40.38
3	41.26	41.32	40.47	40.88
4	40.96	41.71	40.56	41.15
Delta	1.19	2.11	0.56	0.78
Rank	2	1	4	3

Table 29: Response Table for Signal to Noise Ratios of Impact Strength (Larger is the better)

Level	MCC	MTT	S	T
1	30.15	30.57	31.91	31.85
2	31.39	31.74	32.01	31.94
3	33.01	32.49	32.25	31.98
4	33.51	33.26	31.88	32.29
Delta	3.36	2.69	0.37	0.43
Rank	1	2	4	3

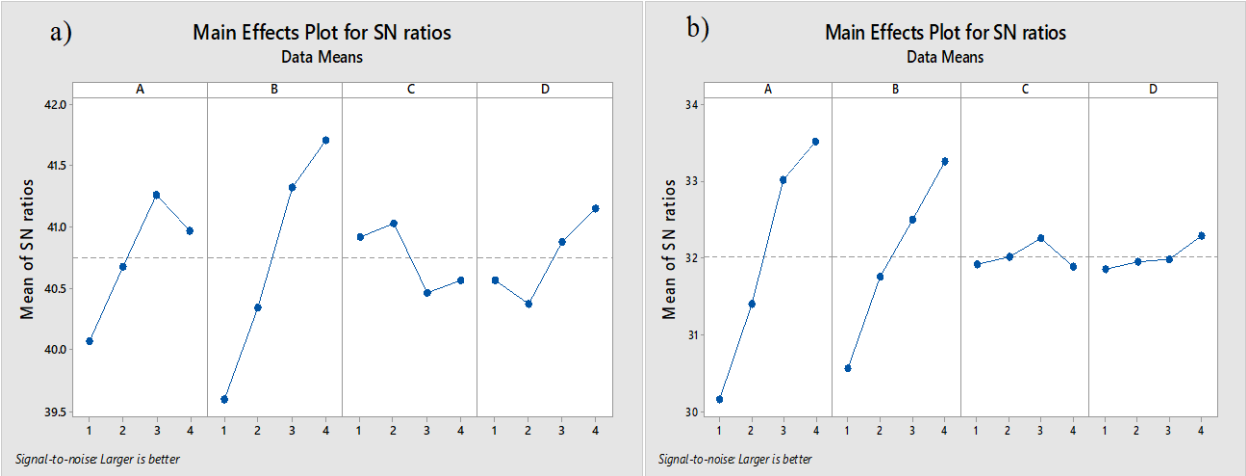

Figure 27: Main effects plot for S/N ratios of (a) hardness and (b) impact strength

Regression Analysis

The regression equation that explains the strength of the relationship between factors with hardness value and impact strength is given as follows;

$$HV = 76.14 + 4.12\ MCC + 9.14\ MTT - 2.39\ S + 2.56\ T \quad \text{..... (31)}$$

$$IS = 17.09 + 5.337\ MCC + 4.033\ MTT - 0.417\ S + 0.458\ T \quad \text{..... (32)}$$

ANOVA for regression model of hardness value and impact strength

The significances of factors incorporated in regression equation of hardness value and impact strength is given in ANOVA Table 30 and 31, respectively. The regression P-value (0.000) for both suggests that a statistically significant relationship occurs between factors and responses in the experimental design and factors P-value lesser than 0.05 shows the most significance element that influences the regression equation. Table 30 presents that MTT P-value 0.000 and F-value 37.06 indicates that MTT is the most significant factor for regression model of hardness value followed by MCC with the p-value of 0.019 and F-value 7.54 and Table 31 presents that MCC is

the most significant factor followed by MTT, and T and S are less significant factor for regression model of impact strength. These results are agree with the S/N ratio analysis of hardness value and impact strength.

Table 30: Analysis of Variance for regression equation of hardness value

Source	DF	Adj SS	Adj MS	F-Value	P-Value
Regression	4	2254.3	563.57	12.51	0.000
MCC	1	339.5	339.49	7.54	0.019
MTT	1	1669.0	1668.96	37.06	0.000
S	1	114.2	114.24	2.54	0.140
T	1	131.6	131.58	2.92	0.115
Error	11	495.4	45.04		
Total	15	2749.7			

Table 31: Analysis of Variance for regression equation of impact strength

Source	DF	Adj SS	Adj MS	F- Value	P-Value
Regression	4	902.671	225.668	78.52	0.000
MCC	1	569.778	569.778	198.26	0.000
MTT	1	325.221	325.221	113.16	0.000
S	1	3.486	3.486	1.21	0.294
T	1	4.186	4.186	1.46	0.253
Error	11	31.613	2.874		
Total	15	934.284			

4.11 Water Absorption and Density

Table 32 displays the water absorption and density of developed bio composite. Under water absorption as clearly observed in Table 32 the combination of MCC, MTT and S addition highly influences the water absorption of PLA. On the experimental setup of higher level of MCC and S such as 6MCC/3MTT/30S/150T and 9MCC/0MTT/30S/125T indicated the higher water absorption of 15.24 and 16.56 %, respectively. This is caused mainly MCC and S has high water absorption trend due higher –OH groups (Abel et al., 2021). Additionally, the water absorption rises with temperature due to the molecular processes. Due to the non-equilibrium vapor pressure at interface increment results increased water molecule absorption of fibers and related to reducing of solid gas interfacial tension improves the water absorption (Songok et al., 2014). The density result shows that the addition of MCC, MTT and S slightly increases the density of PLA. In related studies, the addition of natural fiber (MTT and MCC) in PLA increases the densities of PLA, this is probably due to the fillers have high densities due to most probably by their size advantages (Olonisakin et al., 2022).

Table 32: Water absorption and density of bio composite with S/N ratios

S.N	Factors				Responses			
	MCC	MTT	S	T	WA (%)	S/N Ratio	Density (g/mm^3)	S/N Ratio
1	0	0	0	100	2.56	-8.17871	0.00130	-57.7211
2	0	3	10	125	6.29	-15.9721	0.00133	-57.523
3	0	6	20	150	8.70	-18.786	0.00135	-57.3933
4	0	9	30	175	10.91	-20.7558	0.00138	-57.2024
5	3	0	10	150	5.66	-15.0569	0.00134	-57.4579
6	3	3	0	175	4.35	-12.7654	0.00134	-57.4579
7	3	6	30	100	12.58	-21.9927	0.00133	-57.523
8	3	9	20	125	7.98	-18.0351	0.00136	-57.3292
9	6	0	20	175	9.82	-19.8386	0.00136	-57.3292
10	6	3	30	150	15.24	-23.6619	0.00137	-57.2656
11	6	6	0	125	5.56	-14.8945	0.00135	-57.3933
12	6	9	10	100	6.67	-16.4782	0.00138	-57.2024
13	9	0	30	125	16.56	-24.3835	0.00136	-57.3292
14	9	3	20	100	10.37	-20.3121	0.00137	-57.2656
15	9	6	10	175	7.19	-17.1293	0.00139	-57.1397
16	9	9	0	150	6.51	-16.2701	0.00141	-57.0156

Probability Plot

The normal probability plot shown in Figure 28 represents the comparison between the actual experimental results and the predicted values of water absorption and density. As clearly shown in the Figure 28 all the experimental data are under the interval of 95% confidence level.

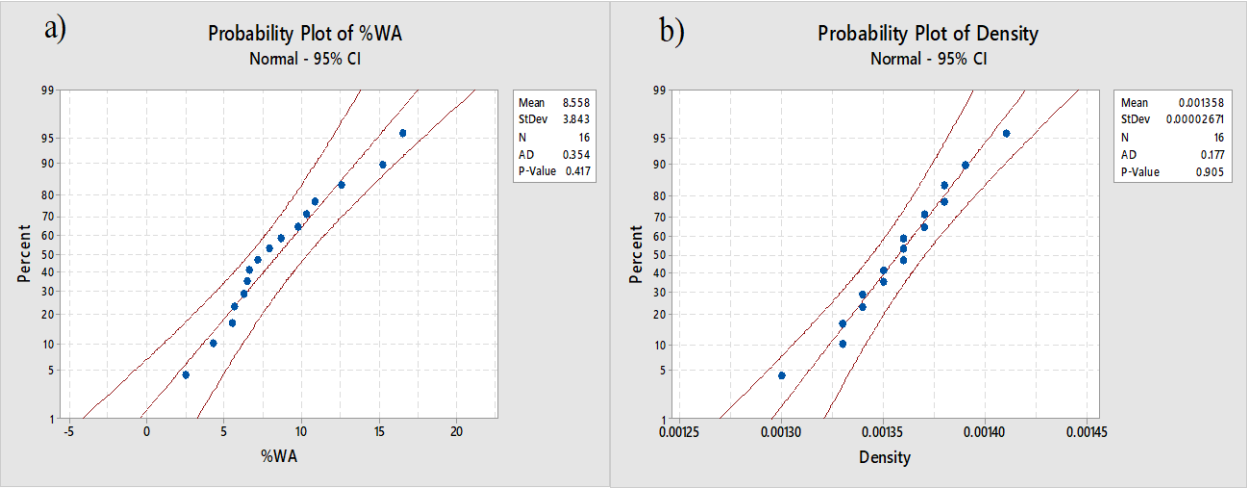

Figure 28: Probability plot for water absorption (a) and density (b) of developed bio composite.

Table 33 and Table 34 shows based on S/N ratio result it can examine which factor has the highest influence on the water absorption and density, respectively. Optimal water absorption factor of controlled variables are investigated on the basis of S/N ratios shown in Table 33 and Fig. 29 (a). The factor highly affect the water absorption are S and MCC, respectively. This is mainly due to a lot of hydroxyl (-OH) groups in these constituents (Lupidi et al., 2023). The optimization of factors of the water absorption in relation to the given factors and levels, with respect to the criterion smaller is the better is at 0MCC/0MTT/0S/100T, which means pure PLA is better in performance of water absorption capacity as shown in Figure 29 (a). Under density the optimal factors are investigated at 9MCC/9MTT/30S/175T as shown in Table 34 and Fig. 29 (b).

Table 33: Response Table for S/N Ratios of water absorption (Smaller is the better)

Level	MCC	MTT	S	T
1	-15.92	-16.86	-13.03	-16.74
2	-16.96	-18.18	-16.16	-18.32
3	-18.72	-18.20	-19.24	-18.44
4	-19.52	-17.88	-22.70	-17.62
Delta	3.60	1.34	9.67	1.70
Rank	2	4	1	3

Table 34: Response Table for S/N Ratios of density (larger is the better)

Level	MCC	MTT	S	T
1	-57.46	-57.46	-57.40	-57.43
2	-57.44	-57.38	-57.33	-57.39
3	-57.30	-57.36	-57.33	-57.28
4	-57.19	-57.19	-57.33	-57.28
Delta	0.27	0.27	0.07	0.15
Rank	1	2	4	3

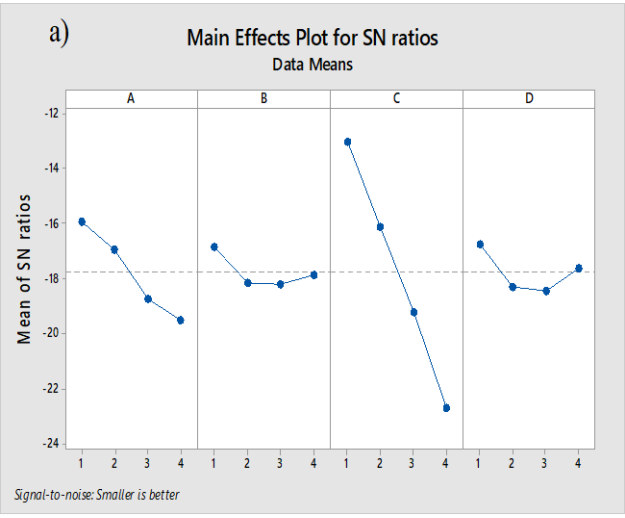

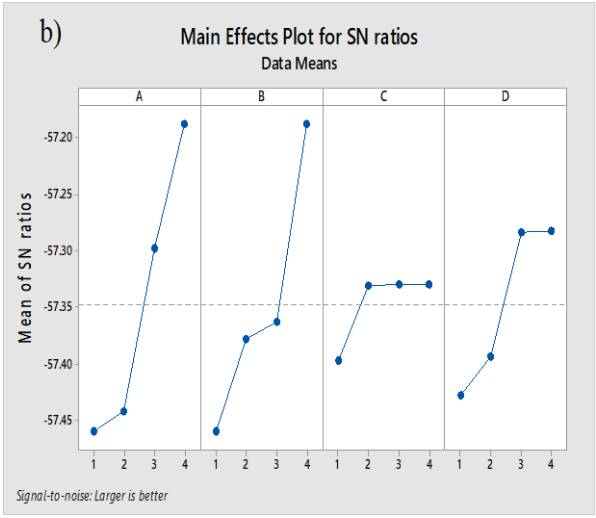

Figure 29: Main effect plot for S/N ratios of water absorption (a) and density (b)

Regression Analysis

The correlation between significant factors and water absorption of developed bio composite is established through linear regression. The regression equation for the % of water absorption and density is shown as follows;

$$\%WA = -1.03 + 1.080\ MCC - 0.247\ MTT + 3.000\ S - 0.001\ T \quad \ldots\ldots (33)$$

$$Density = 0.001259 + 0.000015\ MCC + 0.000013\ MTT + 0.000003\ S + 0.000009\ T \quad \ldots.. (34)$$

ANOVA for regression model of water absorption and density of developed bio composite

The significances of factors incorporated in regression equation of water absorption and density is given in ANOVA Table 35 and 36, respectively. The regression P-value (0.000) suggests, a statistically significant relationship occurs between factors and responses in the experimental design and factors P-value lesser than 0.05 shows the most significance element that influences the regression equation. Table 35 presents that S and MCC are the most significant factor for regression model of water absorption and Table 36 presents MCC, MTT and T are the most significant factor for regression model of density. The same result was observed on S/N analysis of both water absorption and density.

Table 35: ANOVA for regression model of water absorption

Source	DF	Adj SS	Adj MS	F-Value	P-Value
Regression	4	204.596	51.149	33.14	0.000
MCC	1	23.349	23.349	15.13	0.003
MTT	1	1.217	1.217	0.79	0.394
S	1	180.030	180.030	116.63	0.000
T	1	0.000	0.000	0.00	0.998
Error	11	16.980	1.544		
Total	15	221.576			

Table 36: Analysis of Variance for regression model of density

Source	DF	Adj SS	Adj MS	F-Value	P-Value
Regression	4	0.000000	0.000000	21.87	0.000
MCC	1	0.000000	0.000000	41.42	0.000
MTT	1	0.000000	0.000000	31.11	0.000
S	1	0.000000	0.000000	1.66	0.224
T	1	0.000000	0.000000	13.30	0.004
Error	11	0.000000	0.000000		
Total	15	0.000000			

4.12 Grey Relational Analysis of Bio Composite

The responses of developed bio composite at various experimental setup is tabulated as shown Table 37, where all the response data were converted into S/N ratio for further subsequent process according to equation 19 and 20. The S/N ratio of responses are the same as Taguchi orthogonal array analysis as per experimental setup of each combination and tabulated as shown in Table 38.

Table 37: Experimental set up and average experimental result values of responses

Run	Coded Factors				Responses							
	A	B	C	D	TS (MPa)	YM (GPa)	FS (MPa)	FM (GPa)	HV	IS (J/m)	WA (%)	DT (g/mm^3)
1	1	1	1	1	55.5	3.28	52.50	4.1	87.1	26.7	2.56	0.00130
2	1	2	2	2	68.8	3.60	60.00	5.3	91.4	30.9	6.29	0.00133
3	1	3	3	3	72.2	3.93	75.00	6.7	108.9	35.2	8.70	0.00135
4	1	4	4	4	77.7	3.70	82.50	7.5	119.0	36.9	10.9	0.00138
5	2	1	2	3	66.6	3.38	60.00	5.5	102.4	30.6	5.66	0.00134
6	2	2	1	4	77.7	4.26	71.25	7.1	113.6	37.1	4.35	0.00134
7	2	3	4	1	67.7	3.44	75.00	7.5	106.1	37.9	12.5	0.00133
8	2	4	3	2	75.5	3.53	93.75	9.7	110.7	44.1	7.98	0.00136
9	3	1	3	4	58.3	3.12	63.75	6.7	98.6	40.1	9.82	0.00136
10	3	2	4	3	72.2	3.75	63.75	7.1	108.4	43.0	15.2	0.00137
11	3	3	1	2	78.8	4.13	67.50	7.7	124.3	45.3	5.56	0.00135
12	3	4	2	1	83.3	3.95	71.25	8.4	134.6	51.2	6.67	0.00138
13	4	1	4	2	66.6	2.55	45.00	5.0	94.6	39.6	16.5	0.00136
14	4	2	3	1	70.5	2.63	56.25	8.1	104.3	45.3	10.3	0.00137
15	4	3	2	4	81.6	2.89	56.25	7.8	127.6	52.2	7.19	0.00139
16	4	4	1	3	78.8	3.21	60.00	8.6	123.8	53.8	6.51	0.00141

Table 38: S/N ratio values of each experimental setup

Run	S/N ratio							
	TS	YM	FS	FM	HV	IS	WA	DT
1	34.8859	10.3175	34.4032	12.2557	38.8004	28.5302	-8.17871	-57.7211
2	36.7518	11.1261	35.5630	14.4855	39.2189	29.7992	-15.9721	-57.523
3	37.1707	11.8879	37.5012	16.5215	40.7406	30.9309	-18.786	-57.3933
4	37.8084	11.3640	38.3291	17.5012	41.5109	31.3405	-20.7558	-57.2024
5	36.4695	10.5783	35.5630	14.8073	40.2060	29.7144	-15.0569	-57.4579
6	37.8084	12.5882	37.0557	17.0252	41.1076	31.3875	-12.7654	-57.4579
7	36.6118	10.7312	37.5012	17.5012	40.5143	31.5728	-21.9927	-57.523
8	37.5589	10.9555	39.4394	19.7354	40.8830	32.8888	-18.0351	-57.3292
9	35.3134	9.8831	36.0896	16.5215	39.8775	32.0629	-19.8386	-57.3292

10	37.1707	11.4806	36.0896	17.0252	40.7006	32.6694	-23.6619	-57.2656
11	37.9305	12.3190	36.5861	17.7298	41.8894	33.1220	-14.8945	-57.3933
12	38.4129	11.9319	37.0557	18.4856	42.5809	34.1854	-16.4782	-57.2024
13	36.4695	8.1308	33.0643	13.9794	39.5178	31.9539	-24.3835	-57.3292
14	36.9638	8.3991	35.0025	18.1697	40.3657	33.1220	-20.3121	-57.2656
15	38.2338	9.2180	35.0025	17.8419	42.1170	34.3534	-17.1293	-57.1397
16	37.9305	10.1301	35.5630	18.6900	41.8544	34.6156	-16.2701	-57.0156

4.12.1 Normalization

The normalization process of each S/N ratios of responses are performed using equation 22 and 23. Each quality responses of all experimental setup would be set into comparability sequence. Equation 22 used for normalization of larger the better characteristics such as tensile, flexural, hardness and impact strength, whereas equation 23 used for normalization of smaller the better characteristics such as water absorption. The normalization results are between 0 and 1. The experimental response that has excellent quality have to a result of 1 and the poorest has 0 value. The normalization values of each experimental setup are tabulated in Table 39.

Table 39: Normalized S/N ratio values of each experimental setups

Run	TS	YM	FS	FM	HV	IS	WA	DT
1	0.0000	0.4906	0.2100	0.0000	0.0000	0.0000	0.0000	0.0000
2	0.5290	0.6720	0.3920	0.2981	0.1107	0.2085	0.4739	0.2810
3	0.6478	0.8429	0.6960	0.5703	0.5132	0.3945	0.6743	0.4402
4	0.8286	0.7254	0.8258	0.7013	0.7170	0.4618	0.7763	0.7532
5	0.4490	0.5491	0.3920	0.3411	0.3718	0.1946	0.4287	0.2810
6	0.8286	1.0000	0.6261	0.6377	0.6103	0.4695	0.2797	0.3849
7	0.4893	0.5834	0.6960	0.7013	0.4534	0.5000	0.8550	0.2906
8	0.7579	0.6337	1.0000	1.0000	0.5509	0.7162	0.6118	0.5656
9	0.1212	0.3931	0.4746	0.5703	0.2849	0.5805	0.7291	0.5831
10	0.6478	0.7515	0.4746	0.6377	0.5026	0.6802	0.9677	0.6862
11	0.8632	0.9396	0.5524	0.7319	0.8171	0.7545	0.3856	0.4856
12	1.0000	0.8528	0.6261	0.8329	1.0000	0.9293	0.5489	0.7282
13	0.4490	0.0000	0.0000	0.2305	0.1898	0.5626	1.0000	0.5656
14	0.5891	0.0602	0.3040	0.7907	0.4140	0.7545	0.7447	0.6437
15	0.9492	0.2439	0.3040	0.7468	0.8773	0.9569	0.5744	0.8268
16	0.8632	0.4485	0.3920	0.8602	0.8078	1.0000	0.5427	1.0000

The normalized result as shown in Table 37 shows that all characteristics are scaled between 0 and 1. This ensures all the data are treated equally even data have different values and units without one objective (maximizing or minimizing) dominating the others. This allows for a balanced and fair optimization of multiple objectives, leading to better decision-making and more robust solutions. The proceeding process, deviation sequence represents the absolute difference between the normalized values of the performance characteristics and the ideal (reference) value. The ideal value is usually 1 for normalized data because normalization scales the data to a range of 0 to 1, where 1 represents the best possible value. Table 40 represents the deviation sequence of the normalized data.

Table 40: Deviation sequence

Run	TS	YM	FS	FM	HV	IS	WA	DT
1	1.0000	0.5094	0.7900	1.0000	1.0000	1.0000	1.0000	1.0000
2	0.4710	0.3280	0.6080	0.7019	0.8893	0.7915	0.5261	0.7190
3	0.3522	0.1571	0.3040	0.4297	0.4868	0.6055	0.3257	0.5598
4	0.1714	0.2746	0.1742	0.2987	0.2830	0.5382	0.2237	0.2468
5	0.5510	0.4509	0.6080	0.6589	0.6282	0.8054	0.5713	0.7190
6	0.1714	0.0000	0.3739	0.3623	0.3897	0.5305	0.7203	0.6151
7	0.5107	0.4166	0.3040	0.2987	0.5466	0.5000	0.1450	0.7094
8	0.2421	0.3663	0.0000	0.0000	0.4491	0.2838	0.3882	0.4344
9	0.8788	0.6069	0.5254	0.4297	0.7151	0.4195	0.2709	0.4169
10	0.3522	0.2485	0.5254	0.3623	0.4974	0.3198	0.0323	0.3138
11	0.1368	0.0604	0.4476	0.2681	0.1829	0.2455	0.6144	0.5144
12	0.0000	0.1472	0.3739	0.1671	0.0000	0.0707	0.4511	0.2718
13	0.5510	1.0000	1.0000	0.7695	0.8102	0.4374	0.0000	0.4344
14	0.4109	0.9398	0.6960	0.2093	0.5860	0.2455	0.2553	0.3563
15	0.0508	0.7561	0.6960	0.2532	0.1227	0.0431	0.4256	0.1732
16	0.1368	0.5515	0.6080	0.1398	0.1922	0.0000	0.4573	0.0000

4.12.2 Grey Relational Coefficient and Grade

Grey relational coefficient (GRC) is investigated to define the correlation between the reference sequence (target or ideal) and actual normalized values. The higher GRC are the nearer reference sequence and actual experimental trials. The GRC was determined using equation (25) and each experimental trials is presented in Table 41. The grey relational grade (GRG) was determined by calculating the mean of GRC using equation (26) and used to find the optimum processing factors. At this stage multiple responses are converted to single GRG and optimized. The optimal level of

parameters will be the highest GRG parameter levels. The GRG of all experimental trials are tabulated in Table 41 with their ranking. As clearly shown in Table 41 the highest weighted GRG is at experiment 12, which is better for approaching ideal value 1. Therefore, the best test sequence for gaining better mechanical and physical properties is at 6 Wt% of MCC, 9Wt% of MTT and 10Wt% of Sorbitol with 100 ^{0}C of Temperature (6%MCC/9%MTT/10%S/100^{0}C T).

Table 41: Grey relational coefficient and grey relational grade

Run	TS	YM	FS	FM	HV	IS	WA	DT	Grade	S/N	Rank
1	0.3333	0.4953	0.3876	0.3333	0.3333	0.3333	0.3333	0.3333	0.36	-8.86	16
2	0.5149	0.6038	0.4512	0.4160	0.3599	0.3872	0.4873	0.4102	0.45	-6.85	14
3	0.5867	0.7609	0.6219	0.5378	0.5067	0.4523	0.6055	0.4718	0.56	-4.91	9
4	0.7447	0.6455	0.7417	0.6260	0.6386	0.4816	0.6909	0.6695	0.65	-3.76	5
5	0.4757	0.5258	0.4512	0.4315	0.4432	0.3830	0.4667	0.4102	0.45	-6.86	15
6	0.7447	1.0000	0.5721	0.5798	0.5620	0.4852	0.4097	0.4484	0.60	-4.43	8
7	0.4947	0.5455	0.6219	0.6260	0.4777	0.5000	0.7751	0.4134	0.55	-5.18	10
8	0.6737	0.5772	1.0000	1.0000	0.5268	0.6379	0.5630	0.5351	0.68	-3.23	3
9	0.3626	0.4517	0.4876	0.5378	0.4115	0.5438	0.6486	0.5453	0.49	-6.04	12
10	0.5867	0.6680	0.4876	0.5798	0.5013	0.6099	0.9393	0.6144	0.62	-4.20	7
11	0.7852	0.8922	0.5277	0.6509	0.7322	0.6707	0.4487	0.4929	0.65	-3.74	6
12	1.0000	0.7725	0.5721	0.7495	1.0000	0.8761	0.5257	0.6479	0.77	-2.20	1
13	0.4757	0.3333	0.3333	0.3938	0.3816	0.5334	1.0000	0.5351	0.49	-6.15	13
14	0.5489	0.3473	0.4181	0.7049	0.4604	0.6707	0.6620	0.5839	0.55	-5.20	11
15	0.9078	0.3981	0.4181	0.6639	0.8029	0.9207	0.5402	0.7428	0.68	-3.40	4
16	0.7852	0.4755	0.4512	0.7815	0.7224	1.0000	0.5223	1.0000	0.71	-2.88	2

Equation 26 was used to calculate the GRG means and S/N ratios for each level of input components, which are shown in Table 41. Higher - the - better characteristics is required for grey relational grade. The combination with the highest S/N ratio represents the optimal settings that has better performances in mechanical and physical properties, and are least affected by noise factors. Additionally, this selected optimal combination is further optimized as a single objective to determine whether there is another, better option than the combination given (L16). Figure 30 allows to conclude that there is another, better ideal or optimal parametric combination than the one mentioned (L16). Therefore, 6 Wt% MCC, 9 Wt% MTT, 10 Wt% S, and 175^{0}C T is the best or optimal parametric combination for better response characteristics. At this parametric combination the improvement of mechanical and physical properties of the synthesized bio composite sample is expected. Having the results of GRG main effects and the effects of factors are presented in Table 42 and Figure 30.

Table 42: Response table for grey relational grade

Parameter	Level				Delta	Rank
	1	2	3	4		
MCC	0.5076	0.5726	0.6355	0.6098	0.1278	2
MTT	0.4504	0.5543	0.6123	0.7086	0.2582	1
S	0.5820	0.5931	0.5763	0.5741	0.0190	4
T	0.5591	0.5704	0.5882	0.6078	0.0487	3

Total mean values of gray relational grade (average of total grade) = **0.581381.**

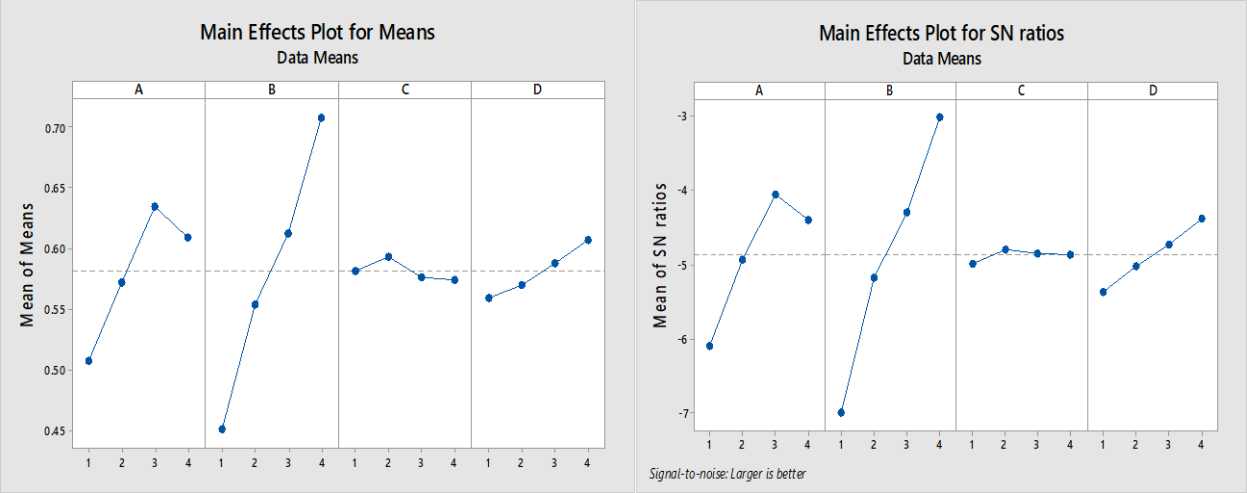

Figure 30: Effects of parameters on grade results

4.12.3 Analysis of Variance (ANOVA) for GRG

Based on grey relational grade result, ANOVA is conducted to isolate the significant processing parameters. As clearly shown in Table 43, the contribution (%) of every parameter on the entire deviation with their degree of consequence on the results obtained, the MTT (73.85%) highly affects MCC/MTT/S/PLA bio composite followed by MCC (19.5%), T (2.86%) and S (0.45%), respectively. This result not implies the non-significances of the materials availability on the developed bio composite but shows the effects of level variation of factor such as MCC, T and S are low relative to MTT in the synthesized bio composite sample. The properties examined in this study such as FS, FM, TS, YM, HV, IS, %WA, and D are highly affected by the availability and the variation of MTT due to distributions of its layered structure, which has a large surface area and aspect ratio (length to thickness) compared to MCC, can greatly increases the interfacial area between the PLA, MCC and MTT, leads to performance improvement of the developed MCC/MTT/S/PLA bio composite.

Table 43: ANOVA for grade of grey relational

Source	DF	Seq SS	Adj SS	Adj MS	F	P	Contribution (%)
A	3	0.037012	0.037012	0.012337	5.89	0.090	19.5
B	3	0.140117	0.140117	0.046706	22.31	0.015	73.85
C	3	0.000866	0.000866	0.000289	0.14	0.931	0.45
D	3	0.005435	0.005435	0.001812	0.87	0.546	2.86
Residual Error	3	0.006279	0.006279	0.002093			
Total	15	0.189709					

S = 0.04575 R-Sq = 96.7% R-Sq(adj) = 83.5%

4.12.4 Optimum value grade prediction and validation test

The optimum grade of grey relation is estimated at the obtained (particular) optimum setting of input factors. The optimal factor with their significant level was formerly identified as MCC6, MMT9, S10 and T175. The predicted grade of grey relational would be determined by Equation (35).

$$\gamma_{(predicted)} = \gamma_t + \sum_{i=1}^{n} (\gamma_i - \gamma_t) \quad \ldots\ldots\ldots\ldots\ldots\ldots\ldots\ldots\ldots\ldots\ldots\ldots (35)$$

Where γ_t - average of entire GRG, γ_i - average of optimal level GRG, and n = the number of bio composite preparation parameters that noticeably influence the multiple performance characteristics. The MCC6, MTT9, S10 and T175 is an optimum factors setting of the composite material identified through GRA and it's treated as an observation of validation. According to Equation (35) the predicted GRG can be achieved. Table 44 shows the responses of validation observation through the optimum input factors. As clearly tabulated on Table 44, the TS is improved from 55.5 to 86.7 MPa, the YM is improved from 3.28 to 4.65, the FS is increased from 52.5 to 79.4 GPa, the FM is improved from 4.1 to 8.82 GPa, the HV is improved from 87.1 to 142.6, the IS is increased from 26.7 to 56.3 J, WA is improved from 2.48 to 6.92% and density also improved from 0.00130 to 0.00137 g/mm^3. Additionally, the predicted GRG value was improved from 0.789 to 0.846, which indicates the enhancement of synthesized bio composite properties when optimum sample preparation factors are used. Therefore, the optimum sample fabricated via optimum parametric combination shows significant mechanical property improvement and GRG value enhancement.

Table 44: Comparison between properties of bio composite using first and optimum preparation factors.

	First observation input factors	Optimum input factors	
		Prediction	Experiment
Combination level	A1B1C1D1	A3B4C2D4	A3B4C2D4

TS (MPa)		55.5	-	86.7
YM (GPa)		3.28	-	4.65
FS (MPa)		52.5	-	79.4
FM (GPa)		4.1	-	8.82
HV		87.1	-	142.6
IS (J/m)		26.7	-	56.3
WA (%)		2.48	-	6.92
DT (g/mm^3)		0.00130	-	0.00137
GRG	Mean	0.3604	0.789625	0.8460
	S/N	-8.865	-1.76532	-1.4527

4.12.5 FTIR Spectroscopy

Figure 31 shows the IR spectra of neat PLA and optimal sample peak. The FTIR spectra of neat PLA shows broad peaks at 3390 cm^{-1} is associated to a bending vibration of various –OH groups and the absorptions at 2928 and 2850 cm^{-1} are corresponds to an unsymmetrical stretching vibration mode of C–H group. The absorptions at 1442 and 1046 cm^{-1} attributed to –CH3 and –OH bending vibrations, the observation at 1089 cm^{-1} is attributed to the stretching vibration of C–O groups. The optimal sample peak contains MTT and MCC as a fillers and S as a plasticizers. The availability of MTT into the PLA is represented by the PLA peak shift of 1046 cm^{-1} to the lower wave number of 1040 cm^{-1} and the peaks showed at 465 and 520 cm^{-1} attributed to stretching vibrations of the Si–O groups of the MTT filler. These modifications in the IR spectra implicates the interaction of MTT filler and PLA using polar interactions of both material functional groups are good. Mainly, the MTT has huge polar sites numbers that uniformly distributed on the surfaces (M. Liu et al., 2013). The peak shifting of PLA based nano composite is probably caused by polar interaction of PLA hydroxyl groups and MTT Si-O groups (Arjmandi, Hassan, Eichhorn, et al., 2015).

The availability of MCC in the optimal sample is represented by the absorption at 2925 cm^{-1} which attributes the stretching vibrations of CH_3 (symmetric) in neat PLA and become sharper in the optimal sample and broader absorption peak at 3390 cm^{-1} that associates to stretching vibration of OH groups, the absorption intensity increased due to MCC and sorbitol occurrence. The position of peak at 1597 cm^{-1} which attributes to band of amide II (N-H bending vibration) and 894 cm^{-1} unchanged shows, the β-glycoside and amino bonds were not involved (W. Zhang et al., 2023). Additionally, the peak observed at 956 cm^{-1} represents the vibration of helical backbone of CH_3 with the occurrences of MCC. The broad peak between 3000 and 3600 cm^{-1} narrowed and slight

shift from PLA implies the availability of sorbitol on the optimal sample and sorbitol disturbed the hydrogen bonds between PLA molecules (Ma et al., 2018).

Moreover, in Fig. 31 IR spectra, the addition of MTT and MCC filler in PLA influences the IR spectra of neat PLA. The observation of new functional group in the spectrum is caused due to the chemical interaction of MTT and PLA. However, MCC interacts only physically with PLA there is no chemical interaction between them, also same opinion was reported by other researcher (Arjmandi et al., 2016; Rasheed et al., 2021). The physical and chemical interaction exist between the polymer matrix and the reinforcing fillers refers the bond and forces exist between them. These interactions play a critical role in determining the overall performance and properties of the bio composite material. The main physical interactions found in polymer bio composites are non-covalent bonds includes; intermolecular forces (van der waals forces, hydrogen bonding), mechanical interlocking, Adsorption and wetting, and etc. The chemical interactions are covalent bonds exist between filler and base material. Therefore, the physical interaction between MCC and PLA lead to an interphase development which yields characteristics which are modifications of those of the individual component.

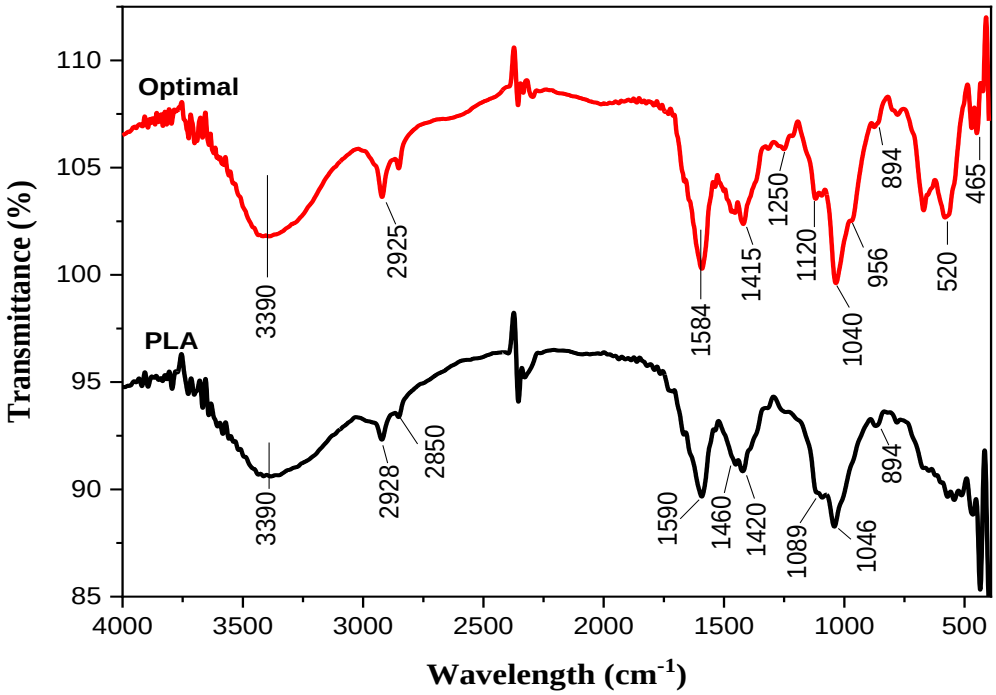

Figure 31: IR spectra of PLA and Optimal sample

4.12.6 X-Ray Diffraction Pattern

The XRD patterns of PLA and optimal bio composite are shown in Fig. 32. For each investigation one sample was used to analyze the structural variation between neat PLA and optimal sample. The diffraction peaks of PLA and optimal sample are noticeably on the same locations, but their intensity is different. The neat PLA X-ray diffraction pattern has average crystalline size of 11.78 nm and 72.98% crystalline index, and the average crystalline size (5.89 nm) of optimal sample is smaller than PLA and the crystalline index is improved by 11.73% found to be 82.67% as shown in Table 45. The larger number of finer crystallinities of optimal sample increases crystallinity of the bio composite. The high peaks at 13.68^0 and 16.8^0, and small peaks observed at 19.3^0, 22.1^0, 25.5^0, 27.2^0, 29.9^0, and 43.8^0 observed at PLA are increased in optimal sample without changing the crystal structure of PLA, this is caused due to the molecular weight of fillers has no considerable molecular chain movement difference on crystallization process (Wu et al., 2020). This growth of optimal sample intensity and reduction in the crystalline size caused for the improvement of mechanical properties of optimal sample from pure PLA. Additionally, the non-development of other diffraction peak indicates that the layers of silicate structure are consistent and randomly spread in PLA at nanosize (Chuayjuljit et al., 2009; W. Zhang et al., 2023). Further, these represents the distributions and intercalation of MMT filler in PLA (Sanusi et al., 2021).

Table 45: Crystalline index of neat PLA and optimal sample.

Sample	The total area of crystalline peaks	Areas of all peaks	Crystalline index (CI %)	Crystallite size (nm)
PLA	19559.08	26799.1	72.98	11.78
Optimal	20209.66	16707.56	82.67	5.89

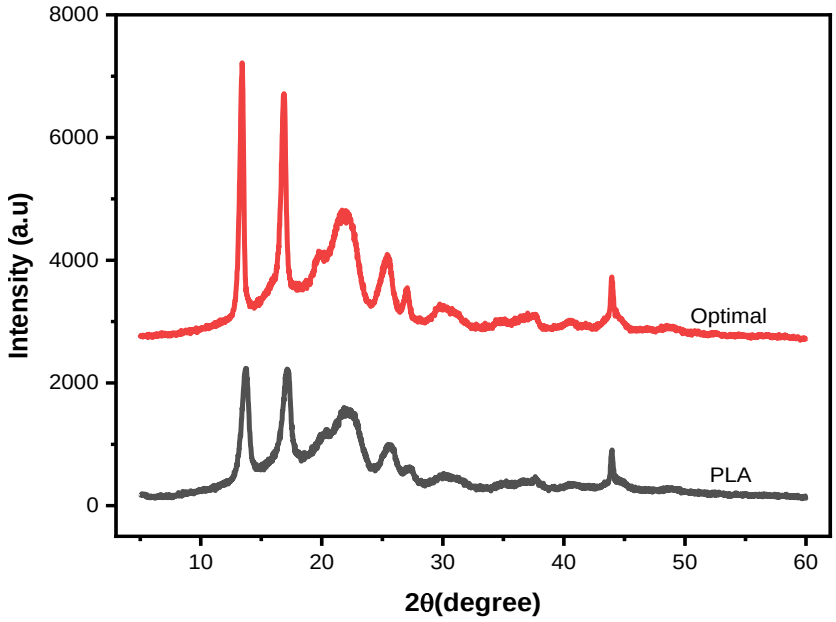

Figure 32: X-ray diffraction pattern of PLA and optimal sample

4.12.7 Thermo-Gravimetric Analysis

TGA and DTG plots of PLA and optimal (MCC/MTT/S/PLA) bio composite sample are presented in Figure 33. For each analysis one sample was used to analyze the thermal variation of optimal sample from the pure PLA sample. From Figure 33 (a) the TGA (Weight, % vs. Temperature, ˚C) plot shows the onset degradation temperature (T_{on}) and maximum weight loss temperature (T_{max}) of neat PLA and optimal sample. The neat PLA begins to degrade nearby 280^{o}C and shows single-step loss of weight in the range of 280-330^{o}C, remaining small quantity (6.6 %) of residue char at 600^{o}C. The inclusion of fillers not significantly affect the thermal degradation point of optimal bio composite sample and it follows the same one-stage weight loss temperature (285-240^{o}C) nearby the range of PLA, similar pattern also observed when PLA blend with epoxidized palm oil (Giita Silverajah et al., 2012) and recycle PLA (Bergaliyeva et al., 2023). However, thermal stability is improved at higher temperature (240^{o}C and above) and the amount of residue char increased significantly from 6.6 to 28.8%, which is probably caused due to the presence of MTT (flame retardant) content. The presence of MTT reduces the heat release rate and increase the smoke yields. In combustion, nano-clays move to the surface of the polymer matrix and to form a dense silicate layer, which resist against the fire as protective layer that slow down the polymer composite for further degradation. Additionally, Nanoclay has the ability to form carbonaceous layer during combustion which will resist the permeability of oxygen but it does not stop the flame (Shah et al., 2017a). The DTG curve of PLA and optimal sample also shows correlated degradation process of

single-stage decomposition pattern characterized by one peak as presented in Figure 33 (b) and exhibits the maximum thermal weight loss rate (WLR_{max}). The similar pattern is observed also when montmorillonite reinforced PLA (Grigora et al., 2022) and similar outcome was stated by (Haafiz et al., 2013) and (Ramesh, Prasad, et al., 2020) when oil palm biomass derived MCC and treated Aloevera fiber and MTT using as reinforcing agent in PLA. The parameters gained from TGA and DTG analysis are tabulated in Table 46.

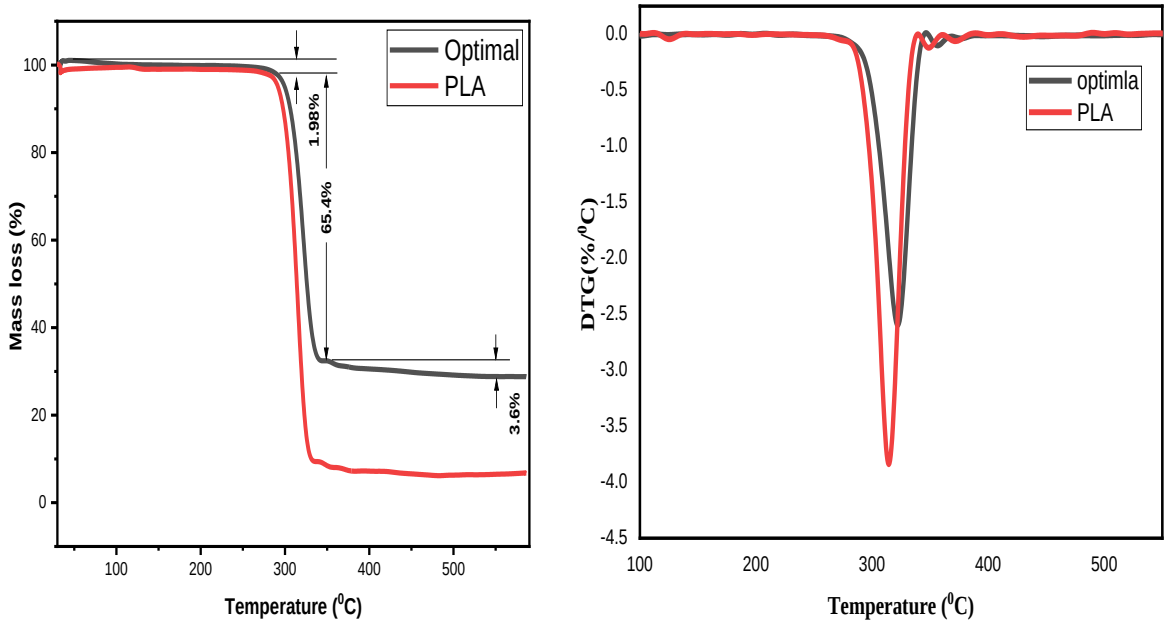

Figure 33: a) TGA and b) DTG analysis of neat PLA and Optimal

Table 46: Variables obtained from TGA and DTG analysis

Samples	T_{on} (^{0}C)	T_{max} (^{0}C)	WLR_{max} (%/^{0}C)	Residue (%)
PLA	280	330	-3.83	6.6
Optimal	285	340	-2.63	28.8

4.12.9 Scanning Electron Microscope

To examine the tensile fractured surfaces of neat PLA and optimal bio composite samples, SEM micrographs were used as shown in Figure 34. For each examinations, one sample was used to study the fracture behavior of samples when exposed to tensile load. The SEM micrograph of neat PLA (a) shows flat fracture surface which represents the characteristics of unfilled matrix and optimal bio composite sample (b) shows rough fracture surface which is typical behavior of filled matrix materials. The dispersion of fillers in the PLA matrix are very well, however they are aggregate (agglomerate) on the matrix material, these significantly affects the mechanical

properties of the synthesized bio composite. The observed characterstics of fillers on PLA is similar to Armandi et al. (Arjmandi, Hassan, Eichhorn, et al., 2015) research work.

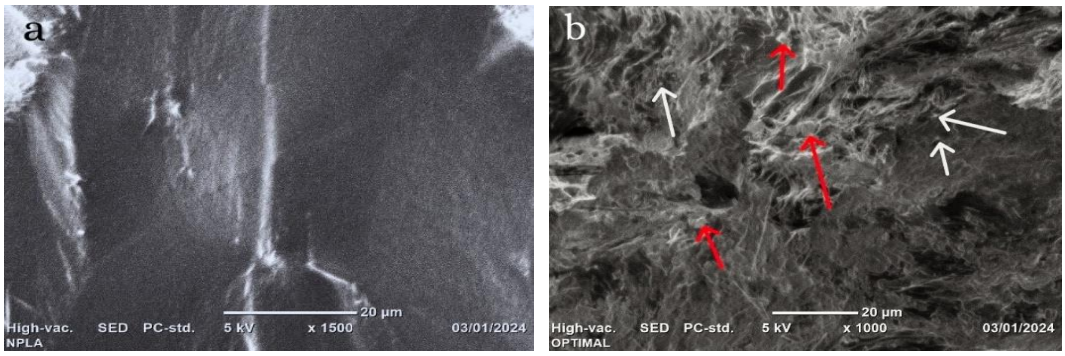

Figure 34: (a) Neat PLA and (b) Optimal sample SEM micrographs of tensile fractured surface. The MCC and MTT fillers are represented by red and white arrows, respectively.

4.12.10 Optical Microscope

The surface of neat PLA and dispersion of MCC/MTT in plasticized PLA were examined through optical microscope. For each examinations, one sample which is selected through purposive sampling was used to study the surface morphology. Figure 35 (a) and (b) presents the surface of neat PLA and optimal (6MCC/9MTT/10S/15T) sample, respectively. Figure 35 (a) indicates that pure PLA surface, and it's observed as smooth surface, similar to SEM analysis. However, Figure 36 (b) indicates that the optimal (MCC/MTT filled plasticized PLA) sample. The dispersion of MCC in PLA is fine but the aggregation of MCC is observed in black spot (indicated by the red arrow) and the dispersion of MTT in PLA is also healthy but the same agglomeration is observed in white spot some areas (indicated by the white arrow), similar observation were reported by Arjmandi et al. (Arjmandi, Hassan, Haafiz, et al., 2015) when the content of fillers (MCC and MTT) are increased.

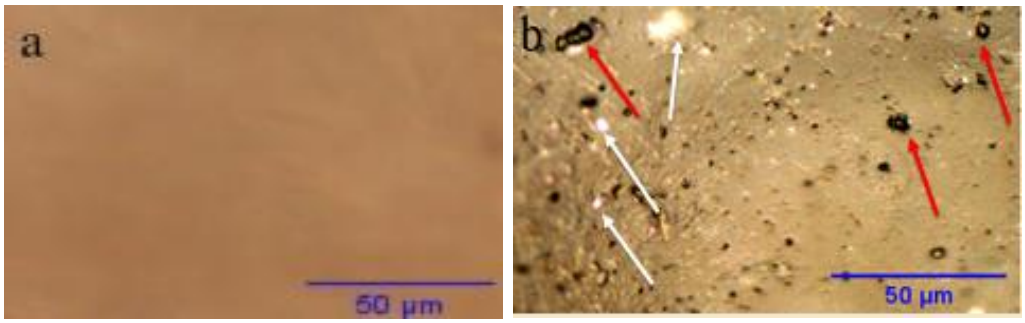

Figure 35: Optical micrographs of (a) neat PLA, (b) optimal sample. The MCC and MTT fillers are represented by red and white arrows, respectively.

4.13 Application of Synthesized MCC/MTT/S/PLA

Based on the findings of the MCC and MTT – filled and sorbitol plasticized PLA, a possible applications are recommended in this section. Currently, neat PLA has been utilized for different nonstructural applications such as automotive, medical, packaging, etc. industries. However, this study investigation shows that the developed PLA based bio composite material properties shows a promising candidate for a future of bio composite material for various applications. Here comparison was made between the materials used in current automotive part components such as bumper, dashboard, fenders and etc., and alternative materials that researchers had suggested for these applications.

According to the information of largest automotive part (GMT) manufacturer, Azdel company handbook and other researcher's investigations. The main failure criterion for automotive bumper's structural application is impact (sudden) load, the impact strength of developed bio composite is better than GMT (50 J/m). Additionally, the tensile strength of optimal sample shows improved properties than the GMT (70 MPa) bumper material and it has lower flexural strength than GMT but it is higher than 50 MPa. According to Bilge et al. (Bilge et al., 2020), the minimum over all material strength required to utilize for automotive bumper is 50 N/mm^2. Therefore, the synthesized bio composite material has the possibility to utilize in the automotive bumper application. Because, in order to sure the employment of this material in automotive bumper some testing of this material is required. The given properties of automotive bumper materials proposed by researchers and GMT material are tabulated in Table 47.

Moreover, the synthesized material has also the possibility to utilize it to other automotive body parts such as dash board, fender, and interior car body parts. According to Shinde et al. (Shinde et al., 2020), the tensile strength (20 to 30 MPa), young modulus (2 to 6 GPa), and density (0.98 to 1.1 g/cm^3) of polymer composites are necessary for usage as dash boards and at least 18 MPa tensile strength is required to use polymer composites for fenders. Furthermore, Koronis et al. (Koronis et al., 2013) states that the tensile strength desired for automotive interior components ranges from 53 to 81.9 MPa.

The synthesized PLA - based bio composite material results demonstrate that the material exhibits the necessary mechanical and thermal properties required to meet the performance standards for

the intended uses. Additionally, its physical and biodegradability properties, making it a possible alternative to conventional petroleum-based polymers and polymer composites. Furthermore, the material's simplicity for process ability, ensures its practicality for large-scale production. Therefore, the synthesized PLA based bio composite material performances meet the standards required for the aforementioned applications and it is a promising candidate for sustainable and high-performance material solutions.

Table 47: Comparative analysis with existing bumper and other automotive bumper materials

Material Used	TS (MPa)	YM (GPa)	FS (MPa)	FM (GPa)	IS (J/m)	Density (g/cm^3)	Reference
Nylon6/Nanoclay for bumper	75.2	5	-	-	-	1.13	(Osokoya, 2017)
Wood fiber/PP for bumper	56.4	3.43	88.5	3.79	-	-	(Panthapulakkal et al., 2006)
Wood fiber/GF/PP	75.3	4.36	123.7	5.54	-	-	(Panthapulakkal et al., 2006)
Kenaf/GF/epoxy	39	2.3	453	36.4	146	0.97	(Atiqah et al., 2014)
GMT	70	5.3	150	5	50	1.15	(Adesina et al., 2019; Davoodi et al., 2010)
MCC/MTT/S/PLA	86	4.65	79	8.8	56	1.37	(This study)

In conclusion, this chapter carefully determines and justifies the chemical composition analysis of CH, extraction of MCC, PLA based bio composite samples mechanical and physical properties, single and multi-objective parametric combination, structural and morphological variations of synthesized bio composite from the neat PLA material and recommendations of possible applications. The chemical composition analysis provides critical insights into the raw materials (CH), guiding the effective extraction of MCC and its yield. The developed bio composite samples revealed the feasibility of integrating extracted MCC into PLA matrix with MTT filler material, while rigorous testing and characterization revealed their mechanical, thermal, and morphological properties. Optimization efforts highlighted the importance of balancing parameters to achieve enhanced performance, ensuring the developed bio composites improved highly to meet specific application requirements. Based on these findings, the study recommends potential applications for the developed bio composites in structural areas, where sustainability and performance are paramount. This work not only advances the understanding of bio composite materials but also emphasizes their potential as ecofriendly alternatives to conventional materials.

CONCLUSIONS AND RECOMMENDATIONS

Conclusions

In this study, waste coffee husks were collected, separated from its outer part (exocarp), washed, and chemically treated with dewaxing, alkalizing, bleaching and hydrolyzing to study the chemical composition and examine the elimination of amorphous parts such as lignin, hemicellulose, and extractives from the surface of coffee husk fiber and to extract MCC. Then extracted MCC filled PLA based bio composite samples were fabricated at different weight ratios of fillers, tested to determine its performances and optimized through Taguchi's based GRA. Additionally, the best optimum sample testing and characterization, and comparative analysis with existing automotive bumper was carried out. Based on the investigation the following conclusion is made;

1. The chemical composition of cellulose, hemicellulose, lignin, extractive and ash contents were (52.9%), (12.5%), (21.9%), (9.4%) and (2.4%), respectively. The morphological and X-RD examination showed the great untreated (UT) fiber sample was greatly reduced into a micro-sized (1-2um) and crystalline region (54.7% yield) BL sample. The highest CI has been determined for the BL sample, i.e., 89.9%. Additionally, the thermal analysis shows that the BL sample has greatest thermal stability at higher temperature. Therefore, the extracted crystalline cellulose has considered as promising agent in bio composite reinforcement application.
2. The developed samples testing result showed that the optimal factor level combinations were FS is 96.5 MPa at 3% MCC and 9% MTT fillers, and 20% S plasticizer and at 175^0C T (3%MCC, 9%MTT, 20%S and 175^0C); FM is 9.8 GPa at 6%MCC, 9%MTT, 20%S and 175^0C; TS is 85.2 MPa at 9%MCC, 9%MTT, 10%S and 175^0C; YM is 4.22 GPa at 6%MCC, 9%MTT, 0%S and 150^0C; HV is 138.2 at 6%MCC, 9%MTT, 10%S and 175^0C; WA found at 0%MCC, 0%MTT, 0%S and 100^0C; and D is found 1.3 to 1.41 g/cm^3 at 9%MCC, 9%MTT, 30%S and 175^0C.
3. The best-performing samples of the synthesized bio composite materials were MCC at level 3 (6%), MTT at level 4 (9%), S at level 2 (10%), and T at level 4 (175^0C).
4. The mechanical and physical properties of the most optimal samples were TS (86.7 MPa), YM (4.65 GPa), FS (79.4 MPa), FM (8.82 GPa), HV (142.6), IS (56.3 J), WA (6.92%) and density (0.00137 g/mm3). ANOVA shows that MTT has the greatest significant effect (73.85%) on

the mechanical and physical properties of MCC/MTT/S/PLA bio composite followed by MCC (19.5%), T (2.86%), and S (0.45%), respectively. The confirmation test indicates that the improvement of weighted GRG from 0.7896 to 0.846, which indicates the enhancement of synthesized bio composite properties when the most optimum sample preparation factors and levels are used.

5. The characterization result indicates that the presence of fillers, modifies the base material, PLA properties noticeably. Additionally, the observation of new functional group in the IR spectra is caused due to the chemical interaction of MTT and PLA. However, MCC interacts physically with the base material. The XRD result reveals that the inclusion of fillers improves the crystalline size and index of PLA. The crystalline index shows an improvement of 11.73%, rising from 72.98% to 82.67%. The thermal analysis shows that the optimal bio composite sample has better thermal stability at higher temperature (240 ^{0}C and above) and the amount of residue char increased up to 28.8%.
6. The performance of optimal samples possible applications is compared with automotive part components such as bumper, dashboard, fenders, etc. The comparison revealed that the examined properties of the synthesized materials were comparable to those required properties for the intended applications. Therefore, the synthesized bio composite sample material performances meet the standards required for the aforementioned structural applications and it is a promising candidate for sustainable and high-performance material solutions.

Therefore, the contribution of this study is to advance the bio composite field by indicating the potential of local extraction of MCC as a filler agent with MTT in plasticized PLA matrix. It also provides an understanding of the material's properties, offers single and multi-objective optimization strategies for enhanced performance, and gives attention to the environmental and economic benefits of using renewable resources. Additionally, this study paves the way for the development of sustainable materials that meet the demands of various industrial applications while addressing global environmental challenges. Finally, it is possible to conclude that the novelty of this research is to develop completely bio degradable polymer composite material for structural application through entire environmental friendly processing method.

Recommendations

The result obtained from this investigations showed that the chemical treatment conducted to remove amorphous parts of the fibers was effective. In order to increase the yield and quality of the extracted MCC, it's suggested that detailed optimization of process parameters such as concentration of chemical, temperature and time is needed. The structural performance of extracted MCC directly affects the mechanical, thermal and physical properties of the material. Therefore, extracting using different techniques will be also leads to better qualities of MCC that improves the properties of synthesized bio composite. Furthermore, addition of compatibilizer and different types of plasticizer may enhance the interfacial bonding between fillers and matrices, in result further improved performances of PLA based bio composite material will be achieved. Finally, the processing method used to develop bio composite materials plays a critical role in determining the final performances of the synthesized material. Different processing techniques can lead to variations in overall properties. Therefore, it is highly recommended to explore and evaluate the performance of bio composite materials produced through alternative processing methods. This investigation would provide a more comprehensive understanding of how different fabrication techniques influence material behavior and could potentially lead to the optimization of material properties for specific applications.

As part of the future work stemming from this study, the fabrication of structural components such as automotive bumper, dashboard, fender and etc. using synthesized bio-composite materials should be undertaken. This would involve not only the production of the structural components but also rigorous testing of their performance under various conditions. These future efforts would contribute to advancing the practical application of synthesizes bio composite materials in structural areas and automotive industry, and provide valuable insights into their suitability for real-world use.

Finally, the developed bio composite material will undergo a cost evaluation. To minimize its water absorption due to sorbitol plasticizer, secondary processing like painting, coating and other methods should be applied in the future to improve its performance and usability.

REFERENCE

Abel, O. M., Chinelo, S., & Chidioka, R. (2021). Enhancing cassava peels starch as feedstock for biodegradable plastic. *J Mater Environ Sci, 12*(2), 169-182.

Abolore, R. S., Jaiswal, S., & Jaiswal, A. K. (2023). Green and sustainable pretreatment methods for cellulose extraction from lignocellulosic biomass and its applications: a review. *Carbohydrate Polymer Technologies and Applications*, 100396.

Achema, F., Yahaya, B., Apeh, E., & Akinyeye, J. (2017). Application of glass fibre reinforced composite in the production of light weight car bumper (a case study of the mechanical properties). *International Journal of Engineering Research & Technology (IJERT), 6*(7).

Achor, M., Oyeniyi, Y., & Yahaya, A. (2014). Extraction and characterization of microcrystalline cellulose obtained from the back of the fruit of Lageriana siceraria (water gourd). *Journal of Applied Pharmaceutical Science, 4*(1), 057-060.

Adamu, A. D., Jikan, S. S., Talip, B. H. A., Badarulzaman, N. A., & Yahaya, S. (2017). *Effect of glycerol on the properties of tapioca starch film.* Paper presented at the Materials Science Forum.

Adedokun, M., Essien, G., Uwah, T., Romanus, A., Josiah, I., & Jackson, C. (2014). Evaluation of the release properties of microcrystalline cellulose derived from Saccharum officinarum L. in paracetamol tablet formulation. *J. Pharm. Sci. Res, 6*(10), 342-346.

Adekunle, K. F. (2015). Surface treatments of natural fibres—A review: Part 1. *Open Journal of Polymer Chemistry, 5*(3), 41-46.

Adel, A. M., Abd El-Wahab, Z. H., Ibrahim, A. A., & Al-Shemy, M. T. (2011). Characterization of microcrystalline cellulose prepared from lignocellulosic materials. Part II: Physicochemical properties. *Carbohydrate polymers, 83*(2), 676-687.

Adeleye, O. A., Bamiro, O. A., Albalawi, D. A., Alotaibi, A. S., Iqbal, H., Sanyaolu, S., . . . Thiripuranathar, G. (2022). Characterizations of Alpha-Cellulose and Microcrystalline Cellulose Isolated from Cocoa Pod Husk as a Potential Pharmaceutical Excipient. *Materials, 15*(17), 5992.

Adesina, O., Jamiru, T., Sadiku, E., Ogunbiyi, O., & Beneke, L. (2019). Mechanical evaluation of hybrid natural fibre–reinforced polymeric composites for automotive bumper beam: a review. *The International Journal of Advanced Manufacturing Technology, 103*, 1781-1797.

Akampumuza, O., Wambua, P. M., Ahmed, A., Li, W., & Qin, X. H. (2017). Review of the applications of biocomposites in the automotive industry. *Polymer Composites, 38*(11), 2553-2569.

Alam, M. A., Sapuan, S., Ya, H., Hussain, P., Azeem, M., & Ilyas, R. (2021). Application of biocomposites in automotive components: A review. *Biocomposite and synthetic composites for automotive applications*, 1-17.

Alex, A. S., Rajeev, R., Krishnaraj, K., Sreenivas, N., Manu, S., Gouri, C., & Sekkar, V. (2017). Thermal protection characteristics of polydimethylsiloxane-organoclay nanocomposite. *Polymer Degradation and Stability, 144*, 281-291.

Alhanish, A., & Abu Ghalia, M. (2021). Developments of biobased plasticizers for compostable polymers in the green packaging applications: A review. *Biotechnology Progress, 37*(6), e3210.

Ali, A., Shaker, K., Nawab, Y., Jabbar, M., Hussain, T., Militky, J., & Baheti, V. (2018). Hydrophobic treatment of natural fibers and their composites—A review. *Journal of Industrial Textiles, 47*(8), 2153-2183.

Alias, A. H., Norizan, M. N., Sabaruddin, F. A., Asyraf, M. R. M., Norrrahim, M. N. F., Ilyas, A. R., . . . Nazrin, A. (2021). Hybridization of MMT/Lignocellulosic Fiber Reinforced Polymer Nanocomposites for Structural Applications: A Review. *Coatings, 11*(11), 1355.

Alotaibi, M. D., Alshammari, B. A., Saba, N., Alothman, O. Y., Sanjay, M., Almutairi, Z., & Jawaid, M. (2019). Characterization of natural fiber obtained from different parts of date palm tree (Phoenix dactylifera L.). *International journal of biological macromolecules, 135*, 69-76.

Amin, M. N., Ahmad, W., Khan, K., & Ahmad, A. (2022). A comprehensive review of types, properties, treatment methods and application of plant fibers in construction and building materials. *Materials, 15*(12), 4362.

Anbupalani, M. S., Venkatachalam, C. D., & Rathanasamy, R. (2020). Influence of coupling agent on altering the reinforcing efficiency of natural fibre-incorporated polymers–A review. *Journal of Reinforced Plastics and Composites, 39*(13-14), 520-544.

Antony, J. (2023). *Design of experiments for engineers and scientists*: Elsevier.

Arief, M., Mubarak, A., & Pujiastuti, D. (2021). *The concentration of sorbitol on bioplastic cellulose based carrageenan waste on biodegradability and mechanical properties*

bioplastic. Paper presented at the IOP Conference Series: Earth and Environmental Science.

Arjmandi, R., Hassan, A., Eichhorn, S. J., Mohamad Haafiz, M., Zakaria, Z., & Tanjung, F. A. (2015). Enhanced ductility and tensile properties of hybrid montmorillonite/cellulose nanowhiskers reinforced polylactic acid nanocomposites. *Journal of Materials Science, 50*, 3118-3130.

Arjmandi, R., Hassan, A., Haafiz, M. M., & Zakaria, Z. (2015). Effect of microcrystalline cellulose on biodegradability, tensile and morphological properties of montmorillonite reinforced polylactic acid nanocomposites. *Fibers and Polymers, 16*, 2284-2293.

Arjmandi, R., Hassan, A., Haafiz, M. M., Zakaria, Z., & Inuwa, I. (2014). Characterization of polylactic acid/microcrystalline cellulose/montmorillonite hybrid composites. *Malaysian J. Anal. Sci, 18*, 642-650.

Arjmandi, R., Hassan, A., Mohamad Haafiz, M., & Zakaria, Z. (2016). Effects of micro-and nano-cellulose on tensile and morphological properties of montmorillonite nanoclay reinforced polylactic acid nanocomposites. *Nanoclay Reinforced Polymer Composites: Natural Fibre/Nanoclay Hybrid Composites*, 103-125.

Asaithambi, B., Ganesan, G., & Ananda Kumar, S. (2014). Bio-composites: Development and mechanical characterization of banana/sisal fibre reinforced poly lactic acid (PLA) hybrid composites. *Fibers and Polymers, 15*, 847-854.

Asif, M., Ahmed, D., Ahmad, N., Qamar, M. T., Alruwaili, N. K., & Bukhari, S. N. A. (2022). Extraction and characterization of microcrystalline cellulose from Lagenaria siceraria fruit pedicles. *Polymers*, *14*(9), 1867.

Asim, M., Jawaid, M., Saba, N., Nasir, M., & Sultan, M. T. H. (2017). Processing of hybrid polymer composites—a review. *Hybrid polymer composite materials*, 1-22.

Atiqah, A., Maleque, M., Jawaid, M., & Iqbal, M. (2014). Development of kenaf-glass reinforced unsaturated polyester hybrid composite for structural applications. *Composites Part B: Engineering, 56*, 68-73.

Azum, N., Jawaid, M., Kian, L. K., Khan, A., & Alotaibi, M. M. (2021). Extraction of microcrystalline cellulose from Washingtonia fibre and its characterization. *Polymers, 13*(18), 3030.

Bae, D. H., Choi, H. J., Choi, K., Do Nam, J., Islam, M. S., & Kao, N. (2017). Fabrication of phosphate microcrystalline rice husk based cellulose particles and their electrorheological response. *Carbohydrate polymers, 165*, 247-254.

Ballesteros, L. F., Teixeira, J. A., & Mussatto, S. I. (2014). Chemical, functional, and structural properties of spent coffee grounds and coffee silverskin. *Food and bioprocess technology, 7*, 3493-3503.

Banerjee, A., & Ray, S. K. (2020). Synthesis of novel composite membranes by in-situ intercalative emulsion polymerization for separation of aromatic-aliphatic mixtures by pervaporation. *Journal of Membrane Science, 597*, 117729.

Banerjee, J., & Dutta, K. (2019). Melt-mixed carbon nanotubes/polymer nanocomposites. *Polymer Composites, 40*(12), 4473-4488.

Baruah, J., Deka, R. C., & Kalita, E. (2020). Greener production of microcrystalline cellulose (MCC) from Saccharum spontaneum (Kans grass): Statistical optimization. *International journal of biological macromolecules, 154*, 672-682.

Barzegar, R., Yozgatligil, A., Olgun, H., & Atimtay, A. T. (2020). TGA and kinetic study of different torrefaction conditions of wood biomass under air and oxy-fuel combustion atmospheres. *Journal of the Energy Institute, 93*(3), 889-898.

Begum, S. A., Rane, A. V., & Kanny, K. (2020). Applications of compatibilized polymer blends in automobile industry *Compatibilization of Polymer Blends* (pp. 563-593): Elsevier.

Behera, K., Chang, Y.-H., Yadav, M., & Chiu, F.-C. (2020). Enhanced thermal stability, toughness, and electrical conductivity of carbon nanotube-reinforced biodegradable poly (lactic acid)/poly (ethylene oxide) blend-based nanocomposites. *Polymer, 186*, 122002.

Bekalo, S. A., & Reinhardt, H.-W. (2010). Fibers of coffee husk and hulls for the production of particleboard. *Materials and structures, 43*(8), 1049-1060.

Belingardi, G., Beyene, A., Koricho, E., & Martorana, B. (2015). Alternative lightweight materials and component manufacturing technologies for vehicle frontal bumper beam. *Composite Structures, 120*, 483-495.

Belkheir, M., Boutaleb, M., Mokaddem, A., & Doumi, B. (2022). Predicting the effect of coconut natural fibers for improving the performance of biocomposite materials based on the poly (methyl methacrylate)-PMMA polymer for engineering applications. *Polymer Bulletin*. doi: 10.1007/s00289-022-04166-6

Bergaliyeva, S., Sales, D. L., Delgado, F. J., Bolegenova, S., & Molina, S. I. (2023). Manufacture and Characterization of Polylactic Acid Filaments Recycled from Real Waste for 3D Printing. *Polymers, 15*(9), 2165.

Beroual, M., Mehelli, O., Boumaza, L., Trache, D., Tarchoun, A. F., Derradji, M., & Khimeche, K. (2021). Synthesis and characterization of microcrystalline cellulose from giant reed using different delignification processes *Materials Research and Applications* (pp. 173-187): Springer.

Bhambure, S., & Rao, A. (2021). Experimental investigation of impact strength of kenaf fiber reinforced polyester composite. *Materials Today: Proceedings, 46*, 1134-1138.

Bharath, K. N., & Basavarajappa, S. (2016). Applications of biocomposite materials based on natural fibers from renewable resources: a review. *Science and Engineering of Composite Materials, 23*(2), 123-133.

Bhasney, S. M., Bhagabati, P., Kumar, A., & Katiyar, V. (2019). Morphology and crystalline characteristics of polylactic acid [PLA]/linear low density polyethylene [LLDPE]/microcrystalline cellulose [MCC] fiber composite. *Composites science and technology, 171*, 54-61.

Bhasney, S. M., Mondal, K., Kumar, A., & Katiyar, V. (2020). Effect of microcrystalline cellulose [MCC] fibres on the morphological and crystalline behaviour of high density polyethylene [HDPE]/polylactic acid [PLA] blends. *Composites science and technology, 187*, 107941.

Bilge, Ç., Aydıner, T., Akdeniz, Ç., Soyer, A. M., & Aksel, L. (2020). Weight Reduction of Automobile Using Glass-Mat Thermoplastic Composites in Spare-Wheel Well. *European Mechanical Science, 4*(1), 7-11.

Bin, Y., Yang, B., & Wang, H. (2018). The effect of a small amount of modified microfibrillated cellulose and ethylene–glycidyl methacrylate copolymer on the crystallization behaviors and mechanical properties of polylactic acid. *Polymer Bulletin, 75*, 3377-3394.

Bitinis, N., Fortunati, E., Verdejo, R., Armentano, I., Torre, L., Kenny, J. M., & López-Manchado, M. Á. (2014). Thermal and bio-disintegration properties of poly (lactic acid)/natural rubber/organoclay nanocomposites. *Applied Clay Science, 93*, 78-84.

Blinová, L., Sirotiak, M., Bartošová, A., & Soldán, M. (2017a). Utilization of waste from coffee production. *Research Papers Faculty of Materials Science and Technology Slovak University of Technology, 25*(40), 91-101.

Blinová, L., Sirotiak, M., Bartošová, A., & Soldán, M. (2017b). Utilization of waste from coffee production. *Vedecké Práce Materiálovotechnologickej Fakulty Slovenskej Technickej Univerzity v Bratislave so Sídlom v Trnave, 25*(40), 91.

Bocqué, M., Voirin, C., Lapinte, V., Caillol, S., & Robin, J. J. (2016). Petro-based and bio-based plasticizers: chemical structures to plasticizing properties. *Journal of Polymer Science Part A: Polymer Chemistry, 54*(1), 11-33.

Bondesson, E. (2015). A nutritional analysis on the by-product coffee husk and its potential utilization in food production.

Bredin, M. (2012). *The ecology of the New Testament: Creation, re-creation, and the environment*: InterVarsity Press.

Budin, S., Maideen, N., Koay, M., Ibrahim, D., & Yusoff, H. (2019). *A comparison study on mechanical properties of virgin and recycled polylactic acid (PLA).* Paper presented at the Journal of Physics: Conference Series.

Bui, T. K. A., Hoa, S. V., Ngo, T. D., & That, M. T. T. (2010). *Effect of addition of nanoclays on properties of vinyl ester.* Paper presented at the Design, Manufacturing and Applications of Composites: Proceedings of the Eighth Joint Canada-Japan Workshop on Composites.

Carmona, V. B., Corrêa, A. C., Marconcini, J. M., & Mattoso, L. H. C. (2015). Properties of a biodegradable ternary blend of thermoplastic starch (TPS), poly (ε-caprolactone)(PCL) and poly (lactic acid)(PLA). *Journal of Polymers and the Environment, 23*(1), 83-89.

Casalini, T., Rossi, F., Castrovinci, A., & Perale, G. (2019). A Perspective on Polylactic Acid-Based Polymers Use for Nanoparticles Synthesis and Applications. *Frontiers in Bioengineering and Biotechnology, 7*. doi: 10.3389/fbioe.2019.00259

Cesarino, I., Carnietto, M., Bronzato, G., & Leao, A. (2020). Fabrication of pineapple leaf fibers reinforced composites. *Pineapple Leaf Fibers: Processing, Properties and Applications*, 265-277.

Chanda, B., Kumar, R., Kumar, K., & Bhowmik, S. (2015). *Optimisation of mechanical properties of wood dust-reinforced epoxy composite using grey relational analysis.* Paper presented at the Proceedings of Fourth International Conference on Soft Computing for Problem Solving: SocProS 2014, Volume 2.

Chandramohan, D., & Kumar, A. J. P. (2017). Experimental data on the properties of natural fiber particle reinforced polymer composite material. *Data in Brief, 13*, 460-468.

Chandrasekar, M., Ishak, M., Sapuan, S., Leman, Z., & Jawaid, M. (2017). A review on the characterisation of natural fibres and their composites after alkali treatment and water absorption. *Plastics, Rubber and Composites, 46*(3), 119-136.

Chandrasekar, M., Kumar, T. S. M., Senthilkumar, K., Radoor, S., Ilyas, R., Sapuan, S., . . . Siengchin, S. (2021). Performance of Natural Fiber Reinforced Recycled Thermoplastic Polymer Composites Under Aging Conditions *Recycling of Plastics, Metals, and Their Composites* (pp. 127-139): CRC Press.

Chattopadhyay, S., Pan, N., Roy, A., Samanta, K. K., & Khan, A. (2022). Two-step bleaching of jute yarn and fabric using hydrogen peroxide and peracetic acid. *Journal of Natural Fibers, 19*(3), 1159-1167.

Chen, G.-Q., & Patel, M. K. (2012). Plastics derived from biological sources: present and future: a technical and environmental review. *Chemical reviews, 112*(4), 2082-2099.

Chen, X., Gu, Y., Zhou, X., & Zhang, Y. (2014). Asparagus stem as a new lignocellulosic biomass feedstock for anaerobic digestion: Increasing hydrolysis rate, methane production and biodegradability by alkaline pretreatment. *Bioresource technology, 164*, 78-85.

Choi, K.-m., Choi, M.-C., Han, D.-H., Park, T.-S., & Ha, C.-S. (2013). Plasticization of poly (lactic acid)(PLA) through chemical grafting of poly (ethylene glycol)(PEG) via in situ reactive blending. *European polymer journal, 49*(8), 2356-2364.

Chowdhury, M. A., & Pandit, P. (2022). Chemical processing of knitted fabrics *Advanced Knitting Technology* (pp. 503-536): Elsevier.

Chuayjuljit, S., Hosililak, S., & Athisart, A. (2009). Thermoplastic cassava starch/sorbitol-modified montmorillonite nanocomposites blended with low density polyethylene: properties and biodegradability study. *Journal of Metals, Materials and Minerals, 19*(1).

Collazo-Bigliardi, S., Ortega-Toro, R., & Boix, A. C. (2018). Isolation and characterisation of microcrystalline cellulose and cellulose nanocrystals from coffee husk and comparative study with rice husk. *Carbohydrate polymers, 191*, 205-215.

Collazo-Bigliardi, S., Ortega-Toro, R., & Chiralt, A. (2019a). Improving properties of thermoplastic starch films by incorporating active extracts and cellulose fibres isolated from rice or coffee husk. *Food Packaging and Shelf Life, 22*, 100383.

Collazo-Bigliardi, S., Ortega-Toro, R., & Chiralt, A. (2019b). Using lignocellulosic fractions of coffee husk to improve properties of compatibilised starch-PLA blend films. *Food Packaging and Shelf Life, 22*, 100423.

Collazo-Bigliardi, S., Ortega-Toro, R., & Chiralt Boix, A. (2018). Reinforcement of thermoplastic starch films with cellulose fibres obtained from rice and coffee husks. *Journal of Renewable Materials, 6*(6), 599-610.

Czitrom, V. (2003). Ch. 1. Guidelines for selecting factors and factor levels for an industrial designed experiment. *Handbook of Statistics, 22*, 3-32.

Dadi, D., Daba, G., Beyene, A., Luis, P., & Van der Bruggen, B. (2019). Composting and co-composting of coffee husk and pulp with source-separated municipal solid waste: a breakthrough in valorization of coffee waste. *International Journal of Recycling of Organic Waste in Agriculture, 8*, 263-277.

Davoodi, M., Sapuan, S., Ahmad, D., Ali, A., Khalina, A., & Jonoobi, M. (2010). Mechanical properties of hybrid kenaf/glass reinforced epoxy composite for passenger car bumper beam. *Materials & Design, 31*(10), 4927-4932.

Dawit, J. B., Regassa, Y., & Lemu, H. G. (2020). Property characterization of acacia tortilis for natural fiber reinforced polymer composite. *Results in Materials, 5*, 100054.

de Oliveira, R. L., da Silva Barud, H., de Assunção, R. M., da Silva Meireles, C., Carvalho, G. O., Filho, G. R., . . . Ribeiro, S. J. L. (2011). Synthesis and characterization of microcrystalline cellulose produced from bacterial cellulose. *Journal of thermal analysis and calorimetry, 106*(3), 703-709.

Debeli, D. K., Qin, Z., & Guo, J. (2018). Study on the pre-treatment, physical and chemical properties of ramie fibers reinforced poly (lactic acid)(PLA) biocomposite. *Journal of Natural Fibers, 15*(4), 596-610.

Debnath, B., Haldar, D., & Purkait, M. K. (2021). A critical review on the techniques used for the synthesis and applications of crystalline cellulose derived from agricultural wastes and forest residues. *Carbohydrate polymers*, 118537.

Degaga, J. (2020). Review on coffee production and marketing in Ethiopia. *Journal of Marketing and Consumer Research, 67*, 7-15.

Dejene, B. K., & Geletaw, T. M. (2024). Development of fully green composites utilizing thermoplastic starch and cellulosic fibers from agro-waste: a critical review. *Polymer-Plastics Technology and Materials, 63*(5), 540-569.

Devnani, G., & Sinha, S. (2019). Extraction, characterization and thermal degradation kinetics with activation energy of untreated and alkali treated Saccharum spontaneum (Kans grass) fiber. *Composites Part B: Engineering, 166*, 436-445.

Ding FangFang, D. F. (2018). Mechanical properties and degradation characteristics of corn straw fibers/polylactic acid composite materials.

Dixit, S., Goel, R., Dubey, A., Shivhare, P. R., & Bhalavi, T. (2017). Natural fibre reinforced polymer composite materials-a review. *Polymers from renewable resources, 8*(2), 71-78.

Dogu, B., & Kaynak, C. (2016). Behavior of polylactide/microcrystalline cellulose biocomposites: effects of filler content and interfacial compatibilization. *Cellulose, 23*, 611-622.

Duressa, E. L. (2018). Discourse Analysis of Origin and Distribution of Coffee Arabica. *American Rsearch Journal, 4*(1), 10.

El Amri, A., Ouass, A., Wardighi, Z., Bouhassane, F. Z., Zarrouk, A., Habsaoui, A., . . . Lebkiri, A. (2022). Extraction and characterization of cellulosic nanocrystals from stems of the reed plant large-leaved cattail (Typha latifolia). *Materials Today: Proceedings*.

Emenike, E. C., Iwuozor, K. O., Saliu, O. D., Ramontja, J., & Adeniyi, A. G. (2023). Advances in the extraction, classification, modification, emerging and advanced applications of crystalline cellulose: a review. *Carbohydrate Polymer Technologies and Applications, 6*, 100337.

Eslami, Z., Elkoun, S., Robert, M., & Adjallé, K. (2023). A review of the effect of plasticizers on the physical and mechanical properties of alginate-based films. *Molecules, 28*(18), 6637.

Evans, M. (2022). *Optimisation of manufacturing processes: a response surface approach*: CRC Press.

Fan, F., Zhu, M., Fang, K., Cao, E., Yang, Y., Xie, J., . . . Cao, X. (2022). Extraction and characterization of cellulose nanowhiskers from TEMPO oxidized sisal fibers. *Cellulose, 29*(1), 213-222.

Farah, S., Anderson, D. G., & Langer, R. (2016). Physical and mechanical properties of PLA, and their functions in widespread applications—A comprehensive review. *Advanced drug delivery reviews, 107*, 367-392.

Ferreira, J., Borrego, L., Costa, J., & Capela, C. (2013). Fatigue behaviour of nanoclay reinforced epoxy resin composites. *Composites Part B: Engineering, 52*, 286-291.

Fouad, H., Kian, L. K., Jawaid, M., Alotaibi, M. D., Alothman, O. Y., & Hashem, M. (2020). Characterization of Microcrystalline Cellulose Isolated from Conocarpus Fiber. *Polymers, 12*(12), 2926.

Fu, S., Sun, Z., Huang, P., Li, Y., & Hu, N. (2019). Some basic aspects of polymer nanocomposites: A critical review. *Nano Materials Science, 1*(1), 2-30. doi: https://doi.org/10.1016/j.nanoms.2019.02.006

Gao, G., Xu, F., & Xu, J. (2022). Parametric optimization of fdm process for improving mechanical strengths using taguchi method and response surface method: A comparative investigation. *Machines, 10*(9), 750.

Garcia-Munoz, P., Valenzuela, L., Wegstein, D., Schanz, T., Lopez, G. E., Ruppert, A. M., . . . Keller, N. (2023). Photocatalytic Synthesis of Hydrogen Peroxide from Molecular Oxygen and Water. *Topics in Current Chemistry, 381*(4), 1-73.

Gaur, V. K., Sharma, P., Sirohi, R., Awasthi, M. K., Dussap, C.-G., & Pandey, A. (2020). Assessing the impact of industrial waste on environment and mitigation strategies: A comprehensive review. *Journal of Hazardous Materials, 398*, 123019.

Geng, W., Narron, R., Jiang, X., Pawlak, J. J., Chang, H.-m., Park, S., . . . Venditti, R. A. (2019). The influence of lignin content and structure on hemicellulose alkaline extraction for non-wood and hardwood lignocellulosic biomass. *Cellulose, 26*(5), 3219-3230. doi: 10.1007/s10570-019-02261-y

Getme, A. S., & Patel, B. (2020). A review: Bio-fiber's as reinforcement in composites of polylactic acid (PLA). *Materials Today: Proceedings, 26*, 2116-2122.

Ghadi, R., Muntimadugu, E., Domb, A., Khan, W., & Zhang, X. (2017). Synthetic biodegradable medical polymer: Polyanhydrides *Science and principles of biodegradable and bioresorbable medical polymers* (pp. 153-188): Elsevier.

Giita Silverajah, V., Ibrahim, N. A., Yunus, W. M. Z. W., Hassan, H. A., & Woei, C. B. (2012). A comparative study on the mechanical, thermal and morphological characterization of poly (lactic acid)/epoxidized palm oil blend. *International journal of molecular sciences, 13*(5), 5878-5898.

Gómez-Salcedo, Y., Oliva-Merencio, D., Rodríguez-Díaz, J. M., & Pereda-Reyes, I. (2021). Contribution of the Environmental Biotechnology to the Sustainability of the Coffee Processing Industry in Developing Countries *Advances in the Domain of Environmental Biotechnology* (pp. 565-589): Springer.

Gowthaman, N., Lim, H., Sreeraj, T., Amalraj, A., & Gopi, S. (2021). Advantages of biopolymers over synthetic polymers: social, economic, and environmental aspects *Biopolymers and their Industrial Applications* (pp. 351-372): Elsevier.

Greco, A., & Ferrari, F. (2021). Thermal behavior of PLA plasticized by commercial and cardanol-derived plasticizers and the effect on the mechanical properties. *Journal of thermal analysis and calorimetry, 146*(1), 131-141.

Grigora, M.-E., Terzopoulou, Z., Tsongas, K., Bikiaris, D. N., & Tzetzis, D. (2022). Physicochemical characterization and finite element analysis-assisted mechanical behavior of polylactic acid-montmorillonite 3D printed nanocomposites. *Nanomaterials, 12*(15), 2641.

Gunti, R., Ratna Prasad, A., & Gupta, A. (2018). Mechanical and degradation properties of natural fiber-reinforced PLA composites: Jute, sisal, and elephant grass. *Polymer Composites, 39*(4), 1125-1136.

Guo, J., Tsou, C.-H., Yu, Y., Wu, C.-S., Zhang, X., Chen, Z., . . . Guzman, M. R. D. (2021). Conductivity and mechanical properties of carbon black-reinforced poly (lactic acid)(PLA/CB) composites. *Iranian Polymer Journal, 30*(12), 1251-1262.

Guo, R., Ren, Z., Bi, H., Xu, M., & Cai, L. (2019). Electrical and thermal conductivity of polylactic acid (PLA)-based biocomposites by incorporation of nano-graphite fabricated with fused deposition modeling. *Polymers, 11*(3), 549.

Haafiz, M. M., Hassan, A., Zakaria, Z., Inuwa, I. M., Islam, M. S., & Jawaid, M. (2013). Properties of polylactic acid composites reinforced with oil palm biomass microcrystalline cellulose. *Carbohydrate polymers, 98*(1), 139-145.

Hachaichi, A., Kouini, B., Kian, L. K., Asim, M., Fouad, H., Jawaid, M., & Sain, M. (2021). Nanocrystalline cellulose from microcrystalline cellulose of date palm fibers as a promising candidate for bio-nanocomposites: isolation and characterization. *Materials, 14*(18), 5313.

Hafid, H. S., Omar, F. N., Zhu, J., & Wakisaka, M. (2021). Enhanced crystallinity and thermal properties of cellulose from rice husk using acid hydrolysis treatment. *Carbohydrate polymers*, *260*, 117789.

Haldar, D., & Purkait, M. K. (2020). Micro and nanocrystalline cellulose derivatives of lignocellulosic biomass: A review on synthesis, applications and advancements. *Carbohydrate polymers*, *250*, 116937.

Haruna, F., Apeji, Y. E., Oparaeche, C., Oyi, A. R., & Gamlen, M. (2020). Compaction and tableting properties of composite particles of microcrystalline cellulose and crospovidone engineered for direct compression. *Future Journal of Pharmaceutical Sciences, 6*(1), 1-9.

Hasanzadeh, R., Azdast, T., Eungkee Lee, R., & Afsari Ghazi, A. (2017). Experimental polymeric nanocomposite material selection for automotive bumper beam using multi-criteria decision making methods. *Iranian Journal of Materials Science and Engineering, 14*(3), 1-10.

Hashim, M. Y., Amin, A. M., Marwah, O. M. F., Othman, M. H., Yunus, M. R. M., & Huat, N. C. (2017). *The effect of alkali treatment under various conditions on physical properties of kenaf fiber*. Paper presented at the Journal of Physics: Conference Series.

He, C., Li, H., Hong, J., Xiong, H., Ni, H., & Zheng, M. (2022). Characterization and Functionality of Cellulose from Pomelo Fruitlets by Different Extraction Methods. *Polymers*, *14*(3), 518.

Hedthong, R., Kittikorn, T., Damsongsee, P., Kadea, S., Khanoonkon, N., Witayakran, S., . . . Chollakup, R. (2023). Investigation of physico-chemical degradation through weathering acceleration of hemp/PLA biocomposite: thermal analysis. *Journal of thermal analysis and calorimetry*, 1-14.

Hernandez, C. C., & dos Santos Rosa, D. (2016). Extraction of cellulose nanowhiskers: natural fibers source, methodology and application. *matrix, 3*, 16.

Hill, K., Swiecki, B., & Cregger, J. (2012). The bio-based materials automotive value chain. *Center for Automotive Research, 112*, 1-92.

Huang, S.-M., Hwang, J.-J., Liu, H.-J., & Zheng, A.-M. (2021). A characteristic study of polylactic acid/organic modified montmorillonite (PLA/OMMT) nanocomposite materials after hydrolyzing. *Crystals, 11*(4), 376.

Ibrahim, N., Jollands, M., & Parthasarathy, R. (2019). *Morphology and mechanical properties of polylactide/montmorillonite composites.* Paper presented at the Journal of Physics: Conference Series.

Ibrahim, N. A., Yunus, W. M. Z. W., Othman, M., Abdan, K., & Hadithon, K. A. (2010). Poly (lactic acid)(PLA)-reinforced kenaf bast fiber composites: the effect of triacetin. *Journal of Reinforced Plastics and Composites, 29*(7), 1099-1111.

Idumah, C. I., & Obele, C. M. (2021). Understanding interfacial influence on properties of polymer nanocomposites. *Surfaces and Interfaces, 22*, 100879. doi: https://doi.org/10.1016/j.surfin.2020.100879

Ihueze, C. C., Achike, M. K., & Okafor, C. Optimal Performance Characteristics and Reinforcement Combinations of Coconut Fibre Reinforced High Density Polyethylene (HDPE) Polymer Matrixes.

Ilangovan, M., Guna, V., Hu, C., Takemura, A., Leman, Z., & Reddy, N. (2021). Dehulled coffee husk-based biocomposites for green building materials. *Journal of Thermoplastic Composite Materials, 34*(12), 1623-1638.

Islam, M. Z., Sarker, M. E., Rahman, M. M., Islam, M. R., Ahmed, A. F., Mahmud, M. S., & Syduzzaman, M. (2022). Green composites from natural fibers and biopolymers: A review on processing, properties, and applications. *Journal of Reinforced Plastics and Composites, 41*(13-14), 526-557.

Jaafar, J., Siregar, J. P., Tezara, C., Hamdan, M. H. M., & Rihayat, T. (2019). A review of important considerations in the compression molding process of short natural fiber composites. *The International Journal of Advanced Manufacturing Technology, 105*(7), 3437-3450. doi: 10.1007/s00170-019-04466-8

Jahan, M. S., Saeed, A., He, Z., & Ni, Y. (2011). Jute as raw material for the preparation of microcrystalline cellulose. *Cellulose, 18*(2), 451-459. doi: 10.1007/s10570-010-9481-z

Jalauddin, M. N., Ali, A., Sahari, B., & Aziz, N. A. (2012). Performance of automotive composite bumper beams and hood subjected to frontal impacts. *Materials Testing, 54*(1), 19-25.

Jankovic, A., Chaudhary, G., & Goia, F. (2021). Designing the design of experiments (DOE)–An investigation on the influence of different factorial designs on the characterization of complex systems. *Energy and Buildings, 250*, 111298.

Jayaramudu, J., Das, K., Sonakshi, M., Reddy, G. S. M., Aderibigbe, B., Sadiku, R., & Ray, S. S. (2014). Structure and properties of highly toughened biodegradable polylactide/ZnO biocomposite films. *International journal of biological macromolecules, 64*, 428-434.

Jem, K. J., & Tan, B. (2020). The development and challenges of poly (lactic acid) and poly (glycolic acid). *Advanced Industrial and Engineering Polymer Research, 3*(2), 60-70.

Jena, D., Mohapatra, R. C., & Das, A. K. (2019). Optimization of mechanical characteristics of rice husk particle reinforced polymer composites using Taguchi Experimental Technique. *World Scientific News, 124*(2), 155-170.

Juntuek, P., Ruksakulpiwat, C., Chumsamrong, P., & Ruksakulpiwat, Y. (2012). Comparison between mechanical and thermal properties of polylactic acid and natural rubber blend using calcium carbonate and vetiver grass fiber as fillers. *Advanced Materials Research, 410*, 59-62.

Kandasamy, M., Chandravathanan, A., & Mohan, M. (2020). An investigation on tribological and mechanical properties of arecanut and borassus flabellifer fiber hybrid composite reinforced with epoxy. *Ind Eng J, 13*(2).

Karali, N., Khanna, N., & Shah, N. (2024). Climate Impact of Primary Plastic Production.

Karimah, A., Ridho, M. R., Munawar, S. S., Adi, D. S., Damayanti, R., Subiyanto, B., . . . Fudholi, A. (2021). A review on natural fibers for development of eco-friendly bio-composite: characteristics, and utilizations. *Journal of materials research and technology, 13*, 2442-2458.

Kashfipour, M. A., Mehra, N., & Zhu, J. (2018). A review on the role of interface in mechanical, thermal, and electrical properties of polymer composites. *Advanced Composites and Hybrid Materials, 1*, 415-439.

Kausar, A., Zohra, S. T., Ijaz, S., Iqbal, M., Iqbal, J., Bibi, I., . . . Nazir, A. (2022). Cellulose-based materials and their adsorptive removal efficiency for dyes: A review. *International journal of biological macromolecules*.

Kelleci, O., Aydemir, D., Altuntas, E., Oztel, A., Kurt, R., Yorur, H., & Istek, A. (2022). Thermoplastic composites of polypropylene/biopolymer blends and wood flour: Parameter optimization with fuzzy-grey relational analysis. *Polymers and Polymer Composites, 30*, 09673911221100968.

Khalid, M. Y., Al Rashid, A., Arif, Z. U., Ahmed, W., Arshad, H., & Zaidi, A. A. (2021). Natural fiber reinforced composites: Sustainable materials for emerging applications. *Results in Engineering*, *11*, 100263. doi: https://doi.org/10.1016/j.rineng.2021.100263

Khenblouche, A., Bechki, D., Gouamid, M., Charradi, K., Segni, L., Hadjadj, M., & Boughali, S. (2019). Extraction and characterization of cellulose microfibers from Retama raetam stems. *Polímeros*, *29*.

Kian, L., Saba, N., Jawaid, M., & Fouad, H. (2020). Characterization of microcrystalline cellulose extracted from olive fiber. *International journal of biological macromolecules*, *156*, 347-353.

Kian, L. K., Jawaid, M., Ariffin, H., & Alothman, O. Y. (2017). Isolation and characterization of microcrystalline cellulose from roselle fibers. *International journal of biological macromolecules*, *103*, 931-940.

Kibria, M. G., Masuk, N. I., Safayet, R., Nguyen, H. Q., & Mourshed, M. (2023). Plastic waste: challenges and opportunities to mitigate pollution and effective management. *International Journal of Environmental Research*, *17*(1), 20.

Kickelbick, G. (2014). Hybrid materials-past, present and future.

Kim, D.-H., Kim, H.-G., & Kim, H.-S. (2015). Design optimization and manufacture of hybrid glass/carbon fiber reinforced composite bumper beam for automobile vehicle. *Composite Structures*, *131*, 742-752.

Kim, Y., Kim, J. S., Lee, S.-Y., Mahajan, R. L., & Kim, Y.-T. (2020). Exploration of hybrid nanocarbon composite with polylactic acid for packaging applications. *International journal of biological macromolecules*, *144*, 135-142.

Komuraiah, A., Kumar, N. S., & Prasad, B. D. (2014). Chemical composition of natural fibers and its influence on their mechanical properties. *Mechanics of composite materials*, *50*, 359-376.

Kopparthi, P. K., Kundavarapu, V. R., Kaki, V. R., & Pathakokila, B. R. (2021). Modeling and multi response optimization of mechanical properties for E-glass/polyester composite using Taguchi-grey relational analysis. *Proceedings of the Institution of Mechanical Engineers, Part E: Journal of Process Mechanical Engineering*, *235*(2), 342-350.

Kormin, S., Kormin, F., & Beg, M. (2019). *Effect of plasticizer on physical and mechanical properties of ldpe/sago starch blend.* Paper presented at the Journal of Physics: Conference Series.

Koronis, G., Silva, A., & Fontul, M. (2013). Green composites: A review of adequate materials for automotive applications. *Composites Part B: Engineering, 44*(1), 120-127.

Kowalczyk, M., Piorkowska, E., Kulpinski, P., & Pracella, M. (2011). Mechanical and thermal properties of PLA composites with cellulose nanofibers and standard size fibers. *Composites Part A: Applied Science and Manufacturing, 42*(10), 1509-1514.

Krapež Tomec, D., Schöflinger, M., Leßlhumer, J., Gradišar Centa, U., Žigon, J., & Kariž, M. (2024). The Effects of Microcrystalline Cellulose Addition on the Properties of Wood–PLA Filaments for 3D Printing. *Polymers, 16*(6), 836.

Kumar, A., Grover, N., Manna, A., Kumar, R., Chohan, J. S., Singh, S., . . . Pruncu, C. I. (2022). Multi-objective optimization of WEDM of aluminum hybrid composites using AHP and genetic algorithm. *Arabian Journal for Science and Engineering, 47*(7), 8031-8043.

Kumar, K. R., Mohanavel, V., & Kiran, K. (2022). Mechanical properties and characterization of polylactic acid/carbon fiber composite fabricated by fused deposition modeling. *Journal of Materials Engineering and Performance, 31*(6), 4877-4886.

Kurda, R., de Brito, J., & Silvestre, J. D. (2019). CONCRETop-A multi-criteria decision method for concrete optimization. *Environmental Impact Assessment Review, 74*, 73-85.

Kus, H., Basar, G., & Kahraman, F. (2018). Modeling and optimization for fly ash reinforced bronze-based composite materials using multi objective Taguchi technique and regression analysis. *Industrial Lubrication and Tribology, 70*(7), 1187-1192.

Lee, S.-Y., Mohan, D. J., Kang, I.-A., Doh, G.-H., Lee, S., & Han, S. O. (2009). Nanocellulose reinforced PVA composite films: effects of acid treatment and filler loading. *Fibers and Polymers, 10*(1), 77-82.

Li, H., Cao, Z., Wu, D., Tao, G., Zhong, W., Zhu, H., . . . Liu, C. (2016). Crystallisation, mechanical properties and rheological behaviour of PLA composites reinforced by surface modified microcrystalline cellulose. *Plastics, Rubber and Composites, 45*(4), 181-187.

Li, H., & Huneault, M. A. (2011). Comparison of sorbitol and glycerol as plasticizers for thermoplastic starch in TPS/PLA blends. *Journal of applied polymer science, 119*(4), 2439-2448.

Liang, Z., Wu, H., Liu, R., & Wu, C. (2021). Preparation of long sisal fiber-reinforced polylactic acid biocomposites with highly improved mechanical performance. *Polymers, 13*(7), 1124.

Liew, F. K., Hamdan, S., Rahman, M., Rusop, M., Lai, J. C. H., & Hossen, M. (2015). Synthesis and characterization of cellulose from green bamboo by chemical treatment with mechanical process. *Journal of Chemistry, 2015*.

Likittanaprasong, N., Seadan, M., & Suttiruengwong, S. (2015). *Impact property enhancement of poly (lactic acid) with different flexible copolymers.* Paper presented at the IOP Conference Series: Materials Science and Engineering.

Liu, H., Hu, J., Zhang, Y., Zhao, J., Wang, X., & Song, J. (2023). A dual role of D-Sorbitol in crystallizing and processing poly (lactic acid). *Journal of Polymer Research, 30*(3), 102.

Liu, M., Zhang, Y., & Zhou, C. (2013). Nanocomposites of halloysite and polylactide. *Applied Clay Science, 75*, 52-59.

Liu, Q., Xing, H., Ju, Y., Ou, Z., & Li, Q. (2014). Quasi-static axial crushing and transverse bending of double hat shaped CFRP tubes. *Composite Structures, 117*, 1-11.

Liu, R., Cao, J., Luo, S., & Wang, X. (2013). Effects of two types of clay on physical and mechanical properties of poly (lactic acid)/wood flour composites at various wood flour contents. *Journal of applied polymer science, 127*(4), 2566-2573.

Liu, X., Wu, Y., Zhao, X., & Wang, Z. (2021). Fabrication and applications of bioactive chitosan-based organic-inorganic hybrid materials: A review. *Carbohydrate polymers, 267*, 118179.

Liu, X., Xiao, W., Ma, X., Huang, L., Ni, Y., Chen, L., . . . Li, J. (2020). Conductive regenerated cellulose film and its electronic devices–a review. *Carbohydrate polymers, 250*, 116969.

Lupidi, G., Pastore, G., Marcantoni, E., & Gabrielli, S. (2023). Recent Developments in Chemical Derivatization of Microcrystalline Cellulose (MCC): Pre-Treatments, Functionalization, and Applications. *Molecules, 28*(5), 2009.

Ma, X., Qiao, C., Zhang, J., & Xu, J. (2018). Effect of sorbitol content on microstructure and thermal properties of chitosan films. *International journal of biological macromolecules, 119*, 1294-1297.

Maheswari, C. U., Reddy, K. O., Muzenda, E., Guduri, B., & Rajulu, A. V. (2012). Extraction and characterization of cellulose microfibrils from agricultural residue–Cocos nucifera L. *Biomass and Bioenergy, 46*, 555-563.

Mahmoud, Y., Belhanche-Bensemra, N., & Safidine, Z. (2022). Impact of microcrystalline cellulose extracted from walnut and apricots shells on the biodegradability of Poly (lactic acid). *Frontiers in Materials, 9*, 1005387.

Malkapuram, R., Kumar, V., & Negi, Y. S. (2009). Recent development in natural fiber reinforced polypropylene composites. *Journal of Reinforced Plastics and Composites, 28*(10), 1169-1189.

Manimekalai, G., Kavitha, S., Divya, D., Indran, S., & Binoj, J. (2021). Characterization of enzyme treated cellulosic stem fiber from Cissus quadrangularis plant: an exploratory investigation. *Current Research in Green and Sustainable Chemistry, 4*, 100162.

Manu, T., Nazmi, A. R., Shahri, B., Emerson, N., & Huber, T. (2022). Biocomposites: A Review of Materials and Perception. *Materials Today Communications*, 103308.

Martinez Villadiego, K., Arias Tapia, M. J., Useche, J., & Escobar Macías, D. (2022). Thermoplastic starch (TPS)/polylactic acid (PLA) blending methodologies: a review. *Journal of Polymers and the Environment, 30*(1), 75-91.

Martins, R. P., Schmatz, A. A., de Freita, L. A., Mutton, M. J. R., & Brienzo, M. (2021). Solubilization of hemicellulose and fermentable sugars from bagasse, stalks, and leaves of sweet sorghum. *Industrial Crops and Products, 170*, 113813.

Mathew, A. P., & Dufresne, A. (2002). Plasticized waxy maize starch: effect of polyols and relative humidity on material properties. *Biomacromolecules, 3*(5), 1101-1108.

Mathew, A. P., Oksman, K., & Sain, M. (2005). Mechanical properties of biodegradable composites from poly lactic acid (PLA) and microcrystalline cellulose (MCC). *Journal of applied polymer science, 97*(5), 2014-2025.

Meng, X., Bocharova, V., Tekinalp, H., Cheng, S., Kisliuk, A., Sokolov, A. P., . . . Ozcan, S. (2018). Toughening of nanocelluose/PLA composites via bio-epoxy interaction: Mechanistic study. *Materials & Design, 139*, 188-197.

Mochane, M., Mokhena, T. C., Mokhothu, T., Mtibe, A., Sadiku, E., Ray, S. S., . . . Daramola, O. (2019). Recent progress on natural fiber hybrid composites for advanced applications: A review.

Mohamad, M., Ting, S. W., Bakar, M. B. A., & Osman, W. H. W. (2020). *The Effect of Alkaline Treatment on Mechanical Properties of Polylactic Acid Reinforced with Kenaf Fiber Mat*

Biocomposite. Paper presented at the IOP Conference Series: Earth and Environmental Science.

Mohammed, A. A., Omran, A. A. B., Hasan, Z., Ilyas, R., & Sapuan, S. (2021). Wheat biocomposite extraction, structure, properties and characterization: a review. *Polymers, 13*(21), 3624.

Morán, J. I., Alvarez, V. A., Cyras, V. P., & Vázquez, A. (2008). Extraction of cellulose and preparation of nanocellulose from sisal fibers. *Cellulose, 15*(1), 149-159.

Moser, K., Schmitt, M., Holzer, A., Bergmann, B., Diemert, J., & Elsner, P. (2016). *Optimization of PLA compounds using novel nucleating agents and plasticizers.* Paper presented at the AIP Conference Proceedings.

Mzimela, Z. N. T., Linganiso, L. Z., Revaprasadu, N., & Motaung, T. E. (2018). Comparison of cellulose extraction from sugarcane bagasse through alkali. *Materials Research, 21*.

Nagarajan, K., Balaji, A., Rajan, S. T. K., & Ramanujam, N. (2020). Preparation of bio-eco based cellulose nanomaterials from used disposal paper cups through citric acid hydrolysis. *Carbohydrate polymers, 235*, 115997.

Nagarajan, K., Balaji, A., & Ramanujam, N. (2018). Isolation and characterization of cellulose nanocrystals from Saharan aloe vera cactus fibers. *International Journal of Polymer Analysis and Characterization*.

Nagarajan, K., Balaji, A., & Ramanujam, N. (2019). Extraction of cellulose nanofibers from cocos nucifera var aurantiaca peduncle by ball milling combined with chemical treatment. *Carbohydrate polymers, 212*, 312-322.

Nagarajan, K., Ramanujam, N., Sanjay, M., Siengchin, S., Surya Rajan, B., Sathick Basha, K., . . . Raghav, G. (2021). A comprehensive review on cellulose nanocrystals and cellulose nanofibers: Pretreatment, preparation, and characterization. *Polymer Composites, 42*(4), 1588-1630.

Naik, V., & Kumar, M. (2021). A review on natural fiber composite material in automotive applications. *Engineered Science, 18*, 1-10.

Nakason, K., Pathomrotsakun, J., Kraithong, W., Khemthong, P., & Panyapinyopol, B. (2019). Torrefaction of agricultural wastes: influence of lignocellulosic types and treatment temperature on fuel properties of biochar. *International Energy Journal, 19*(4).

Naz, S., Ahmad, N., Akhtar, J., Ahmad, N. M., Ali, A., & Zia, M. (2016). Management of citrus waste by switching in the production of nanocellulose. *IET nanobiotechnology*, *10*(6), 395-399.

Nazir, M. S., Mohamad Kassim, M. H., Mohapatra, L., Gilani, M. A., Raza, M. R., & Majeed, K. (2016). Characteristic properties of nanoclays and characterization of nanoparticulates and nanocomposites. *Nanoclay reinforced polymer composites: Nanocomposites and bionanocomposites*, 35-55.

Nechifor, M., Tanasă, F., Teacă, C.-A., & Şulea, D. (2022). Maleated coupling agents for the surface treatment of natural fibers. *Surface treatment methods of natural fibres and their effects on biocomposites*, 95-123.

Nehra, P., & Chauhan, R. P. (2022). Facile synthesis of nanocellulose from wheat straw as an agricultural waste. *Iranian Polymer Journal*, *31*(6), 771-778.

Neoh, K., Tshai, K. Y., Khiew, P., & Chia, C. H. (2012). Micro palm and kenaf fibers reinforced PLA composite: effect of volume fraction on tensile strength. *Applied Mechanics and Materials*, *145*, 1-5.

Ngo, T.-D. (2018). Natural fibers for sustainable bio-composites. *Natural and artificial fiber-reinforced composites as renewable sources*, 107-126.

Nguyen, K. T., & Zhao, Y. (2015). Engineered hybrid nanoparticles for on-demand diagnostics and therapeutics. *Accounts of chemical research*, *48*(12), 3016-3025.

Nie, K., Song, Y., Liu, S., Han, G., Ben, H., Ragauskas, A. J., & Jiang, W. (2019). Preparation and Characterization of Microcellulose and Nanocellulose Fibers from Artemisia Vulgaris Bast. *Polymers*, *11*(5), 907.

Nofar, M., Tabatabaei, A., Sojoudiasli, H., Park, C., Carreau, P., Heuzey, M.-C., & Kamal, M. (2017). Mechanical and bead foaming behavior of PLA-PBAT and PLA-PBSA blends with different morphologies. *European polymer journal*, *90*, 231-244.

Nwadiogb, J., Igwe, A., Okoye, N., & Chime, C. (2015). Extraction and characterization of microcrystalline cellulose from mango kernel: A waste management approach.

Nwajiobi, C., Otaigbe, J., & Oriji, O. (2019). Physicochemical, spectroscopic and tableting properties of microcrystalline cellulose obtained from the African breadfruit seed hulls. *African Journal of Biotechnology*, *18*(18), 371-382.

Nyambo, C., Mohanty, A. K., & Misra, M. (2011). Effect of maleated compatibilizer on performance of PLA/wheat Straw-Based green composites. *Macromolecular Materials and Engineering*, *296*(8), 710-718.

Okafor, E. G., Abba, M. T., Mohammad, M. H., Ubadike, O. C., Jemitola, P. O., & Sule, G. (2021). THERMO-MECHANICAL INVESTIGATION OF HYBRID PARTICULATE BANANA/SISAL FIBER REINFORCED POLYESTER MATRIX COMPOSITE. *Journal of Southwest Jiaotong University*, *56*(4).

Oladele, I. O., Omotosho, T. F., & Adediran, A. A. (2020a). Polymer-based composites: an indispensable material for present and future applications. *International Journal of Polymer Science*, *2020*.

Oladele, I. O., Omotosho, T. F., & Adediran, A. A. (2020b). Polymer-based composites: an indispensable material for present and future applications. *International Journal of Polymer Science*, *2020*(1), 8834518.

Olonisakin, K., Li, R., He, S., Aishi, W., Lifei, F., Mengting, C., . . . Yang, W. (2022). Flame rating of nano clay/MCC/PLA composites with both reinforced strength and toughness. *Journal of Polymer Research*, *29*(12), 502.

Olorunsola, E., Bhatia, P., Tytler, B., & Adikwu, M. (2016). Hydration and swelling dynamics of some tropical hydrophilic polymers. *Nigerian Journal of Pharmaceutical Sciences*, *15*(1), 41-47.

Omrani, E., Menezes, P. L., & Rohatgi, P. K. (2016). State of the art on tribological behavior of polymer matrix composites reinforced with natural fibers in the green materials world. *Engineering Science and Technology, an International Journal*, *19*(2), 717-736.

Onyedum, O., Aduloju, S. C., Sheidu, S. O., Metu, C. S., & Owolabi, O. B. (2015). Comparative mechanical analysis of okra fiber and banana fiber composite used in manufacturing automotive car bumpers. *American Journal of Engineering, Technology and Society*, *2*(6), 193-199.

Onyekwere, O. S., Oladeinde, M. H., & Edokpia, R. O. (2021). Multi-Response optimization of bamboo fiber reinforced unsaturated polyester composites using hybrid Taguchi–grey relational analysis method. *Journal of Industrial and Production Engineering*, *38*(2), 98-107.

Osokoya, O. (2017). An evaluation of polymer composites for car bumper beam. *International Journal of Automotive Composites, 3*(1), 44-60.

Ostafinska, A., Fortelny, I., Nevoralova, M., Hodan, J., Kredatusova, J., & Slouf, M. (2015). Synergistic effects in mechanical properties of PLA/PCL blends with optimized composition, processing, and morphology. *RSC advances, 5*(120), 98971-98982.

Othman, S. H., Hassan, N., Talib, R. A., Kadir Basha, R., & Risyon, N. P. (2017). Mechanical and thermal properties of PLA/halloysite bio-nanocomposite films: Effect of halloysite nanoclay concentration and addition of glycerol. *Journal of Polymer Engineering, 37*(4), 381-389.

Pachuau, L., Vanlalfakawma, D. C., Tripathi, S. K., & Lalhlenmawia, H. (2014). Muli bamboo (Melocanna baccifera) as a new source of microcrystalline cellulose. *Journal of Applied Pharmaceutical Science, 4*(11), 087-094.

Pan, Y., Farmahini-Farahani, M., O'Hearn, P., Xiao, H., & Ocampo, H. (2016). An overview of bio-based polymers for packaging materials. *J. Bioresour. Bioprod, 1*(3), 106-113.

Panke, D. (2018). Research design & method selection: Making good choices in the social sciences.

Panthapulakkal, S., Law, S., & Sain, M. (2006). Performance of injection molded natural fiber—hybrid thermoplastic composites for automotive structural applications. *SAE Transactions*, 27-32.

Park, W., Shin, H., Choi, B., Rhim, W.-K., Na, K., & Han, D. K. (2020). Advanced hybrid nanomaterials for biomedical applications. *Progress in Materials Science, 114*, 100686.

Peter, Z. (2021). Order in cellulosics: Historical review of crystal structure research on cellulose. *Carbohydrate polymers, 254*, 117417.

Pickering, K. L., Efendy, M. A., & Le, T. M. (2016). A review of recent developments in natural fibre composites and their mechanical performance. *Composites Part A: Applied Science and Manufacturing, 83*, 98-112.

Piotr Konieczka, P., Aliaño-González, M. J., Ferreiro-González, M., Barbero, G. F., & Palma, M. (2020). Characterization of arabica and robusta coffees by ion mobility sum spectrum. *Sensors, 20*(11), 3123.

Platnieks, O., Gaidukovs, S., Barkane, A., Sereda, A., Gaidukova, G., Grase, L., . . . Skute, M. (2020). Bio-based poly (butylene succinate)/microcrystalline cellulose/nanofibrillated

cellulose-based sustainable polymer composites: Thermo-mechanical and biodegradation studies. *Polymers, 12*(7), 1472.

Pongtanayut, K., Thongpin, C., & Santawitee, O. (2013). The effect of rubber on morphology, thermal properties and mechanical properties of PLA/NR and PLA/ENR blends. *Energy Procedia*, *34*, 888-897.

Poyilil, S., Palatel, A., & Chandrasekharan, M. (2021). Physico-chemical characterization study of coffee husk for feasibility assessment in fluidized bed gasification process. *Environmental Science and Pollution Research*, 1-13.

Prabhakaran, S., Chinnarasu, K., & Kumar, M. S. (2012). Design and fabrication of composite bumper for light passenger vehicles. *International Journal of Modern Engineering Research, 2*(4), 2552-2556.

Prevot, V., & Bourgeat-Lami, E. (2020). Recent advances in layered double hydroxide/polymer latex nanocomposites: from assembly to in situ formation. *Layered double hydroxide polymer nanocomposites*, 461-495.

Puthumana, M., Santhana Gopala Krishnan, P., & Nayak, S. K. (2020). Chemical modifications of PLA through copolymerization. *International Journal of Polymer Analysis and Characterization, 25*(8), 634-648.

Rafiee, R., & Shahzadi, R. (2019). Mechanical properties of nanoclay and nanoclay reinforced polymers: a review. *Polymer Composites, 40*(2), 431-445.

Rajamani, D., Balasubramanian, E., Dilli Babu, G., & Ananthakumar, K. (2022). Experimental investigations on high precision abrasive waterjet cutting of natural fibre reinforced nano clay filled green composites. *Journal of Industrial Textiles, 51*(3_suppl), 3786S-3810S.

Rajaram, S., Venkatesan, K., Jenish, I., & Bhaskar, G. (2023). Study of mechanical properties on abaca/sisal fibre–reinforced epoxy resin–based hybrid composites. *Biomass Conversion and Biorefinery*, 1-14.

Rajeshkumar, G., Seshadri, S. A., Devnani, G., Sanjay, M., Siengchin, S., Maran, J. P., . . . Sivarajasekar, N. (2021). Environment friendly, renewable and sustainable poly lactic acid (PLA) based natural fiber reinforced composites–A comprehensive review. *Journal of Cleaner Production, 310*, 127483.

Rajeshkumar, G., Seshadri, S. A., Ramakrishnan, S., Sanjay, M., Siengchin, S., & Nagaraja, K. (2021). A comprehensive review on natural fiber/nano-clay reinforced hybrid polymeric composites: Materials and technologies. *Polymer Composites, 42*(8), 3687-3701.

Ramasubbu, R., & Madasamy, S. (2022). Fabrication of automobile component using hybrid natural fiber reinforced polymer composite. *Journal of Natural Fibers, 19*(2), 736-746.

Ramchandra, C. G. (2020). Some Studies on Characterization of Composite Material for Automotive Application.

Ramesh, P., Durga Prasad, B., & Narayana, K. (2020). *Characterization of Kenaf/Aloevera fiber reinforced PLA-hybrid biocomposite.* Paper presented at the Advances in Applied Mechanical Engineering: Select Proceedings of ICAMER 2019.

Ramesh, P., Prasad, B. D., & Narayana, K. (2020). Effect of MMT clay on mechanical, thermal and barrier properties of treated aloevera fiber/PLA-hybrid biocomposites. *Silicon, 12*(7), 1751-1760.

Ramesh, P., Prasad, B. D., & Narayana, K. (2021). Influence of montmorillonite clay content on thermal, mechanical, water absorption and biodegradability properties of treated kenaf fiber/PLA-hybrid biocomposites. *Silicon, 13*(1), 109-118.

Ranakoti, L., Gangil, B., Mishra, S. K., Singh, T., Sharma, S., Ilyas, R., & El-Khatib, S. (2022). Critical review on polylactic acid: properties, structure, processing, biocomposites, and nanocomposites. *Materials, 15*(12), 4312.

Rasheed, M., Jawaid, M., Karim, Z., & Abdullah, L. C. (2020). Morphological, physiochemical and thermal properties of microcrystalline cellulose (MCC) extracted from bamboo fiber. *Molecules, 25*(12), 2824.

Rasheed, M., Jawaid, M., Parveez, B., Hussain Bhat, A., & Alamery, S. (2021). Morphology, structural, thermal, and tensile properties of bamboo microcrystalline cellulose/poly (lactic acid)/poly (butylene succinate) composites. *Polymers, 13*(3), 465.

Rashid, M., Gafur, M. A., Sharafat, M. K., Minami, H., Miah, M. A. J., & Ahmad, H. (2017). Biocompatible microcrystalline cellulose particles from cotton wool and magnetization via a simple in situ co-precipitation method. *Carbohydrate polymers, 170*, 72-79.

Rawoof, S. A. A., Kumar, P. S., Vo, D.-V. N., Devaraj, K., Mani, Y., Devaraj, T., & Subramanian, S. (2021). Production of optically pure lactic acid by microbial fermentation: a review. *Environmental Chemistry Letters, 19*(1), 539-556. doi: 10.1007/s10311-020-01083-w

Reddy, K. O., Uma Maheswari, C., Muzenda, E., Shukla, M., & Rajulu, A. V. (2016). Extraction and characterization of cellulose from pretreated ficus (peepal tree) leaf fibers. *Journal of Natural Fibers, 13*(1), 54-64.

Reddy, K. O., Zhang, J., Zhang, J., & Rajulu, A. V. (2014). Preparation and properties of self-reinforced cellulose composite films from Agave microfibrils using an ionic liquid. *Carbohydrate polymers, 114*, 537-545.

Reddy, N., & Yang, Y. (2009). Extraction and characterization of natural cellulose fibers from common milkweed stems. *Polymer Engineering & Science, 49*(11), 2212-2217.

Reis, R. S., Tienne, L. G., de HS Souza, D., Maria de Fátima, V. M., & Monteiro, S. N. (2020). Characterization of coffee parchment and innovative steam explosion treatment to obtain microfibrillated cellulose as potential composite reinforcement. *Journal of materials research and technology, 9*(4), 9412-9421.

Ren, H., Shen, J., Pei, J., Wang, Z., Peng, Z., Fu, S., & Zheng, Y. (2019). Characteristic microcrystalline cellulose extracted by combined acid and enzyme hydrolysis of sweet sorghum. *Cellulose, 26*, 8367-8381.

Rico, M., Rodríguez-Llamazares, S., Barral, L., Bouza, R., & Montero, B. (2016). Processing and characterization of polyols plasticized-starch reinforced with microcrystalline cellulose. *Carbohydrate polymers, 149*, 83-93.

Risite, H., Salim, M. H., Oudinot, B. T., Ablouh, E.-h., Joyeux, H. T., Sehaqui, H., . . . Kassab, Z. (2022). Artemisia annua stems a new sustainable source for cellulosic materials: Production and characterization of cellulose microfibers and nanocrystals. *Waste and Biomass Valorization, 13*(4), 2411-2423.

Riyanti, F. (2023). Turnitin Extraction of Cellulose from Kepok Banana Peel (Musa parasidiaca L.) for Adsorption Procion Dye.

Rodiah, M., Jamilah, B., Sharifah Kharidah, S., & Russly, A. (2019). Physico-chemical and antioxidant properties of mesocarp and exocarp from Borassus flabellifer. *International Food Research Journal, 26*(5).

Romruen, O., Karbowiak, T., Tongdeesoontorn, W., Shiekh, K. A., & Rawdkuen, S. (2022). Extraction and Characterization of Cellulose from Agricultural By-Products of Chiang Rai Province, Thailand. *Polymers, 14*(9), 1830.

Sachin, S. R., Kannan, T. K., & Rajasekar, R. (2020). Effect of wood particulate size on the mechanical properties of PLA biocomposite. *Pigment & Resin Technology*, *49*(6), 465-472.

Safaei, M., Taran, M., Imani, M. M., Moradpoor, H., Rezaei, F., Jamshidy, L., & Rezaei, R. (2019). Application of Taguchi method in the optimization of synthesis of cellulose-MgO bionanocomposite as antibacterial agent. *Polish Journal of Chemical Technology*, *21*(4).

Sahu, P., & Gupta, M. (2022). Water absorption behavior of cellulosic fibres polymer composites: A review on its effects and remedies. *Journal of Industrial Textiles*, *51*(5_suppl), 7480S-7512S.

Saidi, M. A., Gorin, A., Kok, H. S., & Jayamani, E. (2018). The optimum sodium hydroxide concentration for high strength pla-rice straw composites. *Journal of Mechanical Engineering and Sciences*, *12*(1), 3472.

Sanusi, O. M., Benelfellah, A., Terzopoulou, Z., Bikiaris, D., & Hocine, N. A. (2021). Properties of polylactide reinforced with montmorillonite/multiwalled carbon nanotube hybrid. *Materials Today: Proceedings*, *47*, 3247-3250.

Scaffaro, R., Lopresti, F., & Botta, L. (2018). PLA based biocomposites reinforced with Posidonia oceanica leaves. *Composites Part B: Engineering*, *139*, 1-11.

Selwyn, T. S. (2021). Formation, characterization and suitability analysis of polymer matrix composite materials for automotive bumper. *Materials Today: Proceedings*, *43*, 1197-1203.

Shah, A. U. R., Prabhakar, M., & Song, J.-I. (2017a). Current advances in the fire retardancy of natural fiber and bio-based composites–A review. *International journal of precision engineering and manufacturing-green technology*, *4*, 247-262.

Shah, A. U. R., Prabhakar, M., & Song, J.-I. (2017b). Current advances in the fire retardancy of natural fiber and bio-based composites–A review. *International journal of precision engineering and manufacturing-green technology*, *4*(2), 247-262.

Shahmaleki, M., Beigmohammadi, F., & Movahedi, F. (2021). Cellulose-Reinforced Starch Biocomposite: Optimization of the Effects of Filler and Various Plasticizers using Design–Expert Method. *Starch-Stärke*, *73*(9-10), 2000028.

Shahruzzaman, M., Hossain, S., Ahmed, T., Kabir, S. F., Islam, M. M., Rahman, A., . . . Rahman, M. M. (2022). Biological macromolecules as antimicrobial agents *Biological Macromolecules* (pp. 165-202): Elsevier.

Shar, A. S., Zhang, C., Song, X., Weng, Y., & Du, Q. (2021). Design of novel PLA/OMMT films with improved gas barrier and mechanical properties by intercalating OMMT interlayer with high gas barrier polymers. *Polymers, 13*(22), 3962.

Sharifzadeh, E., & Cheraghi, K. (2021). Temperature-affected mechanical properties of polymer nanocomposites from glassy-state to glass transition temperature. *Mechanics of Materials, 160*, 103990.

Sharma, A., Thakur, M., Bhattacharya, M., Mandal, T., & Goswami, S. (2019). Commercial application of cellulose nano-composites–A review. *Biotechnology Reports, 21*, e00316.

Shekar, H. S., & Ramachandra, M. (2018). Green composites: a review. *Materials Today: Proceedings, 5*(1), 2518-2526.

Shi, S.-C., & Liu, G.-T. (2021). Cellulose nanocrystal extraction from rice straw using a chlorine-free bleaching process. *Cellulose, 28*(10), 6147-6158.

Shinde, N. G., & Patel, D. M. (2020). *A short review on automobile dashboard materials.* Paper presented at the IOP Conference Series: Materials Science and Engineering.

Shuvo, S. N., Shorowordi, K. M., & Islam, M. A. (2015). Effect of nanoclay on jute fiber reinforced polyester composites. *International Journal of Advanced Engineering and Nano Technology, 2*(8), 20-26.

Siakeng, R., Jawaid, M., Ariffin, H., & Sapuan, S. (2019). Mechanical, dynamic, and thermomechanical properties of coir/pineapple leaf fiber reinforced polylactic acid hybrid biocomposites. *Polymer Composites, 40*(5), 2000-2011.

Sirbu, E.-E., Dinita, A., Tănase, M., Portoacă, A.-I., Bondarev, A., Enascuta, C.-E., & Calin, C. (2024). Influence of Plasticizers Concentration on Thermal, Mechanical, and Physicochemical Properties on Starch Films. *Processes, 12*(9), 2021.

Siva, R., Kesavaram, B., Martin, J. J., Mathiselvan, G., Navas, K. B., & Sangeetha, M. (2021). Mechanical behavior of sisal and banana fiber reinforced hybrid epoxy composites. *Materials Today: Proceedings, 44*, 3692-3696.

Songok, J., Salminen, P., & Toivakka, M. (2014). Temperature effects on dynamic water absorption into paper. *Journal of colloid and interface science, 418*, 373-377.

Storz, H., & Vorlop, K.-D. (2013). Bio-based plastics: status, challenges and trends. *Appl Agric For Res*, *63*, 321-332.

Sun, Z., Zhang, L., Liang, D., Xiao, W., & Lin, J. (2017). Mechanical and thermal properties of PLA biocomposites reinforced by coir fibers. *International Journal of Polymer Science*, *2017*.

Sung, S. H., Chang, Y., & Han, J. (2017). Development of polylactic acid nanocomposite films reinforced with cellulose nanocrystals derived from coffee silverskin. *Carbohydrate polymers*, *169*, 495-503.

Sungsanit, K., Kao, N., & Bhattacharya, S. (2012). Properties of linear poly (lactic acid)/polyethylene glycol blends. *Polymer Engineering & Science*, *52*(1), 108-116.

Suriani, M., Ilyas, R., Zuhri, M., Khalina, A., Sultan, M., Sapuan, S., . . . Harussani, M. (2021). Critical review of natural fiber reinforced hybrid composites: Processing, properties, applications and cost. *Polymers*, *13*(20), 3514.

Swift, L. ENZYMATIC DEGRADATION OF CELLULOSIC WASTES.

Syafri, E., Kasim, A., Abral, H., & Asben, A. (2018). Cellulose nanofibers isolation and characterization from ramie using a chemical-ultrasonic treatment. *Journal of Natural Fibers*.

Szymańska-Chargot, M., Cieśla, J., Pękala, P., Pieczywek, P. M., Oleszek, W., Żyła, M., . . . Zdunek, A. (2022). The Influence of High-Intensity Ultrasonication on Properties of Cellulose Produced from the Hop Stems, the Byproduct of the Hop Cones Production. *Molecules*, *27*(9), 2624.

Taib, N.-A. A. B., Rahman, M. R., Huda, D., Kuok, K. K., Hamdan, S., Bakri, M. K. B., . . . Khan, A. (2023). A review on poly lactic acid (PLA) as a biodegradable polymer. *Polymer Bulletin*, *80*(2), 1179-1213. doi: 10.1007/s00289-022-04160-y

Tang, S., Li, J., Wang, R., Zhang, J., Lu, Y., Hu, G. H., . . . Zhang, L. (2022). Current trends in bio-based elastomer materials. *SusMat*, *2*(1), 2-33.

Tarchoun, A. F., Trache, D., Klapötke, T. M., Derradji, M., & Bessa, W. (2019). Ecofriendly isolation and characterization of microcrystalline cellulose from giant reed using various acidic media. *Cellulose*, *26*(13), 7635-7651.

Tee, Y. B., Talib, R. A., Abdan, K., Chin, N. L., Basha, R. K., & Yunos, K. F. M. (2014). Toughening poly (lactic acid) and aiding the melt-compounding with bio-sourced plasticizers. *Agriculture and Agricultural Science Procedia*, *2*, 289-295.

Teramoto, Y. (2021). Recent Advances in Multi-Scale Experimental Analysis to Assess the Role of Compatibilizers in Cellulosic Filler-Reinforced Plastic Composites. *Journal of Composites Science*, *5*(5), 138.

Thygesen, A., Oddershede, J., Lilholt, H., Thomsen, A. B., & Ståhl, K. (2005). On the determination of crystallinity and cellulose content in plant fibres. *Cellulose*, *12*(6), 563-576.

Tian, H., Liu, D., Yao, Y., Ma, S., Zhang, X., & Xiang, A. (2017). Effect of sorbitol plasticizer on the structure and properties of melt processed polyvinyl alcohol films. *Journal of food science*, *82*(12), 2926-2932.

Trache, D., Hussin, M. H., Chuin, C. T. H., Sabar, S., Fazita, M. N., Taiwo, O. F., . . . Haafiz, M. M. (2016). Microcrystalline cellulose: Isolation, characterization and bio-composites application—A review. *International journal of biological macromolecules*, *93*, 789-804.

Turku, I., & Kärki, T. (2014). Research progress in wood-plastic nanocomposites: a review. *Journal of Thermoplastic Composite Materials*, *27*(2), 180-204.

Väisänen, T., Das, O., & Tomppo, L. (2017). A review on new bio-based constituents for natural fiber-polymer composites. *Journal of Cleaner Production*, *149*, 582-596.

Vieira, M. G. A., Da Silva, M. A., Dos Santos, L. O., & Beppu, M. M. (2011). Natural-based plasticizers and biopolymer films: A review. *European polymer journal*, *47*(3), 254-263.

Wang, G., Zhang, D., Li, B., Wan, G., Zhao, G., & Zhang, A. (2019). Strong and thermal-resistance glass fiber-reinforced polylactic acid (PLA) composites enabled by heat treatment. *International journal of biological macromolecules*, *129*, 448-459.

Wang, X., Cui, X., Che, Y., Zhou, S., Dan, Z., Yan, B., . . . Wang, T. (2021). Gasification of Tibetan herb residue: Thermogravimetric analysis and experimental study. *Biomass and Bioenergy*, *146*, 105952.

Wardhono, E. Y., & Kanani, N. (2019). Development of polylactic acid (PLA) bio-composite films reinforced with bacterial cellulose nanocrystals (BCNC) without any surface modification. *Journal of Dispersion Science and Technology*.

Woyesa, T., & Kumar, S. (2021). Potential of coffee tourism for rural development in Ethiopia: a sustainable livelihood approach. *Environment, development and sustainability, 23*, 815-832.

Wu, Y., Li, L., Chen, S., Qin, J., Chen, X., Zhou, D., & Wu, H. (2020). Synthesis, characterization, and crystallization behaviors of poly (D-lactic acid)-based triblock copolymer. *Scientific reports, 10*(1), 3627.

Xian, X., Wang, X., Zhu, Y., Guo, Y., & Tian, Y. (2018). Effects of MCC content on the structure and performance of PLA/MCC biocomposites. *Journal of Polymers and the Environment, 26*, 3484-3492.

Xiong, R., Zhang, X., Tian, D., Zhou, Z., & Lu, C. (2012). Comparing microcrystalline with spherical nanocrystalline cellulose from waste cotton fabrics. *Cellulose, 19*(4), 1189-1198.

Yan, Z., Chen, S., Wang, H., Wang, B., & Jiang, J. (2008). Biosynthesis of bacterial cellulose/multi-walled carbon nanotubes in agitated culture. *Carbohydrate polymers, 74*(3), 659-665.

Yoganandam, K., Shanmugam, V., Vasudevan, A., Vinodh, D., Nagaprasad, N., Stalin, B., . . . Bharani, M. (2021). Investigation of dynamic, mechanical, and thermal properties of Calotropis procera particle-reinforced PLA biocomposites. *Advances in Materials Science and Engineering, 2021*, 1-7.

Zadorozhnyy, V., Tomilin, I., Berdonosova, E., Gammer, C., Zadorozhnyy, M., Savvotin, I., . . . Bazlov, A. (2022). Composition design, synthesis and hydrogen storage ability of multi-principal-component alloy TiVZrNbTa. *Journal of Alloys and Compounds, 901*, 163638.

Zhang, L., Zhong, J., & Ren, X. (2017). Natural fiber-based biocomposites. *Green Biocomposites: Manufacturing and Properties*, 31-70.

Zhang, Q., Shi, L., Nie, J., Wang, H., & Yang, D. (2012). Study on poly (lactic acid)/natural fibers composites. *Journal of applied polymer science, 125*(S2), E526-E533.

Zhang, W., Zhou, W., Zhang, Z., Zhang, D., Guo, Z., Ren, P., & Liu, F. (2023). Effect of Nano-silica and sorbitol on the properties of chitosan-based composite films. *Polymers, 15*(19), 4015.

Zhao, B., Zhang, Y., & Ren, H. (2020). Effects of microcrystalline cellulose surface modification on the mechanical and thermal properties of polylactic acid composite films. *Plastics, Rubber and Composites, 49*(10), 450-455.

Zhao, T., Chen, Z., Lin, X., Ren, Z., Li, B., & Zhang, Y. (2018). Preparation and characterization of microcrystalline cellulose (MCC) from tea waste. *Carbohydrate polymers*, *184*, 164-170.

Zhou, Y., Zhang, X., Zhang, J., Cheng, Y., Wu, J., Yu, J., & Zhang, J. (2021). Molecular weight characterization of cellulose using ionic liquids. *Polymer testing*, *93*, 106985.

Zwawi, M. (2021). A Review on Natural Fiber Bio-Composites, Surface Modifications and Applications. *Molecules*, *26*(2), 404.

APPENDIX

Appendix 1: Flexural strength and modulus analysis of raw data

Sample	Average force - elongation		Sample size			FS (MPa)	FM (MPa)
			L(mm)	W(mm)	t(mm)		
	d (mm)	F (KN)					
1	0.86	0.14	40	10	4	52.5	4069.76
2	0.75	0.16	40	10	4	60	5333.33
3	0.74	0.2	40	10	4	75	6756.75
4	0.73	0.22	40	10	4	82.5	7534.24
5	0.72	0.16	40	10	4	60	5555.55
6	0.67	0.19	40	10	4	71.25	7089.55
7	0.66	0.2	40	10	4	75	7575.75
8	0.64	0.25	40	10	4	93.75	9765.62
9	0.63	0.17	40	10	4	63.75	6746.03
10	0.6	0.17	40	10	4	63.75	7083.33
11	0.58	0.18	40	10	4	67.5	7758.62
12	0.56	0.19	40	10	4	71.25	8482.14
13	0.6	0.12	40	10	4	45	5000.00
14	0.46	0.15	40	10	4	56.25	8152.17
15	0.48	0.15	40	10	4	56.25	7812.50
16	0.46	0.16	40	10	4	60	8695.65

Appendix 2: Tensile strength raw data and its analysis

Sample	Avg. Force (KN)	Cross sectional area (mm^2)	TS (MPa)
1	1	18	55.5
2	1.2	18	68.8
3	1.3	18	72.2
4	1.4	18	77.7
5	1.2	18	66.6
6	1.4	18	77.7
7	1.2	18	67.7
8	1.35	18	75.5
9	1.05	18	58.3
10	1.3	18	72.2
11	1.4	18	78.8
12	1.5	18	83.3
13	1.2	18	66.6
14	1.26	18	70.5
15	1.47	18	81.6

16	1.4	18	78.8

Appendix 3: Water absorption raw data and analysis

Sample	Mass of Sample		Volume (mm^3)	Wet – dry mass	WA	% WA	density (g/mm^3)
	Dry mass	Wet mass					
1	1.56	1.59	1200	0.038688	0.0248	2.48	0.00130
2	1.596	1.69	1200	0.0962388	0.0603	6.03	0.00133
3	1.608	1.75	1200	0.1411824	0.0878	8.78	0.00135
4	1.656	1.83	1200	0.1760328	0.1063	10.63	0.00138
5	1.596	1.68	1200	0.0884184	0.0554	5.54	0.00134
6	1.608	1.67	1200	0.0673752	0.0419	4.19	0.00134
7	1.596	1.79	1200	0.1966272	0.1232	12.32	0.00133
8	1.632	1.76	1200	0.1274592	0.0781	7.81	0.00136
9	1.632	1.79	1200	0.1587936	0.0973	9.73	0.00136
10	1.644	1.89	1200	0.2502168	0.1522	15.22	0.00137
11	1.62	1.70	1200	0.082782	0.0511	5.11	0.00135
12	1.656	1.77	1200	0.1149264	0.0694	6.94	0.00138
13	1.632	1.89	1200	0.2638944	0.1617	16.17	0.00136
14	1.644	1.81	1200	0.1647288	0.1002	10.02	0.00137
15	1.668	1.79	1200	0.1214304	0.0728	7.28	0.00139
16	1.692	1.80	1200	0.1160712	0.0686	6.86	0.00141